COMPLEMENTARY EFFECTS OF *Polygonum minus* EXTRACT IN COMBINATION WITH 5-FLUOROURACIL IN CT26 MURINE COLON CANCER CELL LINE *IN VITRO* AND *IN VIVO*

By

YANG ZHONGMING

Thesis Submitted to the School of Graduate Studies, Universiti Putra Malaysia, in Fulfilment of the Requirements for the Degree of Doctor of Philosophy

January 2025

IB 2025 1

DEDICATION

This thesis is dedicated to:

Yang Fupei – Dad

Lv Junhua – Mom

Yang Zhongguo – Bro

China – motherland

Abstract of thesis presented to the Senate of Universiti Putra Malaysia in fulfilment of the requirement for the degree of Doctor of Philosophy

COMPLEMENTARY EFFECTS OF *Polygonum minus* EXTRACT IN COMBINATION WITH 5-FLUOROURACIL IN CT26 MURINE COLON CANCER CELL LINE *IN VITRO* AND *IN VIVO*

By

YANG ZHONGMING

January 2025

Chairman : Professor Md Zuki bin Abu Bakar @ Zakaria, PhD
Institute : Bioscience

Colon cancer (CC) is the third most common cancer and the second leading cause of cancer-related deaths worldwide. Treatment strategies typically begin with surgery, followed by chemotherapy, radiation therapy, or targeted therapies such as monoclonal antibodies. 5-Fluorouracil (5-FU) is a key chemotherapeutic agent in CC treatment, but its efficacy is often compromised by toxicity and drug resistance. Plant-derived compounds have gained attention for their potential to enhance chemotherapy while reducing side effects. *Polygonum minus* (PM), a medicinal and dietary plant, has demonstrated various bioactivities, yet its potential synergy with 5-FU remains unexplored.

This study investigates the combinatorial effects of the PM hexane fraction (PM-H-H) and 5-FU on CC using both *in vitro* and *in vivo* models. *In vitro* assays demonstrated that PM-H-H selectively enhanced 5-FU cytotoxicity in murine CC cells (CT26), induced apoptosis, and caused cell cycle arrest at the G0/G1 phase. The combination

treatment also inhibited cell migration, clonogenic survival, and spheroid growth, suggesting a potential role in suppressing metastasis. Metabolomics and proteomics analyses identified significant alterations in metabolic and signaling pathways, highlighting the mechanistic basis of the combination's efficacy.

In vivo experiments using a CT26 tumor-bearing BALB/c mouse model further confirmed these findings. The combination of PM-H-H and 5-FU significantly reduced tumor volume and weight compared to individual treatments while mitigating systemic toxicity. Histopathological analysis revealed enhanced tumor destruction and reduced adverse effects on vital organs, supporting the safety of this approach.

Overall, this study provides strong evidence that PM-H-H enhances the therapeutic effects of 5-FU while reducing its toxicity. These findings suggest that PM-H-H could serve as a promising adjuvant to improve CC treatment outcomes. Further research is needed to validate its clinical potential and long-term safety.

Keywords: Colon cancer; 5-Fluorouracil; *Polygonum minus*; Chemotherapy adjuvant; Molecular therapeutic mechanism

SDG: GOAL 3: Good Health and Well-being

Abstrak tesis yang dikemukakan kepada Senat Universiti Putra Malaysia
sebagai memenuhi keperluan untuk ijazah Doktor Falsafah

KESAN KOMPLEMENTARI EKSTRAK *Polygonum minus* DALAM KOMBINASI DENGAN 5-FLUOROURASIL TERHADAP SEL KANSER KOLON CT26 TIKUS SECARA *IN VITRO* DAN *IN VIVO*

Oleh

YANG ZHONGMING

Januari 2025

Pengerusi : Profesor Md Zuki bin Abu Bakar @ Zakaria, PhD
Institut : Biosains

Kanser kolon (CC) ialah kanser ketiga paling kerap berlaku dan penyebab kedua utama kematian berkaitan kanser di seluruh dunia. Strategi rawatan biasanya bermula dengan pembedahan, diikuti dengan kemoterapi, terapi radiasi, atau terapi sasaran seperti antibodi monoklonal. 5-Fluorourasil (5-FU) merupakan agen kemoterapi utama dalam rawatan CC, tetapi keberkesanannya sering terjejas akibat ketoksikan dan rintangan dadah. Sebatian daripada tumbuhan semakin mendapat perhatian kerana potensinya dalam meningkatkan keberkesanan kemoterapi sambil mengurangkan kesan sampingan. *Polygonum minus* (PM), tumbuhan yang digunakan dalam perubatan dan pemakanan, telah menunjukkan pelbagai aktiviti bioaktif, namun potensinya dalam sinergi dengan 5-FU masih belum diterokai.

Kajian ini menyiasat kesan gabungan pecahan heksana PM (PM-H-H) dan 5-FU terhadap CC menggunakan model *in vitro* dan *in vivo*. Ujian *in vitro* menunjukkan bahawa PM-H-H secara selektif meningkatkan ketoksikan 5-FU terhadap sel CC tikus

(CT26), mendorong apoptosis, dan menyebabkan perencatan kitaran sel pada fasa G0/G1. Rawatan kombinasi ini turut menghalang migrasi sel, daya tahan klonogenik, dan pertumbuhan sferoid, menunjukkan potensi dalam menekan metastasis. Analisis metabolomik dan proteomik mengenal pasti perubahan ketara dalam laluan metabolic dan isyarat sel, menonjolkan asas mekanistik keberkesanan gabungan ini.

Eksperimen *in vivo* menggunakan model tikus BALB/c yang membawa tumor CT26 mengesahkan penemuan ini. Kombinasi PM-H-H dan 5-FU mengurangkan isipadu dan berat tumor dengan lebih ketara berbanding rawatan individu sambil mengurangkan ketoksikan sistemik. Analisis histopatologi menunjukkan peningkatan kerosakan tumor dan pengurangan kesan buruk terhadap organ penting, menyokong keselamatan pendekatan ini.

Secara keseluruhan, kajian ini memberikan bukti kukuh bahawa PM-H-H meningkatkan kesan terapeutik 5-FU sambil mengurangkan ketoksikannya. Penemuan ini mencadangkan bahawa PM-H-H berpotensi sebagai agen tambahan untuk memperbaiki hasil rawatan CC. Kajian lanjut diperlukan untuk mengesahkan potensinya dalam aplikasi klinikal serta keselamatan jangka panjangnya.

Kata kunci: Kanser kolon; 5-Fluorourasil; *Polygonum minus*; Ajuvan kemoterapi; Mekanisme terapeutik molekul

SDG: MATLAMAT 3: Kesihatan dan Kesejahteraan yang Baik

ACKNOWLEDGEMENTS

The past three years at Universiti Putra Malaysia have been a period of intense learning, personal growth, and resilience. Despite these difficulties, each experience has been a stepping stone that helped me evolve, both intellectually and emotionally. These three years have tested my limits but also taught me invaluable lessons about perseverance, patience, and the pursuit of knowledge. As I stand at the end of this chapter, I am deeply grateful for the support, guidance, and encouragement that have surrounded me.

First and foremost, I owe my deepest gratitude to my supervisor, Prof. Dr Md Zuki Abu Bakar @ Zakaria. His unwavering support, intellectual insight, and constant encouragement have been the cornerstone of my academic progress. He has always believed in my potential, even when I doubted myself, and has pushed me to achieve beyond what I thought was possible. His expertise, generosity with time, and dedication to my development have shaped thesis in more ways than words can express.

I am also deeply grateful to my co-supervisor, Prof. Dr Norhaizan Mohd Esa, Assoc. Prof. Dr Ahmad Faizal Mohd Razis, Dr Norsharina Ismail, and Dr Chan Kim Wei, for their insightful feedback and continuous support throughout my research. Their guidance has helped me refine my ideas and strengthen the quality of this work.

In addition to my supervisory committee, I owe a special thanks to Dr Chia, whose expertise and assistance have been crucial in shaping various aspects of my research. Dr Chia's generosity with time and knowledge has helped me navigate through challenging moments in my research. A sincere thank you to the laboratory staff Mr Salman and Ms Nurnajwa, whose expertise, advice, and assistance made the long hours

of research and experimentation both productive and manageable.

I would also like to acknowledge the valuable contributions of Deng Xi, Han Mingzhao, Zanna, and Tahil, who have provided tremendous support throughout my research. Each of you has played a vital role, whether through sharing your knowledge, offering feedback, or providing encouragement during the most challenging moments, whether through late-night conversations or simply offering a listening ear, your presence has made all the difference. I am lucky to have such a strong network of friends who have stood by me through thick and thin.

My heartfelt gratitude goes to my family, who have been my constant source of strength and love. To my parents, your unwavering belief in my abilities and your endless support has given me the courage to pursue my dreams. You have sacrificed so much for me, and I cannot thank you enough for your guidance, understanding, and encouragement. To my brother, thank you for always being there, for your words of encouragement, and for believing in me even when I struggled to believe in myself.

Finally, as I reflect on this chapter of my life, I feel an overwhelming sense of gratitude for all the people and experiences that have shaped this thesis. With all my heart, I thank each and every one of you. As I move forward into the next phase of my life, I do so with humility and gratitude, ready to embark on new challenges, knowing that I carry with me the lessons, support, and love from this journey. I will continue to set off, driven by the desire to contribute positively to the world, with all the knowledge and experiences that I have been privileged to receive.

This thesis was submitted to the Senate of Universiti Putra Malaysia and has been accepted as fulfilment of the requirement for the degree of Doctor of Philosophy. The members of the Supervisory Committee were as follows:

Md Zuki bin Abu Bakar @ Zakaria, PhD
Professor
Faculty of Veterinary Medicine
Universiti Putra Malaysia
(Chairman)

Norhaizan binti Mohd Esa, PhD
Professor
Faculty of Medicine and Health Sciences
Universiti Putra Malaysia
(Member)

Ahmad Faizal bin Abdull Razis, PhD
Associate Professor
Faculty of Food Science and Technology
Universiti Putra Malaysia
(Member)

Norsharina binti Ismail, PhD
Senior Research Officer
Institute of Bioscience
Universiti Putra Malaysia
(Member)

Chan Kim Wei, PhD
Senior Research Officer
Institute of Bioscience
Universiti Putra Malaysia
(Member)

ZALILAH MOHD SHARIFF, PhD
Professor and Dean
School of Graduate Studies
Universiti Putra Malaysia

Date: 8 May 2025

TABLE OF CONTENTS

LIST OF TABLES

LIST OF FIGURES

LIST OF ABBREVIATIONS

5-FU	5-fluorouracil
AA	arachidonic acid
ABC	ATP-binding cassette
ADP	adenosine diphosphate
ALP	alanine phosphatase
ALT	alanine aminotransferase
AML	acute myeloid leukemia
AO	acridine orange
ARP3	actin-related protein
AST	aspartate aminotransferase
BC	blank control
BER	base excision repair
BHT	butylhydroxytoluene
CC	colon cancer
CEACAM5	carcinoembryonic antigen cellular adhesion molecule-5
CI	combination index
CIN	chromosomal instability
CPMG	Carr-Purcell-Meiboom-Gill
CRN	colorectal neoplasia
D	dichloromethane
D-2-HG	D-2-hydroxyglutarate
D_2O	Deuterium Oxide
DEPs	differentially expressed proteins

DHFU	5,6-dihydro-5-fluorouracil
DPD	dihydropyrimidine dehydrogenase
DPEP1	dipeptidase-1
DRI	dose-reduction index
dThdPase	thymidine phosphorylase
dUTP	deoxyuridine triphosphate
ELISA	enzyme-linked immunosorbent assay
emPAI	exponentially modified protein abundance index
FBAL	α-fluoro-β-alanine
FDG-PET	fluorodeoxyglucose-positron emission tomography
FDR	false discovery rate
FdUMP	fluorodeoxyuridine monophosphate
FdUTP	fluorodeoxyuridine triphosphate
FUDR	fluorodeoxyuridine
FUMP	fluorouridine monophosphate
FUTP	fluorouridine triphosphate
GAE	gallic acid equivalent
GC-MS	gas chromatography-mass spectrometry
GI	gastrointestinal
GO	Gene Ontology
H	hexane
HDAC	histone deacetylase
HPLC	high-performance liquid chromatography
HSP47	heat shock protein 47
HSV-1	herpes simplex virus type-1

IC_{50}	50% inhibitory concentration
IDH	isocitrate dehydrogenase
KEGG	Kyoto Encyclopedia of Genes and Genomes
L	leave
LC	liquid chromatography
LC_{50}	median lethal concentration
LV	leucovorin
M	methanol
MALDI-MSI	matrix-assisted laser desorption/ionization mass spectrometric imaging
MCM5	minichromosome maintenance 5
MCs	moderately cytotoxic
MRSI	magnetic resonance spectroscopic imaging
MS	mass spectrometry
MVBs	multivesicular bodies
NC	negative control
NCs	non-cytotoxic
NER	nucleotide excision repair
NMR	nuclear magnetic resonance
OPLS-DA	orthogonal partial least squares-discriminant analysis
OPLS-DA	orthogonal partial least squares-discriminant analysis
OPRT	orotate phosphoribosyltransferase
OXPHOS	oxidative phosphorylation
PCA	principal component analysis
PDAC	pancreatic ductal adenocarcinoma

PHGDH	phosphoglycerate dehydrogenase
Phgdh	phosphoglycerate dehydrogenase
PI	propidium iodide
PM	*polygonum minus*
PM-H-A	PM leave hexane extract acetonitrile partition
PM-H-H	PM leave hexane extract hexane partition
PM-H-M	PM leave hexane extract methanol partition
PM-H-W	PM leave hexane extract water partition
PM-L-D	PM leave dichloromethane extract
PM-L-H	PM leave hexane extract
PM-L-M	PM leave methanol extract
PM-L-W	PM leave water extract
PM-S-D	PM stem dichloromethane extract
PM-S-H	PM stem hexane extract
PM-S-M	PM stem methanol extract
PM-S-W	PM stem water extract
PRDX6	peroxiredoxin-6
PRL3	phosphatase of regenerating liver 3
Psat1	proteins phosphoserine aminotransferase 1
ROS	reactive oxygen species
S	stem
SAH	S-adenosyl-L-homocysteine
Shmt2	serine hydroxymethyltransferase 2
TCA	tricarboxylic acid
Tiam1	T lymphoma invasion and metastasis 1

TK	thymidine kinase
TPC	total phenolic content
TS	thymidylate synthase
UK	uridine kinase
UPLC/TOF-MS	ultra-high performance liquid chromatography/time-of-flight mass spectrometry
UrdPase	uridine phosphorylase
VIP	variable importance projection
VSV	vesicular stomatitis virus
VTN	vitronectin
W	water
WCs	weakly cytotoxic

CHAPTER 1

INTRODUCTION

1.1 Background

Cancer is the second leading cause of death worldwide following cardiovascular diseases (Oh et al., 2020). It is estimated that there will be 152,810 cases of cancer and 53,010 deaths from cancer worldwide in 2024 (Siegel et al., 2024). The incidence and mortality of colon cancer (CC) have been rising rapidly worldwide, the third most common cancer and the second leading cause of cancer-related deaths (Shao et al., 2023). Globally, the incidence and mortality rates of CC are rising every year, with more than 2.2 million new cases and 1.1 million deaths expected by 2030 (Liu et al., 2023). According to global cancer statistics, in 2020, there were 1.9 million new cases and 1.8 million deaths attributable to CC, accounting for 9.6% of all cancer incidences and 9.3% of cancer-related deaths (Bray et al., 2024). In Malaysia, CC is the second most frequently diagnosed cancer (Isah Tsamiya et al., 2024; Tamin et al., 2020). It is the most common cancer among men and the second most common among women (Abu Hassan et al., 2016).

Colon cancer, also known as bowel cancer, colorectal cancer, or rectal cancer, is a type of cancer that develops from the colon or rectum (parts of the large intestine) (Krasteva & Georgieva, 2022; Tian et al., 2023). Genetic mutation, unhealthy food habits, or lifestyle factors contribute to CC (Esmeeta et al., 2022). Three major mechanisms are involved in the carcinogenesis of CC: chromosomal instability, CpG island methylator phenotype, and microsatellite instability (Jung et al., 2020). Among environmental

factors, nutritional aspects leading to obesity and energy intake are also risk factors for CC (Song et al., 2020). CC commonly begins as noncancerous polyps on the mucous membrane of the colon or rectum (Alrushaid et al., 2023). These polyps can develop into cancer if not treated early, making early detection and removal crucial. Various types of polyps, including adenomas, have a high potential to become cancerous. CC typically progresses from aberrant crypt foci to early and then advanced adenomas (Mezzapesa et al., 2022).

Colon cancer treatment includes surgery, radiation therapy, and chemotherapy, with these approaches tailored to the stage and characteristics of the cancer (Krasteva & Georgieva, 2022). Surgery, commonly the first line of treatment, is aimed at removing the tumor and the affected sections of the colon or rectum, particularly in the early stages of cancer (Wlodarczyk & Lee, 2022). Radiation therapy is typically used for rectal cancer to shrink the tumor before surgery or eliminate any remaining cells after surgery (Gash et al., 2017). Chemotherapy is essential in treating CC, particularly in advanced stages (Golshani & Zhang, 2020). A cornerstone of chemotherapy for CC is the 5-fluorouracil (5-FU) due to its effectiveness in inhibiting cancer cell growth, improving survival rates, and enhancing the overall efficacy of treatment regimens (Vodenkova et al., 2020). However, its effectiveness comes with a range of associated side effects that can significantly impact patient well-being. Specifically, around 20–30% of patients experience severe toxicity (Knikman et al., 2021), including diarrhea, nausea, vomiting, mucositis, neutropenia, and hand-foot syndrome (Alzahrani et al., 2023; Yan et al., 2024). Severe-related toxicity can be fatal in up to 1% of patients (Knikman et al., 2021). Moreover, 5-FU resistance also limits its use in CC (Gui et al., 2024; Liu et al., 2020a; Yang et al., 2020).

Combination therapy allows targeting simultaneously different pathways involved in cancer, taking advantage of different mechanisms of action in order to reduce the development of tumor drug resistance (Leary et al., 2018). Several studies published in recent years have shown that cancer treatment through a combinatorial approach is much more effective than the use of drugs individually (Kano et al., 2023). Also, chemosensitization by means of phytochemicals, based on the use of a natural compound to increase the activity of a drug through modulation of its resistance pathways, is one of the strategies proposed to overcome chemoresistance, one of the main challenges in CC treatment (Zou et al., 2024), it is necessary for researchers to mathematically assess the nature of these interactions between molecules (Redondo-Blanco et al., 2017). This is often made by using the Chou-Talay combination index (CI), based on the median-effect equation (Redondo-Blanco et al., 2017):

$$(\mathrm{CI})\mathrm{x} = \frac{(\mathrm{D})1}{(\mathrm{Dx})1} + \frac{(\mathrm{D})2}{(\mathrm{Dx})2},$$

where, (Dx)1 is the dose of the drug D1 alone that inhibits the clonogenic capacity of cell by x%, (Dx)2 is the dose of the drug D2 alone that inhibits the clonogenic capacity of cell by x%, (D)1 and (D)2 are the doses of the drugs D1 and D2 in combination that also inhibit the growth of cells by x%. CI shows an additive interaction between two drugs when it is equal to 1, synergism when CI < 1, and antagonism when CI > 1 (Duarte & Vale, 2022).

In recent years, plants have gradually become a new focus of cancer treatment research due to their natural origin, diversity, and relatively low toxicity and side effects (Y. Zhu et al., 2022). These plants contain a variety of bioactives that can inhibit tumor cell growth, invasion, and metastasis through different mechanisms, and can enhance the efficacy of traditional chemotherapy drugs (Yuan et al., 2022). Specifically, some

plants have been demonstrated to increase tumor cell sensitivity to 5-FU through chemosensitization, thereby improving treatment efficacy without increasing drug dosage (Gao et al., 2022; Ng et al., 2022). On the other hand, some plants were reported to mitigate the toxic effects of 5-FU (Fu et al., 2018; Karimi et al., 2019; Pezzani et al., 2019).

Polygonum minus Huds. (PM), also known as *Persicaria minor* (Huds.) Opiz, or "*laksa leaves*" in Malaysia, is an aromatic plant in the Polygonaceae family, widely utilized in the food industry (Z. Yang et al., 2024). Traditionally, PM leaves have been used in various medicinal applications (Hassan et al., 2015). They have been employed to treat digestive disorders (Han et al., 2024), reduce dandruff (Z. Muhammad & Mustafa, 2015), improve eyesight (Jarukamjorn & Nemoto, 2008), warm the body (Embong, 2007), enhance blood circulation (George, Ng, et al., 2014), treat fungal infections (Ong & Nordiana, 1999), alleviate body aches (Amiruddin et al., 2020; Wiart, 2006)), and as a postpartum beverage (Christapher, Xin, et al., 2015). Recent research has highlighted a range of pharmacological activities of PM, including cytoprotective, antibacterial, antifungal, antiulcer, antiviral, antioxidant, anticancer, antitumor, anti-inflammatory, analgesic, and insecticidal effects (Shen et al., 2018; Vikram et al., 2014). Although there have been reports PM extract has the potency to reduce the side effect of chemotherapy agent cisplatin (Abd Rashid et al., 2021), so far, no literature has reported PM extract can enhance the anticancer effects of chemotherapeutic drug 5-FU and reduce its toxic side effects, and the underlying mechanism.

1.2 Problem statement

Given the high frequencies of occurrence and recurrence of CC following treatment, the main problems with the chemotherapeutic drug 5-FU are its side effects, toxicity, and drug resistance. Thus, research on the use of plant extract in cancer treatment, especially combined with chemotherapeutic drugs, is very important. PM extract has been studied as a potential medicinal herb for the treatment of cancers due to its various bioactivities. In addition, there have been reports PM extract has the potency to reduce the side effects of the chemotherapy agent cisplatin. However, no studies to date have specifically examined its ability to enhance the anticancer effects of the chemotherapeutic drug 5-FU while reducing its toxic side effects, nor have they explored the underlying mechanisms.

1.3 Hypotheses

The combination of PM extract and 5-FU exhibits synergistic anticancer effects against CC by enhancing cytotoxicity, inducing apoptosis, and modulating key therapeutic pathways *in vitro*. Furthermore, this combination improves anti-tumor efficacy *in vivo* by inhibiting tumor growth and reducing systemic toxicity in CT26 tumor-bearing BALB/c mice.

1.4 Objectives

1.4.1 General objective

This study aims to evaluate the complementary effects of PM extract in combination with 5-FU against CC *in vitro* and *in vivo*.

1.4.2 Specific objectives

i. To prepare the PM extract and optimize its bioactive compounds via a cytotoxicity assay on the CC CT26 cell line.

ii. To evaluate the anticancer effects of PM extract in combination with 5-FU on the CC CT26 cell line.

iii. To explore the therapeutic mechanisms of the combination of PM extract and 5-FU *in vitro*.

iv. To determine the anti-tumor efficacy of the PM extract in combination with 5-FU on CT26 tumor-bearing BALB/c mice.

CHAPTER 2

LITERATURE REVIEW

2.1 Colon cancer

2.1.1 Epidemiology of colon cancer

Cancer is the second leading cause of death worldwide following cardiovascular diseases (Oh et al., 2020). The incidence and mortality of colon cancer (CC) have been rising rapidly worldwide, the third most common cancer and the second leading cause of cancer-related deaths (Shao et al., 2023). While the prevalence of CC is lower in Asia compared to Western countries, the region has the highest number of cases (CS Wong et al., 2019). In Malaysia, CC is the second most frequently diagnosed cancer, accounting for 13.5% of all new cases from 2012 to 2016 (Isah Tsamiya et al., 2024; Tamin et al., 2020). It is the most common cancer among men and the second most common among women (Abu Hassan et al., 2016). The age-standardized incidence rate of 14.8 per 100,000 for men and 11.1 per 100,000 for women. Additionally, the incidence of CC is highest among the Chinese population, compared to Malays and Indians in Malaysia (Muhamad et al., 2023).

2.1.2 Causes of colon cancer

Numerous risk factors are associated with the development of CC (Esmeeta et al., 2022). Genetic mutations, such as the activation of proto-oncogenes into oncogenes, have been linked to CC (Baidoun et al., 2020). Age is another significant factor, with individuals over 50 being particularly vulnerable (Hofseth et al., 2020). Dietary factors

also contribute, especially diets low in fiber and high in animal protein and fat, along with excessive alcohol intake, smoking, and the consumption of processed foods (Zargar et al., 2021). Excessive alcohol leads to the accumulation of acetaldehyde, which damages DNA, while smoking induces oxidative stress that can result in DNA damage and uncontrolled cell growth. Processed foods, which metabolize into N-nitroso compounds, also pose a risk by damaging DNA and increasing CC susceptibility (Esmeeta et al., 2022). Additionally, a sedentary lifestyle, lack of physical activity, and obesity are associated with higher CC incidence (Friedenreich et al., 2021). A personal history of colorectal polyps or inherited syndromes, such as familial adenomatous polyposis, hereditary nonpolyposis CC, and Lynch syndrome, further elevates the risk (Kastrinos et al., 2020). Other contributing factors include type-II diabetes and inflammatory bowel diseases, such as ulcerative colitis and Crohn's disease (J. Kim et al., 2020). Figure 2.1 illustrates these potential causes and risk factors.

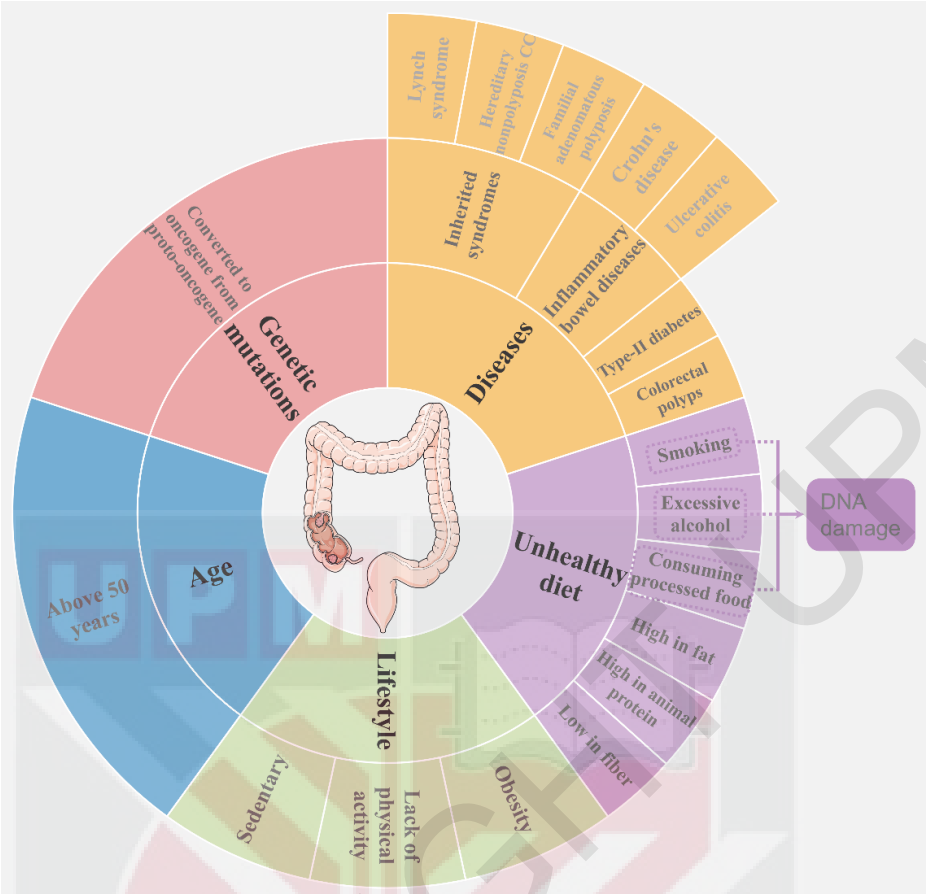

Figure 2.1: Risk factors for colon cancer.

2.1.3 Pathophysiology of colon cancer

Colon cancer often begins as noncancerous polyps on the mucous membrane of the colon or rectum (Alrushaid et al., 2023). Without early detection and treatment, these polyps can progress into cancer, highlighting the importance of timely intervention. Certain types of polyps, such as adenomas, have a higher likelihood of becoming cancerous. The progression of CC typically follows a sequence from aberrant crypt foci to early-stage adenomas, eventually advancing to more severe forms (Mezzapesa et al., 2022). Colonoscopy is the primary method for detecting these abnormalities, successfully identifying approximately 90% of polyps. However, some polyps may resemble normal tissue, making them harder to detect visually, though their molecular characteristics can reveal their cancerous potential. Other effective screening methods

include sigmoidoscopy, fecal occult blood tests, and fecal immunochemical tests (Randel et al., 2021).

2.1.4 Developmental stages of colon cancer

The development of CC is categorized into stages using the TNM system, initially developed by the Union for International Cancer Control and later adopted by the American Joint Committee on Cancer (Alrushaid et al., 2023). This system assesses the primary tumor (T), including its size, growth, and the layers it has invaded, as illustrated in Figure 2.2. In stage 1, the tumor extends to the submucosa without lymph node involvement (Ebbehøj et al., 2021). Stage 2 is subdivided into three sub-stages: stage 2A, where the tumor reaches the outer layers of the colon or rectum but does not penetrate them; stage 2B, where it involves the visceral peritoneum; and stage 2C, where the cancer invades nearby organs or structures (D. Xie et al., 2021). Stage 3 is also divided into three sub-stages: stage 3A, where the tumor spreads to nearby lymph nodes; stage 3B, where it affects up to four lymph nodes; and stage 3C, where it extends beyond the muscular layers and involves four or more lymph nodes (Moon et al., 2022). The final stage, stage 4, is subdivided into stage 4A, where the tumor has metastasized to one distant site (e.g., liver, lungs, or distant lymph nodes); stage 4B, where it has spread to two or more distant sites; and stage 4C, indicating cancer spread throughout the peritoneum (Alrushaid et al., 2023).

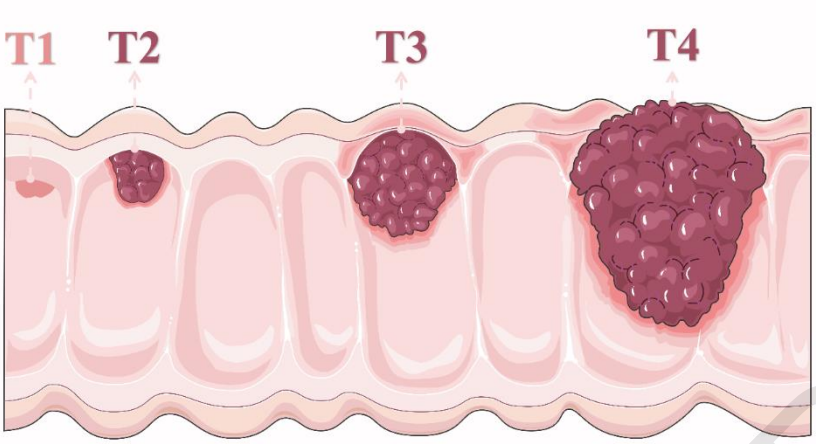

Figure 2.2: **Illustration of the growth of a tumor through the mucosa layer of the colon or rectum, and different colon cancer stages based (T1, T2, T3, and T4) on the TNM system**.

2.1.5 Treatments for colon cancer

Colon cancer treatment typically involves surgery, radiation therapy, and chemotherapy, with the approach tailored to the cancer's stage and characteristics (as shown in Figure 2.3) (Krasteva & Georgieva, 2022). Surgery, often the first line of treatment, aims to remove the tumor along with affected sections of the colon or rectum, particularly in early-stage cancer (Wlodarczyk & Lee, 2022). The extent of colon resection depends on tumor location and severity; in partial colectomy, only the cancerous portion and a margin of healthy tissue are removed, whereas in total colectomy, the entire colon is excised, typically in cases of widespread disease or inherited conditions like familial adenomatous polyposis. In rectal cancer, a proctectomy may be performed, sometimes requiring a permanent colostomy if the anus cannot be preserved (Wlodarczyk & Lee, 2022). Radiation therapy is primarily used in rectal cancer to shrink the tumor before surgery or to eliminate remaining cancer cells afterward (Gash et al., 2017). Chemotherapy plays a crucial role in CC treatment across all stages. In the early stages, it helps reduce tumor size before surgery (neoadjuvant therapy) and eliminate residual cells afterward (adjuvant therapy)

(O'Reilly et al., 2023). This dual approach reduces the risk of recurrence and improves overall treatment outcomes. In metastatic cases, chemotherapy is essential for controlling cancer growth, relieving symptoms, and extending survival (B. Huang et al., 2015).

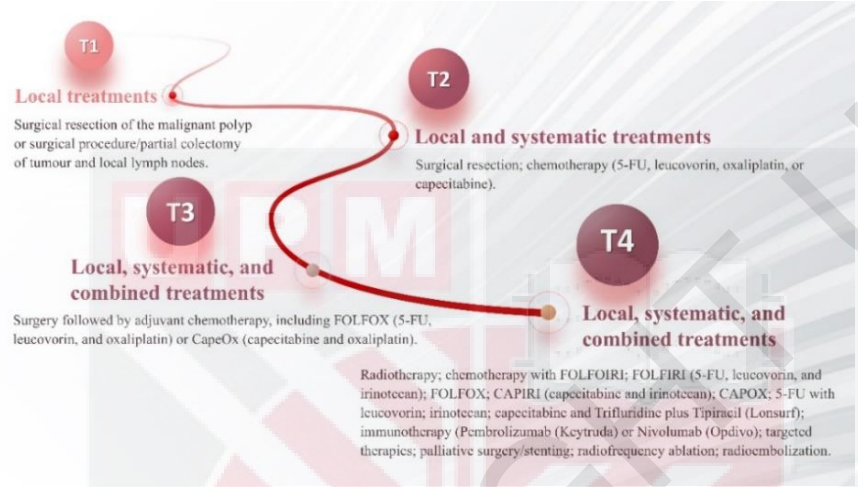

Figure 2.3: Treatments for each stage of colon cancer.

Chemotherapy is crucial in treating CC at all stages, especially advanced stages, as it targets cancer cells that surgery may not remove (McQuade et al., 2017). Several chemotherapy drugs are used in standard treatment protocols, including oxaliplatin, irinotecan, and capecitabine, often in combination regimens such as FOLFOX (5-fluorouracil (5-FU), leucovorin, and oxaliplatin) and FOLFIRI (5-FU, leucovorin, and irinotecan). These combinations improve treatment efficacy by targeting multiple pathways involved in cancer progression (Vodenkova et al., 2020). Among these agents, 5-fluorouracil (5-FU) remains a cornerstone of CC chemotherapy due to its proven effectiveness in inhibiting cancer cell growth and improving survival rates (Sethy & Kundu, 2021). The recommended dosage of 5-FU in human treatment varies depending on the regimen. In the FOLFOX and FOLFIRI protocols, 5-FU is typically administered at a bolus dose of 400 mg/m^2 intravenously (IV) on day 1, followed by a

continuous infusion of 2400 – 3000 mg/m^2 over 46 – 48 hours every two weeks. Additionally, oral 5-FU is administered at 1000 – 1250 mg/m^2 twice daily for 14 days in a 21-day cycle (Karthika et al., 2021). The focus on 5-FU in this study is justified by its widespread clinical use, well-characterized mechanisms of action, and ongoing challenges related to resistance and toxicity. By investigating strategies to enhance 5-FU's efficacy and reduce its side effects, this study aims to improve its therapeutic potential, thereby addressing a critical need in CC treatment.

2.2 5-Fluorouracil

2.2.1 Metabolism of 5-fluorouracil

2.2.1.1 5-Fluorouracil anabolism

5-FU is a chemotherapeutic agent resembling uracil but with a fluorine atom at the C-5 position, facilitating its cellular entry using uracil transport mechanisms (Leelakanok et al., 2018). Once inside the cell, 5-FU is metabolized into active compounds that disrupt RNA and DNA functions, leading to cell death (Sethy & Kundu, 2021). The primary active metabolites include fluorouridine triphosphate (FUTP), which integrates into RNA, causing processing alterations, and fluorodeoxyuridine triphosphate (FdUTP) along with fluorodeoxyuridine monophosphate (FdUMP), which incorporates into DNA, causing damage and inhibiting thymidylate synthase (TS) (Chalabi-Dchar et al., 2021). 5-FU activation involves its conversion to fluorouridine monophosphate (FUMP) via orotate phosphoribosyltransferase (OPRT) or indirectly through uridine phosphorylase (UrdPase) and uridine kinase (UK) (Hruba et al., 2023). Another pathway includes conversion by thymidine phosphorylase (dThdPase) to fluorodeoxyuridine (FUDR), which thymidine kinase (TK) then

phosphorylates to FdUMP (Ghafouri-Fard et al., 2021). This metabolic complexity ensures that FUTP, FdUTP, and FdUMP inflict substantial damage on cellular RNA and DNA.

Additionally, the conversion of 5-FU in the gastrointestinal (GI) tract and bone marrow can lead to significant toxicities, such as GI toxicity and myelotoxicity, primarily due to the incorporation of FdUMP into DNA (Gmeiner, 2020b). Studies have demonstrated that GI toxicity is associated with fluorinated pyrimidines, while myelotoxicity is closely linked to the incorporation of 5-FU into DNA (Derissen & Beijnen, 2020). Notably, a meta-analysis of clinical trials indicated that patients receiving bolus 5-FU infusions experienced higher grades of hematologic toxicity compared to those receiving continuous infusions (Lan et al., 2023).

2.2.1.2 5-Fluorouracil catabolism

Dihydropyrimidine dehydrogenase (DPD) is an enzyme found in the liver, intestinal mucosa, and other tissues that catabolizes 5-FU into 5,6-dihydro-5-fluorouracil (DHFU), eventually producing α-fluoro-β-ureido-propionic acid and α-fluoro-β-alanine (FBAL) (Danesh Pouya et al., 2022). A study by Imamaki et al. (2024) showed that 60-90% of administered 5-FU is excreted as FBAL within 24 hours (Imamaki et al., 2024). While most patients tolerate 5-FU, those with DPD deficiency face severe toxicities, including diarrhea, mucositis, neurotoxicity, and potentially death (García-Alfonso et al., 2021). FBAL neurotoxicity has been extensively studied since the 1970s (Koenig & Patel, 1970). Experiments on cats revealed that continuous administration of FBAL into the brain ventricle caused neuropathological changes like vacuoles and necrosis, which were more severe than those caused by monofluoroacetic acid and

similar to changes seen in patients treated with oral 5-FU (Okeda et al., 1990). Additionally, FBAL is linked to cardiotoxicity (Deac et al., 2020). The incidence of fluoropyrimidine cardiotoxicity is relatively rare but significant. The most common clinical manifestation is coronary vasospasm, which can lead to angina, myocardial infarction, and even sudden cardiac death (Deac et al., 2020). Other reported cardiac events include heart failure, arrhythmias, pericarditis, coronary dissection, QT prolongation, and sudden cardiac death (Kanduri et al., 2019).

2.2.1.3 Ternary complex

FdUMP forms a stable ternary complex with TS and CH2THF, inhibiting TS and blocking dUMP from accessing the TS nucleotide-binding site (Ma et al., 2022). This inhibition causes deoxynucleotide pool imbalances, particularly increasing deoxyuridine triphosphate (dUTP) levels, leading to DNA damage. The depletion of dTMP results in reduced dTTP levels, disrupting DNA synthesis and repair (Derissen & Beijnen, 2020; Mullen & Singh, 2023). Despite TS inhibition causing dUMP accumulation and increased dUTP, thymidylate can be salvaged from thymidine via TK, which may confer resistance to 5-FU (Backer et al., 2023; Walter & Herr, 2022). The molecular mechanisms downstream of TS inhibition by 5-FU remain unclear, and the clinical significance of TS has not been definitively proven. A review by Showalter et al. (2008) found no clear link between TS expression and patient response to 5-FU, suggesting that factors like administration routes, types of 5-FU drugs, and leucovorin (LV) effects may influence 5-FU metabolism and efficacy.

2.2.2 Anti-colon cancer mechanism of 5-fluorouracil

5-FU stands as a cornerstone in CC treatment, leveraging multiple mechanisms to impede cancer cell proliferation. As a fluorinated pyrimidine analog, 5-FU undergoes intracellular activation, yielding active metabolites such as FdUMP and FUTP (Gmeiner, 2020a). FdUMP exerts pivotal action by forming a stable ternary complex with TS and 5,10-methylene tetrahydrofolate (CH_2THF), inhibiting TS and disrupting de novo thymidine nucleotide synthesis required for DNA replication (Masci et al., 2023). This disruption induces a nucleotide pool imbalance, notably elevating dUTP levels, which incorporate into DNA instead of thymidine, impairing DNA synthesis and prompting cellular apoptosis (Z. H. Wang et al., 2024). Moreover, FUTP incorporates into RNA, altering RNA metabolism and protein synthesis critical for tumor cell viability (Therizols et al., 2022). This dual interference with DNA and RNA synthesis pathways underpins 5-FU potent cytotoxicity against rapidly dividing CC cells as shown in Figure 2.4.

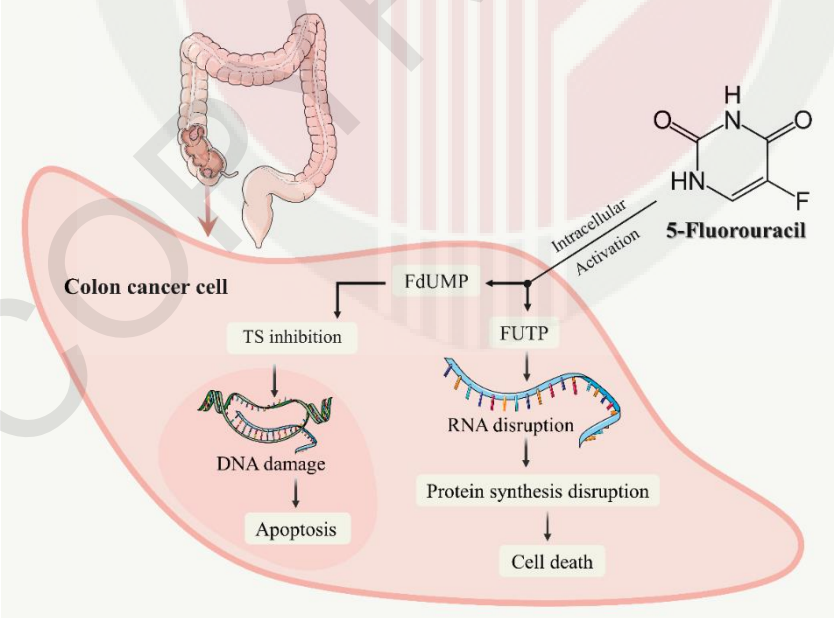

Figure 2.4: Mechanisms of 5-fluorouracil against colon cancer.

2.2.3 Side effects of 5-fluorouracil

5-FU is a widely used chemotherapeutic agent known for its efficacy in treating various cancers, including colorectal, breast, gastric, pancreatic, and skin cancers (Tian et al., 2021; Vodenkova et al., 2020). However, its use is associated with a range of side effects (shown in Figure 2.5), the severity of which can vary depending on dosage, route of administration, and individual patient factors (Gmeiner, 2021; Zafar et al., 2021). Acute side effects, such as nausea, vomiting, and neutropenia, can occur after a single dose, while cumulative toxicity, including cardiotoxicity and neurotoxicity, is more commonly observed after multiple cycles of treatment (Zafar et al., 2021).

Additionally, higher doses or prolonged continuous infusion of 5-FU increase the likelihood of severe adverse effects, such as mucositis and hand-foot syndrome (Gmeiner, 2021). Understanding these dose-dependent toxicities is critical for optimizing treatment regimens and minimizing patient discomfort.

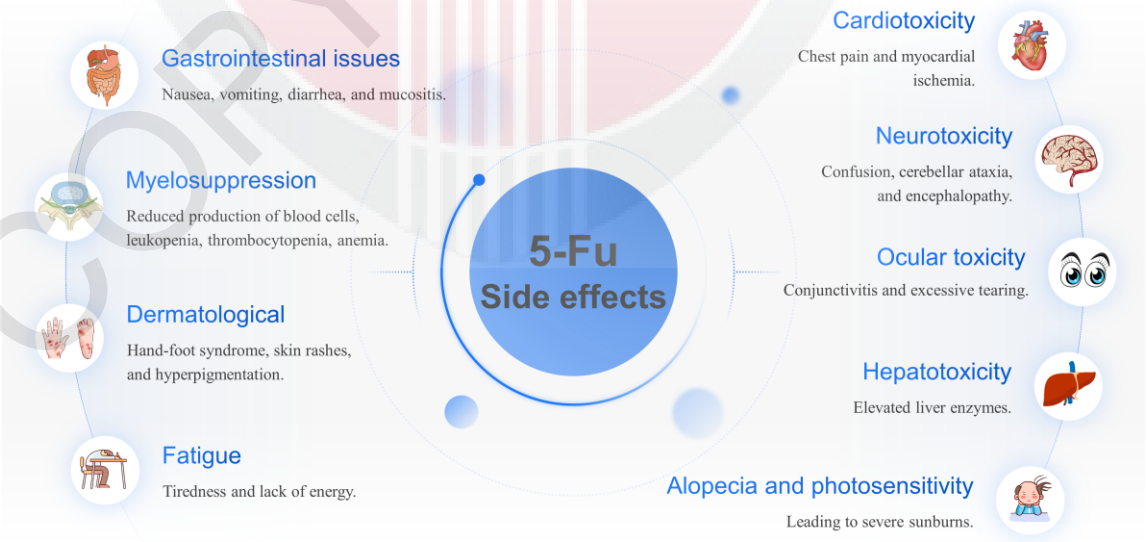

Figure 2.5: Side effects of 5-fluorouracil.

Gastrointestinal issues are frequent with 5-FU treatment, including nausea, vomiting, diarrhea, and mucositis (inflammation and ulceration of the oral and gastrointestinal mucosa) (Mohammed et al., 2023). These symptoms can usually be managed with antiemetic and antidiarrheal medications, along with maintaining hydration and using symptomatic treatments for mucositis (Garutti et al., 2023). Another common side effect is myelosuppression, which results in decreased blood cell production, leading to leukopenia (a decrease in white blood cells), thrombocytopenia (a decrease in platelets), and anemia (a decrease in red blood cells) (Ishibashi et al., 2021). These conditions increase the risk of infection, bleeding, and fatigue, respectively, necessitating regular blood tests to monitor and manage these effects. 5-FU also frequently causes dermatological effects (Ewert de Oliveira et al., 2021). 5-FU-induced hand-foot syndrome is characterized by redness, swelling, pain, and peeling of the skin on the palms and soles, which can be particularly distressing (Punt et al., 2023). In addition, rash and hyperpigmentation are observed, and patients are advised to protect their skin from sunlight. Fatigue, a general feeling of tiredness and lack of energy, is another frequently reported side effect (Parment et al., 2022).

Moreover, 5-FU can cause serious side effects such as cardiotoxicity and neurological effects (More et al., 2021). Cardiotoxicity manifests as chest pain and myocardial ischemia caused by coronary artery spasms, with the risk of severe heart problems, especially in patients with pre-existing heart disease (Jurczyk et al., 2021). Neurological effects, including neurotoxicity, lead to confusion, cerebellar ataxia (uncoordinated movements), and encephalopathy (Cordier et al., 2011). Although these symptoms are typically reversible upon discontinuation of the drug, careful monitoring is still required. Other potential side effects include ocular toxicity (manifested by conjunctivitis and excessive tearing) and hepatotoxicity (manifested by

elevated liver enzymes) (Güçlü et al., 2018). Rarely, patients may experience alopecia (hair loss) and photosensitivity, leading to severe sunburns (Reyes-Habito & Roh, 2014). Management of these side effects generally requires dose adjustments, supportive care with medications such as antiemetics and analgesics, and regular monitoring of liver and kidney functions (Anaka & Abdel-Rahman, 2022; Hashimoto et al., 2020; Smith et al., 2020).

2.2.4 Molecular mechanisms of drug resistance for 5-fluorouracil

Although 5-FU is effective, drug resistance can significantly limit its therapeutic benefits over time. Several mechanisms contribute to the development of 5-FU resistance. One of the primary mechanisms of resistance involves alterations in enzymes involved in 5-FU metabolism (Blondy et al., 2020). Within cells, 5-FU is converted into active metabolites that inhibit thymidylate synthase (TS), a crucial enzyme for DNA synthesis (A. Kumar et al., 2023). Resistance develops when TS is mutated or overexpressed, thereby reducing the effectiveness of 5-FU inhibition (Negrei et al., 2016). Additionally, alterations in other enzymes in the metabolic pathway, such as dihydropyrimidine dehydrogenase (DPD) responsible for the breakdown of 5-FU, can lead to reduced intracellular levels of the active drug, thus promoting drug resistance (Verma et al., 2022). Another significant mechanism is the enhancement of DNA repair mechanisms in cancer cells (Sethy & Kundu, 2021). 5-FU exerts cytotoxic effects by incorporating into DNA and RNA, causing DNA damage and ultimately cell death (Blondy et al., 2020). However, cancer cells develop drug resistance by upregulating DNA repair pathways, such as nucleotide excision repair (NER) and base excision repair (BER), which effectively repair the damage caused by 5-FU, thereby reducing its cytotoxic effects (Gomes et al., 2017).

Moreover, alterations in cellular signaling pathways contribute to 5-FU resistance (Sethy & Kundu, 2021). Activation of survival pathways, such as the PI3K/AKT pathway or the MAPK pathway, promotes cell survival and proliferation despite exposure to 5-FU-induced stress (Azwar et al., 2021). These pathways enhance cell survival, allowing cancer cells to escape the cytotoxic effects of 5-FU. Furthermore, changes in drug transport mechanisms can influence 5-FU resistance (Blondy et al., 2020). Efflux pumps, such as ATP-binding cassette (ABC) transporters, actively pump 5-FU out of cancer cells, thereby reducing its intracellular concentration and effectiveness (Cui et al., 2015). Overexpression of these transporters, such as P-glycoprotein (P-gp), can confer resistance to 5-FU by preventing the accumulation of 5-FU within cancer cells (Asif et al., 2020).

2.3 Combination therapy

Combination therapy enhances cancer treatment by targeting multiple pathways simultaneously, improving efficacy, and reducing drug resistance (Redondo-Blanco et al., 2017). In CC, combination strategies are particularly relevant due to the complex molecular mechanisms involved in tumor initiation and progression, such as chromosomal instability (CIN), DNA mismatch repair deficiencies, and aberrant signaling pathways (Amiri et al., 2013; Singh et al., 2013).

The effectiveness of combination therapy is typically assessed using the Chou-Talalay combination index (CI), based on the median-effect equation: $CI = a/A + b/B$ (Chou & Talalay, 1984). In this formula, A and B represent the doses of drugs A and B, respectively, needed to achieve a specified effect when used individually, while a and b represent the doses required to produce the same effect in combination. A CI value

of 1 indicates an additive effect, CI < 1 signifies synergism, and CI > 1 indicates antagonism between the two drugs (Tallarida, 2002). This approach is widely used in chemotherapy optimization, including natural compound-based chemosensitization, which enhances drug efficacy by modulating resistance pathways (Amiri et al., 2013). Natural compounds, particularly plant extracts, have gained attention in cancer therapy due to their bioactive components, low toxicity, and ability to enhance conventional chemotherapy (Y. Zhu et al., 2022). Several studies have demonstrated that certain plant extracts improve tumor cell sensitivity to 5-FU, reducing the required dosage and minimizing side effects (Gao et al., 2022; Ng et al., 2022). This study evaluates the synergistic effects of PM extract and 5-FU, assessing their combined anticancer activity using *in vitro* and *in vivo* models to explore potential mechanisms of action and clinical applicability.

2.4 *Polygonum minus*

Polygonum minus Huds. (PM), also known as *Persicaria minor* (Huds.) Opiz, or "laksa leaves" in Malaysia, is an aromatic plant in the Polygonaceae family, widely utilized in the food industry (Christapher, Parasuraman, et al., 2015; Z. Yang et al., 2024). In Japan, China, and Europe, PM has long been used as a hot-tasting spice (Ahmad et al., 2014). In Malaysia, it is frequently added to vegetable salads and various dishes, such as laksa (spicy noodle dish), kerabu (fried herbal rice), asam pedas (spicy tamarind curry), and tom yam (spicy tangy soup) (Abdullah et al., 2017; Rahim et al., 2022; Vimala et al., 2003). The Malaysian Government has included PM in the National Agro-Food Policy to ensure an adequate food supply (Embong, 2007). In Indonesia, particularly in West Kalimantan, PM is a key ingredient in padas porridge, a unique local dish (Alves et al. 2001; Phatik, Das & Boruah 2014). Additionally, PM

is valued for its wide range of ethnobotanical uses due to its diverse therapeutic properties.

Traditionally, PM leaves have been used in various medicinal applications (Hassan et al., 2015). They have been employed to treat digestive disorders (Han et al., 2024), reduce dandruff (Z. Muhammad & Mustafa, 2015), improve eyesight (Jarukamjorn & Nemoto, 2008), warm the body (Embong, 2007), enhance blood circulation (George, Ng, et al., 2014), treat fungal infections (Ong & Nordiana, 1999), alleviate body aches (Amiruddin et al., 2020; Wiart, 2006)), and as a postpartum beverage (Christapher, Xin, et al., 2015). In India, PM has been used as diuretics, central nervous system stimulants, diaphoretics, and styptics (Ahmad et al., 2016). Additionally, many Chinese Buddhists consume PM leaves to reduce sexual desire, leading monks to cultivate PM in their gardens as part of their celibate lifestyle (Abubakar et al., 2015).

2.4.1 Safety of *polygonum minus*

A primary concern regarding the toxicity of herbal remedies is their potential to cause adverse effects or even lethality when consumed (Azad et al., 2022). Herbal plants are distinguished by their secondary metabolites, which serve as natural defense mechanisms and can offer substantial therapeutic benefits. However, these compounds may also be harmful if consumed in excessive amounts (van Wyk & Prinsloo, 2020). Thus, assessing the toxicity of medicinal plants is crucial for their safe application in medicine and pharmacology (Pham et al., 2023).

2.4.1.1 Acute toxicity

An acute toxicity study assesses the potential harmful effects of a test substance when

organisms are exposed to single or multiple doses over a 24-hour period, through various routes such as oral, dermal, or inhalation (Saganuwan, 2017). The data from these studies are crucial for establishing safe dosage levels in long-term toxicity studies and other animal research (Erhirhie et al., 2018).

Although PM has well-established traditional uses in folk medicine and is generally regarded as safe, it is important to evaluate its safety. Acute toxicity tests of PM aqueous leaf extract show promising results. During a 14-day observation period, no adverse effects were observed in experimental animals. Specifically, oral administration of 2000 mg/kg of the PM aqueous extract did not result in mortality, behavioral changes, or alterations in physiological functions (Ming et al., 2013; N. Muhammad et al., 2013). Even at the highest dose of 5000 mg/kg body weight (bw), no toxicity was observed, as liver and kidney examinations in treated rats showed no significant changes compared to the control group. Hematological and clinical biochemistry values were consistent with those of control animals, indicating that the PM aqueous leaf extract is relatively non-toxic (Wasman et al., 2010). Additionally, a study on the methanol extract of PM at 2000 mg/kg also showed no signs of acute toxicity, suggesting an LD_{50} greater than 2000 mg/kg (Christapher et al., 2017). According to Sharma et al. (2020), all test animals remained healthy and displayed normal behavior throughout the study, supporting the safety of this herb. Therefore, PM holds potential for development into medications addressing contemporary health issues (Table 2.1).

2.4.1.2 Sub-acute toxicity

Sub-acute toxicity studies are crucial for evaluating the safety of a substance when it

is administered repeatedly over an extended period (Christapher et al., 2017). These studies help identify any long-term adverse effects resulting from continuous daily exposure (Nakakaawa et al., 2023).

In a 28-day sub-acute oral toxicity study, no mortality or toxic signs were observed with oral administration of PM aqueous extract at doses of 125, 500, and 1000 mg/kg (Ming et al., 2013). Similarly, a study conducted by Muhammad and colleagues found no evidence of toxicity, behavioral changes, or fatalities at these doses. However, at a higher dose of 2000 mg/kg body weight for 14 days, the study reported significant reductions in hemoglobin, calcium, and sodium levels, alongside elevated potassium levels. This indicates that while PM leaf extract generally does not cause sub-acute toxicity in male rats, extremely high doses may lead to electrolyte imbalances, anemia, and hypocalcemia (N. Muhammad et al., 2013). Furthermore, research by Christapher et al. (2017) showed that the methanol extract of PM leaves did not exhibit neurotoxicity, with no observed changes in locomotor activity or mental function in treated animals. The chronic administration of PM methanol extracts up to 2000 mg/kg also did not result in any mortality (Table 2.1).

Table 2.1: *Polygonum minus*-induced toxic effects.

Category	Plant part	Solvent used in extraction	Animal Model	Highest dose	Results	Reference
Acute toxicity	Leaf	Water	Rats	5000 mg/kg bw	Non-toxic	(Wasman et al., 2010)
	Stem and leaf	Water		2000 mg/kg bw		(Ming et al., 2013)
	Leaf	Water		2000 mg/kg bw		(N. Muhammad et al., 2013)
	Leaf	Methanol		2000 mg/kg bw		(Christapher et al., 2017)
Sub-acute toxicity	Stem and leaf	Water	Rats	1000 mg/kg bw	Non-toxic	(Ming et al., 2013)
	Leaf	Water	Rats	2000 mg/kg bw	Large dose whereby it may lead to electrolyte imbalance, anemia, and hypocalcemia	(N. Muhammad et al., 2013)
	Leaf	Methanol	Rats	2000 mg/kg bw	Non-toxic	(Christapher et al., 2017)
Genotoxicity	Leaf	Water	Human lymphocytes	\	No genotoxic	(Wan-Ibrahim et al., 2010)
	Stem and leaf	Methanol	Zebrafish	\	No teratogenic	(Omar et al., 2020)

To date, sub-chronic and chronic toxicological studies on various parts and solvent extracts of PM have not been conducted. Therefore, a comprehensive toxicological assessment is necessary to establish the safety of PM extracts before considering them as safe herbal drugs.

2.4.1.3 Genotoxicity

Research has indicated that certain plants commonly used in folk medicine may have genotoxic potential (Ananthi et al., 2010; Marques et al., 2003; Melo-Reis et al., 2011; Regner et al., 2011; Shin et al., 2011). However, Wan-Ibrahim et al. (2010) demonstrated that the aqueous extract of PM does not exhibit genotoxic effects on human lymphocytes. Additionally, Omar and colleagues assessed the teratogenic potential of PM using a zebrafish model and found that the methanol extract of PM did not disrupt zebrafish embryonic development (Table 2.1) (Omar et al., 2020).

2.4.2 Pharmacological effects of *polygonum minus*

2.4.2.1 Pre-clinical studies Antioxidant capacity

Several studies have documented the antioxidant activity of PM using assays such as DPPH radical scavenging, TBARS, and FRAP. The observed antioxidant effects are attributed to the high levels of polyphenols, vitamin C, and β-carotene present in PM (Baharum et al., 2010; Hamidi et al., 1996). Extracts of PM, including those obtained with aqueous, methanol, and ethanol solvents, have demonstrated significant antioxidant potential, comparable to synthetic antioxidants like butylhydroxytoluene (BHT) and gallic acid (Azlim Almey et al., 2010; Faujan et al., 2007; Gorinstein et al., 2007; Huda-Faujan et al., 2009; Qader et al., 2011; Sumazian et al., 2010). Specifically,

the total phenolic content (TPC) in the methanol and ethanol extracts of PM leaves was reported as 31.38 mg and 21.06 mg Gallic Acid Equivalent (GAE) per gram of extract, respectively. The aqueous leaf extract of PM showed notable antioxidant properties with a high TPC of 2800.6 mg/100 g GAE (Vimala et al., 2011). Additionally, the TPC for the aqueous, methanol, and ethanol extracts of the whole PM plant were reported as 55.5 mg, 122.1 mg, and 207 mg GAE per gram, respectively (Qader et al., 2011; Saputri & Jantan, 2011). The total ascorbic acid content was measured at 0.54 mg/g fresh weight, and the flavonoid content was 2.46 mg/g dry weight (Sumazian et al., 2010).

2.4.2.2 Role in LDL oxidation

Saputri and Jantan reported that PM exhibits inhibitory effects on LDL oxidation induced by collagen (Saputri & Jantan, 2011). The study measured the LDL oxidation activity of various concentrations of methanol extract of PM in relation to copper-mediated oxidation in isolated human LDL. The results demonstrated that the inhibition of LDL oxidation was dose-dependent, with higher concentrations of the extract leading to greater inhibition (Saputri & Jantan, 2011). This study highlights a correlation between high phenolic content in PM and its effectiveness in inhibiting LDL oxidation.

2.4.2.3 Anti-platelet aggregation activity

Saputri and Jantan investigated the inhibitory effects of PM's methanol extract on human platelet aggregation (Saputri & Jantan, 2011). The study assessed the extract's efficacy against several platelet aggregation inducers, including arachidonic acid (AA),

adenosine diphosphate (ADP), and collagen. The results indicated that the extract was only moderately effective against AA and ADP-induced platelet aggregation, with inhibition percentages of 25.6 ± 0.8 and 24.0 ± 2.1, respectively (Saputri & Jantan, 2011).

2.4.2.4 Gastro-protective activity

The aqueous extract of the entire PM plant was evaluated for its ulcer-preventive properties using an ethanol-induced ulcer model (Wasman et al., 2010). The study found that pretreatment with PM significantly reduced ulcerated areas in rats, with the effect being dose-dependent. Notably, the extract at a dose of 250 mg/kg was as effective as omeprazole at 20 mg/kg. The gastroprotective effect of the bioactive fraction (EA= 1:1) of PM leaves may be attributed to changes in mucus production, hexosamine levels, and PGE2 synthesis in rodent (Qader et al., 2012). Christapher et al. also investigated the antiulcer effects of methanol and aqueous extracts of PM leaves using a pyloric ligation model. The methanol extract exhibited significant gastroprotective (antiulcer) effects at a dose of 200 mg/kg BW, while the aqueous extract did not show any gastroprotective effects in Wistar rats (Christapher, Xin, et al., 2015).

2.4.2.5 Antimicrobial activity

Plant extracts were evaluated for their antimicrobial properties against various bacteria, viruses, and fungi. The antibacterial activity was primarily assessed against Helicobacter pylori, a bacterium associated with duodenal ulcers. It was found that petroleum ether, methanol, and chloroform extracts of PM exhibited significant inhibition zones against Helicobacter pylori, whereas the aqueous extract did not show

any inhibition (Uyub et al., 2010). Musa et al. reported that PM demonstrated antibacterial activity against ten isolated pathogenic bacteria from fish (Lee et al., 2008). Additionally, PM was slightly more effective than the control in inhibiting microbial growth in refrigerated duck meatballs. The antiviral activity of PM's ethanol extract was tested against Herpes simplex virus type-1 (HSV-1) and Vesicular stomatitis virus (VSV). The extract showed strong antiviral activity against HSV-1 but weak activity against VSV (Hamidi et al., 1996).

Johnny et al. investigated the antifungal properties of 15 Malaysian plants, including PM, against Colletotrichum gloeosporioides isolated from mangoes. The study used various solvents for extraction, and the methanol extract of PM was found to be more effective in inhibiting fungal growth compared to chloroform and acetone extracts (Johnny et al., 2011). Traditionally, PM is combined with a small amount of kerosene and applied topically as a paste to treat fungal infections (Ong & Nordiana, 1999).

2.4.2.6 Digestive enhancing activity

Vimala et al. identified oxalic acid in PM using High-Performance Liquid Chromatography (HPLC) at a concentration of 200 nm. Given that oxalic acid is known to aid digestion, this finding supports the traditional use of kesum as a stimulant for the digestive system (Eastwood & Nyhlin, 1995; Vimala et al., 2011).

2.4.2.7 Immunomodulatory effect

George et al. (2014) investigated the immunomodulatory effects of the aqueous extract of PM on Swiss albino mice using an *in vivo* carbon clearance assay. The phagocytic

effect refers to the ability of immune cells, particularly macrophages and neutrophils, to engulf and eliminate pathogens, cellular debris, and foreign particles, playing a crucial role in innate immunity. Their findings indicated a dose-dependent increase in the phagocytic index, with doses of 200 and 400 mg/kg demonstrating enhanced phagocytic activity. Notably, the phagocytic index at 400 mg/kg was comparable to that of the standard drug Levamisole (2.5 mg/kg body weight), suggesting a significant immunostimulatory effect.

2.4.2.8 Cytotoxicity

The PM leaf extracts, including 50%, 70%, and 100% ethanol extracts, exhibited significant suppression of cell viability in colon cancer (HCT116, HT29, and CT26) cell lines. The 100% ethanol extract also demonstrated antiproliferative activity against cervical cancer (HeLa) cells (Ali et al., 1996; Rohin et al., 2020). Conversely, the acetone extract from PM leaves showed no toxicity towards colon cancer (HCT116, HT29, and CT26) cell lines, suggesting that the efficacy of the extracts may be influenced by the choice of extraction solvent. Additionally, the ethyl acetate extract of PM leaves exhibited potent cytotoxicity against colon cancer (HCT116, HT29, CT26), cervical cancer (HeLa), and liver cancer (HepG2) cells (Abdullah et al., 2017; Mohd Ghazali et al., 2014; Rohin et al., 2020). While the ethyl acetate extract showed cytotoxicity against breast cancer (MCF7) cells, the IC_{50} was >250 µg/mL (Mohd Ghazali et al., 2014). The hexane extract from PM leaves demonstrated promising cytotoxicity against colon cancer (HCT116) cells, with an IC_{50} value of 40 µg/mL (Abdullah et al., 2017). Another study found that the methanol extract of PM leaves had antiproliferative effects on colon cancer (HCT116, HT29, CT26) and cervical cancer (HeLa) cells and exhibited cytotoxicity towards liver cancer (HepG2) and

breast cancer (MCF7) cells, though the IC_{50} was >250 µg/mL (Christapher et al., 2016; Mohd Ghazali et al., 2014; Rohin et al., 2020). The petroleum ether extract also suppressed growth in colon cancer (HCT116), cervical cancer (HeLa), liver cancer (HepG2), and breast cancer (MCF7) cells (Mohd Ghazali et al., 2014). Furthermore, *in vitro* studies indicated that the water extract of PM leaves had antiproliferative effects against a range of cancer cells, including colon cancer (HCT116, HT29, CT26), cervical cancer (HeLa), liver cancer (HepG2), and breast cancer (MCF7) cells (Christapher et al., 2016; Mohd Ghazali et al., 2014; Rohin et al., 2020).

For normal cells, the water, ethanol, ethyl acetate, methanol, and petroleum ether extracts of PM leaves showed no activity against human fibroblast (Hs888Lu) and kidney epithelial (Vero) cells, and exhibited an IC_{50} >250 µg/mL for normal colon (CCD841), liver (Chang liver and WRL-68) cells (Abdullah et al. 2017; Mohd Ghazali et al. 2014; Qader et al. 2011; Vimala et al. 2011; Wahab, Bunawan & Ibrahim 2015). In addition, the hexane, methanol, and water extracts of PM leaves demonstrated cytotoxicity towards normal colon (CCD841) and human endothelial (EA.hy926) cells, while the methanol extract from PM stems exhibited cytotoxicity against kidney epithelial (Vero) cells (Abdullah et al., 2017; Christapher et al., 2016; Wahab et al., 2015).

These findings suggest that certain PM extracts are effective in treating cancers due to their selective toxicity, which results in minimal adverse effects on normal cells, thereby making them a promising option for cancer management and treatment.

2.4.2.9 Anti-inflammatory and analgesic activity

Christapher et al. investigated the anti-inflammatory and analgesic properties of methanol and aqueous extracts from PM leaves in rodent models. The results indicated that the aqueous extract exhibited significant analgesic effects in various assays, including the formalin test, acetic acid-induced writhing, and tail immersion test, as well as anti-inflammatory activity in the carrageenan-induced inflammation model. In contrast, the methanol extract demonstrated analgesic effects but did not show any anti-inflammatory activity (Christapher, Xin, et al., 2015).

2.4.2.10 Cognitive enhancing effect

George et al. investigated the impact of PM water extract on learning and memory, reporting that the extract demonstrated protective effects against scopolamine-induced cognitive deficits in a Barnes maze rat model (George, Ng, et al., 2014).

2.4.2.11 Sexual performance and well-being

Udani et al. (2014) conducted a randomized, double-blind, placebo-controlled clinical trial to assess the effects of Eurycoma longifolia (200 mg/day) combined with PM water extract (100 mg/day) in healthy male volunteers aged 45-65. The results indicated that the combination significantly improved sexual performance compared to the placebo group (Udani et al., 2014). In clinical studies, dosages are often expressed in "mg/day", which refers to a fixed daily dose for all participants, regardless of body weight. This approach is commonly used in human trials where a standardized dose is given to ensure consistency across individuals. In contrast, "mg/kg" is used in preclinical studies and animal experiments, where the dosage is adjusted according to body weight. This method accounts for differences in metabolism and physiological

responses among different-sized subjects, making it more suitable for dose extrapolation from animals to humans. The use of “mg/day” in this clinical study ensures a controlled and uniform dose among participants, whereas “mg/kg” would be necessary in studies where weight-based adjustments are required for accurate dosing.

2.5 Metabolomics

Metabolomics involves the analysis of metabolites within cells and tissues, which can be detected in various body fluids. The presence of a tumor can disrupt an individual’s overall metabolism, leading to alterations in fuel utilization to meet the energy requirements of the tumor. Additionally, tumor metabolism may evolve as the disease advances. Given that metabolic dysregulation is a key characteristic of cancer, metabolomics presents a promising approach for studying the disease (Nannini et al., 2020).

2.5.1 Cancer cell metabolism

One of the earliest and most well-known metabolic changes in cancer cells is their increased glucose consumption. This heightened glucose uptake by tumors can be detected using fluorodeoxyglucose-positron emission tomography (FDG-PET) imaging, which is utilized for initial cancer staging, evaluating treatment response, and monitoring. The discovery by Otto Warburg and others nearly a century ago showed that tumor cells exhibit elevated glucose uptake and produce large amounts of lactate, even in the presence of oxygen. This has firmly established the link between altered metabolism and cancer cells (Heiden et al., 2009; Koppenol et al., 2011; Warburg, 1924, 1956). During the genomic era, research predominantly focused on how

signaling pathways and transcription factors control cancer cell growth and the cell cycle. However, there has been a resurgence of interest in understanding the role of metabolic alterations in cancer pathogenesis. Several factors, such as tumor hypoxia, stromal composition, immune cell infiltration, and genetic mutations are crucial in shaping cancer cell metabolism. Genetic and epigenetic changes offer cancer cells a survival advantage, particularly in nutrient-deprived environments. This renewed focus on cancer metabolism initially stemmed from the recognition that dysregulated signaling pathways and transcriptional reprogramming lead to metabolic alterations in cancer cells (Dang & Semenza, 1999; De Berardinis & Chandel, 2016; Hsu & Sabatini, 2008; Shaw, 2009). Subsequent research has shown that the activation of oncogenes or the loss of tumor suppressors is enough to drive metabolic changes in cancer cells (Dang, 2013; Kimmelman, 2015; Vousden & Ryan, 2009). Consequently, tumor-associated metabolic changes are now recognized as an emerging hallmark of cancer (Hanahan & Weinberg, 2011).

2.5.2 Methodology and Instrumentation

An overview of key technologies utilized in metabolomics is shown in Figure 2.6. The primary focus is on mass spectrometry (MS) and nuclear magnetic resonance (NMR), both of which are effective for detecting compounds in various biofluids or cell/tissue extracts in liquid form. NMR is also applicable to solid-phase samples, including cell membranes and even whole cells and tissues. Other techniques, such as matrix-assisted laser desorption/ionization mass spectrometric imaging (MALDI-MSI) and NMR-based *in vivo* imaging methods like magnetic resonance spectroscopic imaging (MRSI), are more specialized and have been discussed in separate reviews (Crecelius et al., 2015; Posse et al., 2013).

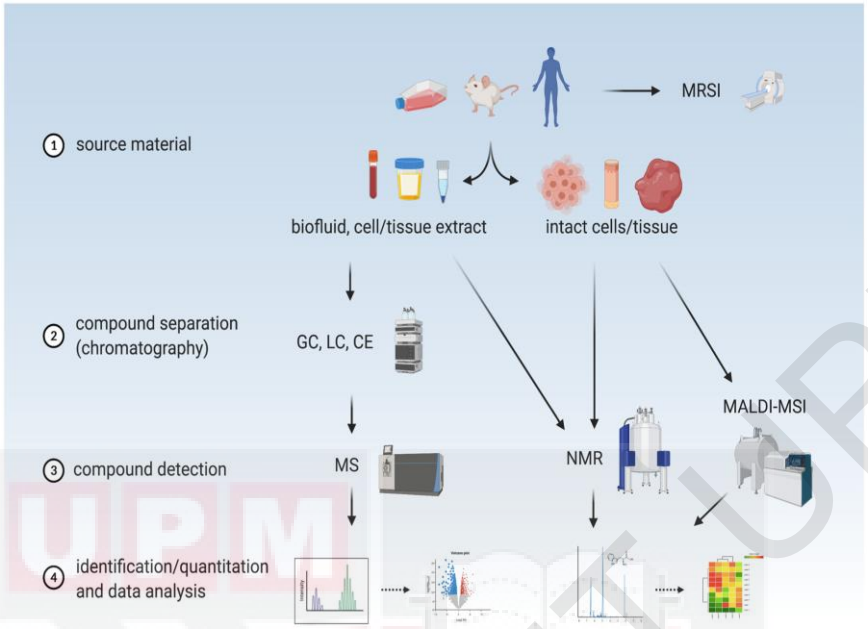

Figure 2.6: The optimal metabolomics workflow depends on source material and application. Various technologies and methods can be used to acquire raw data, which then provide the starting point for computational analysis. See text for details. CE indicates capillary electrophoresis; GC, gas chromatography; LC, liquid chromatography; MALDI-MSI, matrix-assisted laser desorption/ionization mass spectrometric imaging; MRSI, magnetic resonance spectral imaging; MS, mass spectrometry; NMR, nuclear magnetic resonance.

2.5.2.1 Nuclear Magnetic Resonance (NMR)

NMR spectroscopy measures the chemical properties of specific atomic nuclei within a molecule. This method is highly versatile, applicable to biospecimen in liquid, solid, or gas phases without requiring extensive sample preparation. In NMR, a sample is exposed to a strong magnetic field and then irradiated with radiofrequency waves. This process temporarily excites certain nuclei, such as ^{1}H, ^{13}C, ^{15}N, or ^{31}P, causing them to change their spin states. As the nuclei return to their original states, they emit energy that creates a distinctive spectroscopic pattern, known as a chemical shift, which provides information about the type, position, and electromagnetic environment of the excited atoms in the molecule. Importantly, NMR does not consume the sample, allowing it to be used for further analyses. However, NMR instruments are large and

have lower sensitivity (micromolar) compared to mass spectrometry (nanomolar) (Emwas et al., 2019). Additionally, while NMR can resolve several hundred unique metabolites, it is less capable of detecting the vast range of chemical species that mass spectrometry can identify, which can extend to thousands of unique features based on their masses.

2.5.2.2 Mass spectrometry (MS)

Mass spectrometry is a fundamental analytical technique in metabolomics, primarily used for determining the mass-to-charge ratio (m/z) of molecules and their fragments. In this process, a sample in either liquid or gas phase is introduced into the mass spectrometer, where it is ionized and then separated based on its m/z ratio. The sample material is consumed during the analysis. MS is often combined with an initial chromatographic step to enhance resolution by separating isobaric compounds and minimizing signal interference from more abundant species.

2.5.2.3 Source material

Metabolomics can be applied to a diverse array of biological materials, including cultured cells and tissues, specimens from laboratory animals, and clinical samples such as tumors and biofluids, whether freshly obtained or properly archived. The volume of starting material required varies depending on the analytical technique used. For nuclear magnetic resonance (NMR) spectroscopy, sample volumes generally range from 0.1 to 0.5 mL for liquid samples. In contrast, mass spectrometry (MS) methods offer greater sensitivity, with detection limits that are 10 to 1000 times lower than those of NMR, allowing the analysis of just a few microliters or milligrams of sample to detect numerous metabolites.

2.5.3 The implication of metabolomics in colon cancer study

In 2018, Loke et al. employed LC–MS metabolomics combined with 16S rRNA next-generation sequencing to explore differences in function and taxonomy between CC and normal tissue samples, suggesting that microbiome dysbiosis may contribute to variations observed at cancer sites. Their findings indicated elevated levels of the metabolite S-adenosyl-L-homocysteine (SAH) in tumors compared to normal tissues (Loke et al., 2018). Metabolomics is also utilized to evaluate the anti-proliferative and apoptotic activities of natural products. For instance, GC–MS metabolomics was used to analyze the anti-proliferative effects of methanol and water extracts of Chamaecyparis obtusa on the HCT-116 human CC cell line, identifying methanol extract and anthricin as key compounds responsible for this activity (H. Y. Kim et al., 2015). A recent 2018 study used rapid ^{1}H-NMR metabolomics to identify secondary metabolites with anti-proliferative effects against human CC cell lines, including HCT-116, HT-29, and Caco-2, revealing two bioactive compounds, cycloartane glycoside and protodioscin derivative, that demonstrated anti-proliferative activity (Graziani et al., 2018).

2.6 Proteomics

Proteomics involves analyzing the structure and function of proteins, including their interactions and roles within biological systems. In the quest for novel CC biomarkers, proteomics research emphasizes identifying differences in protein expression between normal and cancerous cells or characterizing distinct proteomic profiles in bodily fluids. Key methodologies for discovering protein biomarkers in cancer include two-

dimensional gel electrophoresis combined with liquid chromatography-mass spectrometry (2-DE-MS), two-dimensional difference gel electrophoresis (2D-DIGE), and liquid chromatography-mass spectrometry (LC-MS) (Boja & Rodriguez, 2014). Advanced quantitative proteomic assays can assess changes in proteins, their interacting partners, isoforms, and post-translational modifications (Boja & Rodriguez, 2014).

2.6.1 Cancer cell proteomics

To uncover and identify proteins implicated in tumor development, experimental approaches are crucial for elucidating aberrant mechanisms in controlled environments. Research has shown that certain cancer cell lines, such as those derived from breast cancer, exhibit chromosomal, genetic, and transcriptional abnormalities similar to those found in primary breast tumors (Neve et al., 2006). This suggests that cell lines can partially represent the heterogeneous nature of breast cancer and provide insights that correlate with human samples. The use of cell lines in cancer research offers several advantages, including the ability to manipulate experimental conditions extensively and the suitability for high-throughput screening. Cultured cell lines are often more homogeneous compared to the diverse cell types found in tissues, which facilitates more controlled studies. However, the applicability of findings from cell line studies is sometimes challenged due to limitations such as *in vitro* artifacts, lack of metabolic activity, restricted cell types, and conditions that differ from the *in vivo* environment. Despite these limitations, *in vitro* proteomics offers controlled experimental conditions, homogeneous cell types, cost-efficiency, and experimental convenience. Utilizing cell lines is valuable for exploring cancer pathogenesis and for hypothesis generation and testing.

2.6.2 Label-free quantitation

Label-free quantification offers a cost-effective alternative to isotope labeling for analyzing cancer proteomes (B. Zhang et al., 2006). There are two primary approaches in label-free quantitative proteomics: relative quantification, which relies on spectral counting of peptides/proteins, and absolute quantification using the exponentially modified protein abundance index (emPAI). Spectral counting assumes that the intensity of precursor ions correlates with peptide abundance (Liu et al., 2004). This method involves analyzing samples separately but following the same data acquisition protocol. The emPAI method, an extension of label-free quantification, correlates protein abundance with the ratio of observed peptides to the theoretical number of peptides for each protein (Ishihama et al., 2005). A significant challenge with label-free mass spectrometry quantification is ensuring reproducibility across sample preparation, liquid chromatography separation, and computational analysis to achieve accurate quantitative results (B. Zhang et al., 2006). Additionally, label-free quantification methods face limitations, such as lower accuracy (semi-quantitative nature), difficulties in quantifying low-abundance or short peptides, reduced throughput, and less precise quantitation due to independent handling of samples (Lill, 2003). Despite these limitations, label-free quantification is cost-effective and has been utilized in various oncoproteomic studies (X. Hu et al., 2009).

2.6.3 The implication of proteomics in colon cancer study

Proteomics enables the identification of proteins that are expressed at low concentrations, which, when consistently different in CC patients, can serve as

biomarkers for diagnosis and treatment (Ahrens et al., 2010; Liu et al., 2004). Using a Fisher-based model system, fragments of complement C3f were detected in the serum of CC patients, distinguishing them from healthy individuals. MALDI-TOF mass spectrometry confirmed that complement C3f is present at lower concentrations in CC patients, marking it as a potential biomarker for differentiation (D. Zhu et al., 2013). Proteomic profiling of human and mouse tissues has revealed novel cancer-associated fibroblasts linked to cancer progression. This research highlighted the roles of proteins such as LTBP2, CDH11, OLFML3, CALU, and FSTL1 in the migration and invasion of CC, identifying them as stromal biomarkers (Torres et al., 2013). A study on tissue secretomes found significant differences between cancerous and healthy colon tissues, noting that cancer tissues secrete 40% nuclear proteins compared to just 5% in healthy tissues. Among these nuclear proteins, minichromosome maintenance 5 (MCM5) is notably overexpressed in CC and could serve as a biomarker (de Wit et al., 2014). Exoproteome analysis has established OLFM4, a member of the olfactomedin family, as a marker for non-metastatic tumors in CC, useful for distinguishing between cancerous and non-cancerous tissues (Besson et al., 2011). Additionally, elevated levels of S100A9, carcinoembryonic antigen cellular adhesion molecule-5 (CEA or CEACAM5), and dipeptidase-1 (DPEP1) proteins have been observed in CC patients, while CEACAM-7 was found to be downregulated (Tu et al., 2017). A cohort study examining immunological changes in colorectal carcinogenesis identified increased levels of $CD4^+$ helper T-cells recognizing tumor cells with HLA DR^+ $CD4^+$, reflecting heightened antigen recognition in cancer patients. Elevated concentrations of cytotoxic T-cells capable of targeting malignant cells were also reported (Berndt et al., 2008). Chromosomal abnormalities, such as aneuploidy, have been identified as prognostic factors in many cancers, including CC. A study induced and maintained chromosomal trisomy in colorectal cell lines to explore its relationship with CC

(Gramolini et al., 2008; Schrimpf et al., 2009). Proteomic analysis revealed differential expression of proteins like PCNA, HMGB1, IDH3A, and PSMB3 in trisomic cells, which are associated with cell growth and proliferation, and their abnormal expression may contribute to colorectal carcinoma (Gemoll et al., 2013). Proteomic profiling of APC mutant cells showed disruptions in cell adhesion proteins, increased cell cycle regulators, altered Wnt signaling proteins, and redistributed β-catenin, highlighting the role of Wnt pathway hyperactivation as an early event in CC initiation (Bell et al., 2009). Understanding these mutations can provide new insights into cancer biology (Goh et al., 2011).

CHAPTER 3

PREPARATION OF *Polygonum minus* EXTRACT AND OPTIMIZATION OF ITS BIOACTIVE COMPOUND VIA CYTOTOXICITY ASSAY ON COLON CANCER CT26 CELL LINE ANALYSIS

3.1 Introduction

In recent years, the exploration of natural products as potential therapeutic agents has gained considerable momentum, driven by their promise of offering effective treatments with reduced toxicity compared to traditional chemotherapy (Kalachaveedu et al., 2023; Weth et al., 2024; Y. Xia et al., 2024). Among the diverse array of medicinal plants, *Polygonum minus* (PM) has emerged as a notable candidate due to its rich phytochemical composition, which includes a variety of bioactive compounds such as flavonoids, phenolic acids, and other secondary metabolites (Z. Yang et al., 2024). These compounds are known for their diverse pharmacological activities, including antioxidant, anti-inflammatory, and anticancer properties (Shen et al., 2018; Vikram et al., 2014).

Colon cancer (CC), a leading cause of cancer-related mortality globally, underscores the urgent need for innovative therapeutic approaches (Xi & Xu, 2021). Despite advancements in treatment, the search for effective and less toxic alternatives remains a critical focus in oncology (Islam et al., 2022). Natural products like PM offer a promising avenue for discovering new treatments with potentially enhanced safety profiles.

This chapter is dedicated to the systematic preparation and optimization of PM extract to evaluate its cytotoxicity against the CT26 CC cell line. The research process involves several sequential steps designed to maximize the yield and efficacy of bioactive compounds from PM. Initially, solvent extraction is employed to obtain crude extracts using four different solvents: hexane, dichloromethane, methanol, and water. Each solvent serves a specific purpose based on its polarity, which affects the solubility and extraction of various compounds (Daud et al., 2022). Hexane and dichloromethane are non-polar solvents that primarily target lipophilic substances, while methanol and water are polar solvents used to extract more hydrophilic compounds (Rajhard et al., 2021; Saini et al., 2021). By utilizing a combination of these solvents, the aim is to capture a comprehensive profile of PM's bioactive constituents.

Following the extraction, the cytotoxicity of each crude extract is assessed against the CT26 cell line. This evaluation is crucial for identifying which extract exhibits the strongest anticancer activity. The selection of the most potent extract is based on its ability to inhibit cancer cell growth and induce cell death, providing an initial indication of its therapeutic potential.

The next phase involves optimizing the selected crude extract through liquid-liquid partition. This technique is employed to further refine the extract by separating it into different fractions based on their solubility in immiscible solvents. Liquid-liquid partition enhances the purity and concentration of bioactive compounds, allowing for a more targeted analysis of their effects. By concentrating and isolating the active components, liquid-liquid partition facilitates a clearer understanding of which

fractions are most responsible for the observed cytotoxicity.

The final step involves evaluating the cytotoxicity of each partitioned extract against the CT26 cell line. This assessment provides a detailed profile of the bioactive fractions, helping to pinpoint the most effective components responsible for the anticancer activity. By comparing the effects of different fractions, the research aims to identify and characterize the key bioactive constituents that hold promise for further development as therapeutic agents for CC.

3.2 Materials and methods

3.2.1 Plant material

In December 2022, fresh plant samples (2.5 months old) were obtained from the Agricultural Conservatory Park at the Institute of Bioscience (IBS), Universiti Putra Malaysia (UPM). The Biodiversity Unit, IBS, UPM identified and cataloged the sample as Voucher No. KM 0087/23.

3.2.2 Crude extract

3.2.2.1 Crude extract preparation

The extraction process was carried out sequentially using hexane (H), dichloromethane (D), methanol (M), and water (W), with a solid-to-liquid ratio of 1:10 (w/v) for H, D, and M, and 1:20 (w/v) for W. Dried leaves (L) and stems (S) of 5g weight, were placed in separate Schott bottles. A 50 mL aliquot of hexane was added to the powdered samples in the Schott bottles, which were then mixed under a fume hood. The mixture was soaked in hexane at 5 °C with continuous shaking at 200 rpm in an incubator

shaker for 1 h. For water extraction, the supernatant was centrifuged at 4000 rpm for 10 min and then filtered through Whatman filter paper (No.1) (Gu et al., 2020). The extraction was repeated twice, and the residue was dried. 10 mL of hexane solvent collected was transferred to a round-bottom flask (DWK Life Sciences, Germany)), labeled, and concentrated under reduced pressure at 50 ℃ using a rotary evaporator (Buchi Rotavapor). The water extract was concentrated at 6 ℃. The concentrated extract in the round-bottom flask was then dried in an oven at 50 ℃ until no solvent remains. The flask was cooled in a desiccator and weighed to a constant weight.

3.2.2.2 Estimation of extraction yield

The extraction yield (%) of PM extracts was calculated according to the method described by Setyani et al. (2023) using the following equations.

Extraction yield (%) = (Dried weight of extract ÷ Dried weight of plant powder) ×100%.

3.2.2.3 Cell culture

The CT26 and NIH/3T3 cell lines were maintained in RPMI 1640 medium supplemented with 10% fetal bovine serum, 100 U/mL penicillin and 100 mg/mL streptomycin, and incubated at 7 ℃ in a 5% CO_2 incubator. Cells in the exponential growth phase were used for experiments.

3.2.2.4 Cytotoxic evaluation (MTT assay)

The MTT colorimetric assay was used to assess the cytotoxicity of the extracts (Z. Yang et al., 2025). Briefly, cells were counted and seeded at a density of 5 × 10

cells/mL in a 96 well flat bottom microplate and then incubated for 24 h. Afterward, the medium was removed, and the cells were treated with varying concentrations of PM extracts (75–300 µg/mL), with an untreated control (blank control) group included for comparison. Following the 24, 48, or 72h of incubation, the treatment was removed, and 20µL of MTT (Livning, China) solution (5 mg/mL) was added to each well. The plates (NEST, China) were then incubated for 4 h in a humidified 5% CO_2 incubator at 7 ℃ in the dark. After incubation, the supernatant was aspirated, and 150 µL of DMSO (SYSTERM, ChemAR, Malaysia) was added to each well to dissolve the dark-blue formazan crystals. The absorbance was measured at 570 nm, with a reference wavelength of 630 nm, using Infinite F50 Absorbance Microplate Reader (Tecan Trading AG, Switzerland). The percentage of cell viability was calculated using the following equation:

Cell viability (%) = (OD treated – OD blank) ÷ (OD control – OD blank) ×100%.

The cytotoxicity of the extracts was expressed as 50% inhibitory concentration (IC_{50}), which is the concentration of the extract that inhibits 50% of cell viability compared to the control group.

The cytotoxicity level of the PM extract was categorized according to the Geran protocol and the guidelines from the National Cancer Institute of the United States. Substances were classified as highly cytotoxic (IC_{50} < 20 µg/mL), moderately cytotoxic (MCs) (IC_{50} of 21–200 µg/mL), weakly cytotoxic (WCs) (IC_{50} of 201–500 µg/mL), or non-cytotoxic (NCs) (IC_{50} > 501 µg/mL) (Youssef et al., 2023).

3.2.2.5 Toxicity assays (Brine shrimp lethality assay)

Briefly, 4 g of non-iodized sea salt was dissolved in 1 L of distilled water to create

simulated seawater, which was placed in a fish tank. *Artemia salina* eggs (1 g), obtained from a pet shop, were added to the saltwater and incubated at room temperature with constant aeration and a 12-h light-dark cycle. After approximately 24 h, the eggs hatched into nauplii (Sahandi et al., 2022). 10 active nauplii were then transferred into each well of a 24-well plate, along with 1 mL of simulated seawater. For this study, PM extract was dissolved in DMSO and diluted with artificial seawater to six different concentrations (50, 100, 250, 500, and 1000 µg/mL). Potassium permanganate (KMnO4) dissolved in artificial seawater at the same concentrations served as a positive control, while DMSO (3.33%) served as a negative control (NC), and artificial seawater was used as a blank control (BC) (Muneer et al., 2020). The respective samples were added to the wells containing the nauplii. After 24 h, the wells were inspected under a microscope, and the number of surviving nauplii was recorded. The experiment was performed in triplicate. The percentage of brine shrimp mortality was calculated using the following equation (Billah et al., 2013):

Mortality (%) = (Total larvae – Alive larvae) × 100/Total larvae.

Three independent tests were conducted, and a nonlinear regression analysis was used to determine the lethal concentration 50 (LC_{50}) values (Shah et al., 2014).

Toxicity was evaluated based on the LC_{50} value using Clarkson's toxicity index (Clarkson et al., 2004), which categorizes substances as non-toxic (LC_{50} >1000 µg/mL), low toxicity (LC_{50}: 500–1,000 µg/mL), medium toxicity (LC_{50}: 100–500 µg/mL), and high toxicity (LC_{50}: 0–100 µg/mL).

3.2.3 Fraction

3.2.3.1 Fractionation of active extracts using liquid-liquid partition

The crude leaves or stem extracts of PM hexane, PM dichloromethane, PM methanol, and PM water were selected based on their cytotoxic activity and submitted to fractionation using liquid-liquid partition. The cytotoxic activity of the solvent extracts was estimated, and the highest cytotoxic activity was found in the case of the PM hexane extract, which was tested against the CC (CT-26) cell line and hence was chosen for liquid-liquid partition.

For further processing (as illustrated in Figure 3.1), the hexane extract was dissolved in n-hexane (solid to liquid ratio of 1:200 (w/v)) and partitioned against fresh distilled water (1:1, v/v) to yield a hexane-soluble fraction and a water fraction. The final mixture was stirred at room temperature for 1 h and then transferred into the separating funnel and allowed to stand until two phases were observed. The organic and aqueous phases were collected separately. Further, the hexane layer was repeatedly washed with water to remove the remaining polar substances, and the collected fractions were dried under reduced pressure at 50 °C using a rotary evaporator. In a similar fashion, the extracts were partitioned with acetonitrile and methanol. Subsequently, all four fractions were subjected to cytotoxic activity analysis.

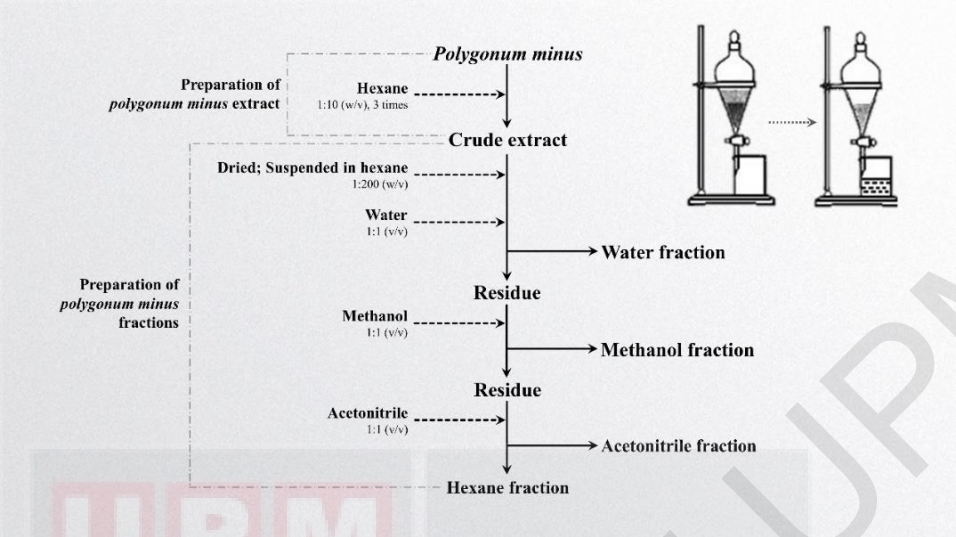

Figure 3.1: The procedure of preparing different fractions of *polygonum minus*.

3.2.4 Statistical analysis

Data were shown as means ± standard deviation (SD) from three independent experiments. SPSS R26.0.0.0 software was used for statistical analysis. The P values were analyzed using ANOVA and $P<0.05$ is considered significant.

3.3 Results and discussion

3.3.1 Extraction yield of crude extract

Extraction yield in various solvents indicates the number of various classes of phytochemicals present in a plant. The extraction yields of different solvents for each part of PM are shown in Table 3.1. Among the leaf extracts, the methanol extract (PM-L-M) had the highest yield of 14.11%, followed by the water extract (PM-L-W) at 13.08%, and the hexane extract (PM-L-H) had the lowest yield of 1.65%. For the stems, the water extract (PM-S-W) had the highest yield of 18.92%, followed by the methanol extract (PM-S-M) at 11.09%, and the hexane extract (PM-S-H) had the lowest yield of

1.02%.

Table 3.1: The extraction yield of PM in different solvents.

PM extract	Hexane	Dichloromethane	Methanol	Water
Leave extract yield (%)	1.65^{A}±0.07	3.39^{B}±0.08	14.11^{C}±0.21	13.08^{D}±0.56
Stem extract yield (%)	1.02^{A}±0.03	1.52^{A}±0.04	11.09^{B}±0.14	18.92^{C}±0.65

Values with different lowercase in the same lines are significantly different ($P<0.05$). Values with different capitals in the same lines are extremely significantly different ($P<0.01$).

In this study, four solvents ranging from non-polar to polar were used to ensure the extraction of various compounds with different polarities from PM. The findings, which showed higher yields of PM extract with polar solvents compared to non-polar ones, align with previous reports (Abdullah et al., 2017; Christapher, Xin, et al., 2015). Additionally, the results confirmed earlier observations that the PM whole plant contains fewer non-polar components (Abdullah et al., 2017).

3.3.2 Cytotoxic evaluation of crude extract

Cytotoxic effects of PM extracts on selected cell lines were evaluated. The IC_{50} values of PM extracts on different cell lines after 72 h of incubation are shown in Table 3.2. PM stem extracts exhibited no cytotoxicity against CC cells CT26 or normal cells (NIH 3T3) (IC_{50}>300 µg/mL in all cases). Similarly, the PM-L-W extract showed no cytotoxicity against CT26 cells. Furthermore, PM leaf polar extracts demonstrated weak cytotoxicity across all tested cell lines, while PM leaf non-polar extracts were moderately cytotoxic. Among these, PM-L-H exhibited the strongest antiproliferative effects.

The CT26 and NIH/3T3 were treated with the PM-L-H for 24, 48, and 72 h and its cytotoxic effects are shown in Table 3.3. PM-L-H showed time-dependent antiproliferative activity, with distinct IC_{50} values for the two cell lines at each time point. Notably, PM-L-H displayed the strongest antiproliferative effect at 48 h, as indicated by the lowest IC_{50} value at this time.

Table 3.2: IC_{50} values of PM extracts on different cell lines after 72 h of incubation.

PM extract	CT26 IC_{50}(µg/mL)	Category	NIH/3T3 IC_{50}(µg/mL)	Category
PM-L-H	126.78^{A}±2.74	MCs	134.27^{a}±1.54	MCs
PM-L-D	149.76^{B}±5.90	MCs	115.09^{Aa}±7.61	MCs
PM-L-M	300.04^{C}±9.48	WCs	221.53^{B}±21.06	WCs
PM-L-W	>300	NCs	265.49^{Bc}±25.95	WCs
PM-S-H	>300	NCs	>300	NCs
PM-S-D	>300	NCs	>300	NCs
PM-S-M	>300	NCs	>300	NCs
PM-S-W	>300	NCs	>300	NCs

PM-L-H: PM leave hexane extract, PM-L-D: PM leave dichloromethane extract, PM-L-M: PM leave methanol extract, PM-L-W: PM leave water extract, PM-S-H: PM stem hexane extract, PM-S-D: PM stem dichloromethane extract, PM-S-M: PM stem methanol extract, PM-S-W: PM stem water extract. MCs: moderately cytotoxic substances, WCs: weakly cytotoxic substances, NCs: non-cytotoxic substances. Values with different lowercase in the same column are significantly different ($P<0.05$). Values with different capitals in the same column are extremely significantly different ($P<0.01$).

Table 3.3: Cytotoxic effect of PM-L-H on CT26 and NIH/3T3 in 24, 48 and 72 h.

Time (h)	CT26 IC_{50}(µg/mL)	Category	NIH/3T3 IC_{50}(µg/mL)	Category
24	143.53^{c}±11.40	MCs	104.14^{B}±5.12	MCs
48	92.91^{A}±7.11	MCs	99.07^{A}±6.41	MCs
72	126.78^{Bb}±2.74	MCs	134.27^{A}±1.54	MCs

Values with different lowercase in the same column are significantly different (P<0.05). Values with different capitals in the same column are extremely significantly different (P<0.01). MCs: moderately cytotoxic substances.

This study is the first to evaluate the cytotoxicity of PM stem extracts. The findings indicate that PM stem extracts exhibit no cytotoxicity for CC and normal cells, providing a basis for further investigation of these extracts. The data revealed that PM leaf non-polar extracts demonstrated moderate cytotoxicity across all tested cell lines, whereas PM leaf polar extracts showed weak or no cytotoxicity (Abdullah et al. 2017; Christapher et al. 2016; Rohin, Hadi & Ridzwan 2020). Additionally, compared to other extracts, PM-L-H exhibited the most significant anti-proliferative effect on CC cells, with the strongest activity observed at 48 h.

3.3.3 Brine shrimp lethality assay of crude extract

The results of the 24h lethality determination of PM extract on brine shrimp are shown in Figure 3.2. All the prepared PM extracts exhibited toxicity with a clear concentration-dependent effect, except for PM-L-H and PM-L-D. The LC_{50} values for PM-L-H and PM-L-D were 631 µg/mL and 375.01 µg/mL, respectively (Table 3.4). According to the toxicity index, PM-L-H is classified as a low-toxicity substance, while PM-L-D is classified as medium-toxicity. The remaining extracts were non-toxic. Figure 3.3 illustrates the toxicity effects of PM-L-H and PM-L-D on brine shrimp at

various concentrations and incubation times. Mortality rates increased with exposure time at the same concentration, with the lowest mortality observed after 12 h and the highest after 48 h, indicating that the toxicity of PM-L-H and PM-L-D escalates over time.

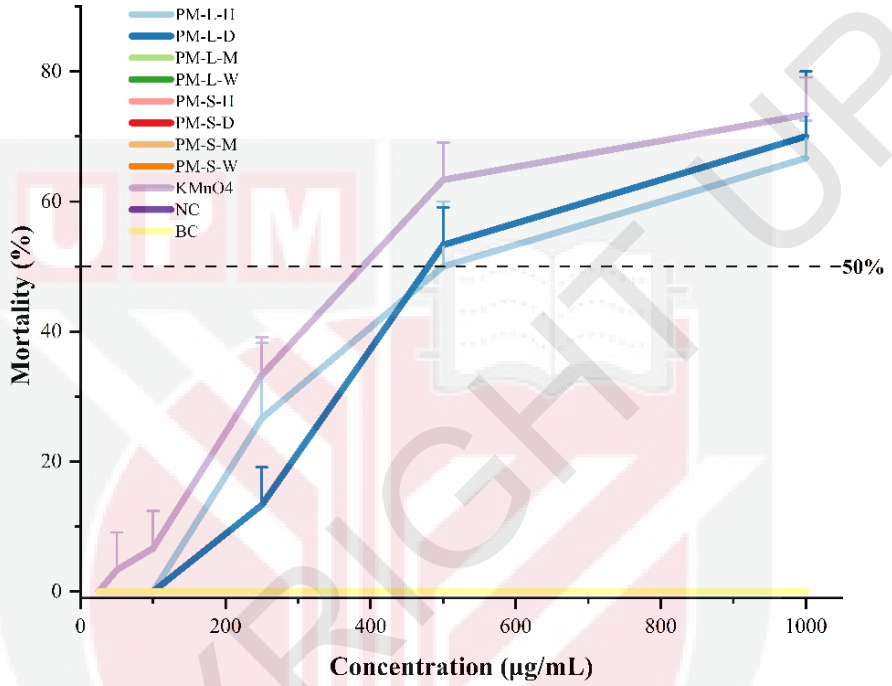

Figure 3.2: Toxicity results after 24 brine shrimp exposure to PM extract from different concentrations. negative control (NC), blank control (BC), positive control (KMnO4).

Table 3.4: LC_{50} of PM extract against brine shrimp lethality assay after 24 h and toxicity level evaluation.

PM extract	LC_{50} (µg/mL)	Toxicity
PM-L-H	631^{A}±52.42	Low toxicity
PM-L-D	375.01^{B}±25.26	Medium toxicity
PM-L-M	>1000	Non-toxic
PM-L-W	>1000	Non-toxic
PM-S-H	>1000	Non-toxic
PM-S-D	>1000	Non-toxic
PM-S-M	>1000	Non-toxic
PM-S-W	>1000	Non-toxic

Values with different lowercase in the same column are significantly different (P<0.05). Values with different capitals in the same column are extremely significantly different (P<0.01).

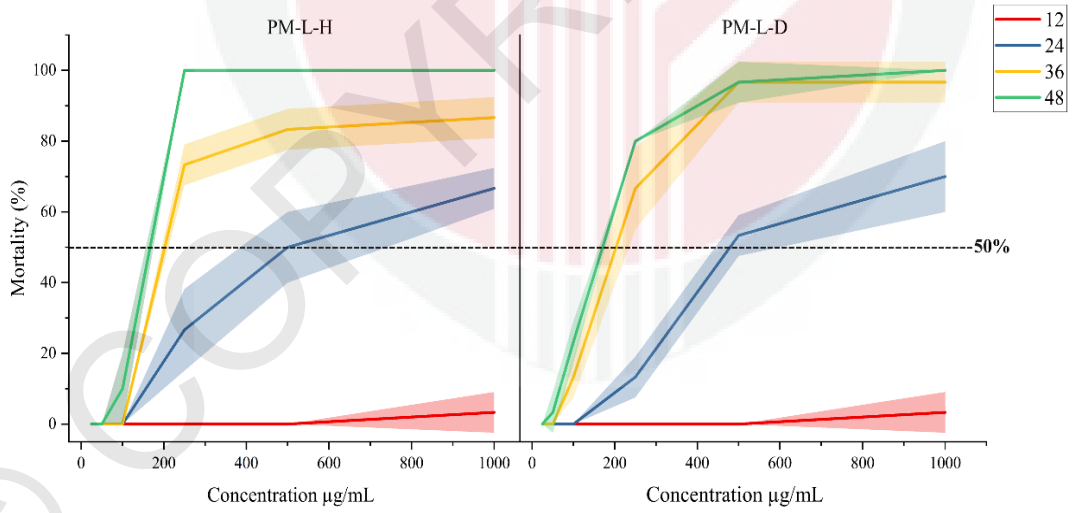

Figure 3.3: PM-L-H and PM-L-D on the mortality rate of brine shrimp after 12, 24, 36, and 48 h.

The toxicity of the plant extracts was assessed using the brine shrimp lethality assay, a widely used method known for its simplicity, cost-effectiveness, and efficiency in evaluating the toxicity of natural products, as well as pure and synthetic organic

compounds (War Naw et al., 2020). Unlike vertebrates, especially mammalian species, *Artemia* species are not typically subject to strict animal research regulations (Clemen-Pascual et al., 2022). Besides, Lagarto Parra et al. (Lagarto Parra et al., 2001) demonstrated a strong correlation ($r = 0.85$; $P < 0.05$) between the LC_{50} of the brine shrimp lethality assay and the LC_{50} of the acute oral toxicity assay in mice. Hence, many researchers advocate for the use of the brine shrimp assay in evaluating plant toxicity (Mwangi et al., 2015).

In this study, neither the blank control (artificial seawater) nor the negative control (3.33% DMSO) exhibited toxic effects or caused mortality after 24 h, confirming that the absence of food and the presence of 3.33% DMSO during the treatment period did not lead to brine shrimp mortality. The positive control (potassium permanganate) demonstrated clear concentration-dependent toxicity, consistent with previous studies (Weli et al., 2020). The inclusion of these control groups enhanced the reliability and validity of the experimental results.

Previous studies have reported that PM-L-W and PM-L-M are non-toxic substances (Christapher et al., 2017; Ming et al., 2013; N. Muhammad et al., 2013; Wasman et al., 2010). The findings align with this research, confirming that PM water extract and PM methanol extract were non-toxic to brine shrimp. However, no toxicity data were available for PM-L-H and PM-L-D, preventing a direct comparison with existing literature. To address this gap, the toxicity of PM-L-H and PM-L-D was investigated on brine shrimp over 12, 36, and 48 hours. The results indicated that both extracts exhibited dose- and time-dependent lethal activity, though the underlying mechanisms require further study.

Based on these studies, PM-L-H is identified as the active extract against CC, as it demonstrated strong anticancer activity and low toxicity. However, considering its moderate ability to inhibit the proliferation of CC cells and its toxicity to brine shrimp, further research should focus on the fractionation of PM-L-H to isolate its active fraction, such as through liquid-liquid partitioning, which may provide a new strategy for CC treatment.

3.3.4 Extraction yield of fraction

The active extract PM-L-H was separated by liquid-liquid separation using three solvents: water, acetonitrile, and methanol, which produced 4 extracts with yields ranging from 1.59% to 65.27%, which varied with the extraction solvent. The liquid-liquid partition yield for PM-L-H decreased as follows: hexane > acetonitrile >methanol > water (Table 3.5).

Table 3.5: The liquid-liquid partition yield for PM-L-H in different solvents.

Solvent	Water	Acetonitrile	Methanol	Hexane
Yield (%)	$1.59^{A}\pm0.15$	$14.06^{C}\pm0.50$	$9.67^{B}\pm0.49$	$65.27^{D}\pm1.80$

Values with different lowercase are significantly different ($P<0.05$). Values with different capitals are extremely significantly different ($P<0.01$).

The experimental results showed that the polar (aqueous) fraction had the lowest extraction yield, at only 1.59%. This occurred because hexane, as a non-polar solvent, extracted only less polar compounds from the plant material, leading to a lower overall yield (Tan et al., 2020). When the polar fraction is removed, the non-polar (hexane) fraction is left.

3.3.5 Brine shrimp lethality assay of fraction

The results of the 24 h lethality determination of PM-L-H partitions on brine shrimp are shown in Figure 3.4. Only PM leaves hexane extract hexane partition (PM-H-H) exhibited non-toxicity in all prepared PM partitions. The LC_{50} values for PM leaves hexane extract water partition (PM-H-W), PM leaves hexane extract acetonitrile partition (PM-H-A) and PM leaves hexane extract methanol partition (PM-H-M) were 380.61 µg/mL, 631µg/mL and 881.33 µg/mL, respectively (Table 3.6). According to the toxicity index, PM-H-W is classified as a medium-toxicity substance, while PM-H-A and PM-H-M are classified as low-toxicity.

Figure 3.5 illustrates the toxicity effects of PM-H-H on brine shrimp at various concentrations and incubation times. No mortality was observed in the 12 h incubation at any concentration tested. For the 24, 36, and 48 h incubation, mortality was observed in brine shrimp only at the maximum concentration of 1000 µg/mL, and mortality increased with increasing exposure time.

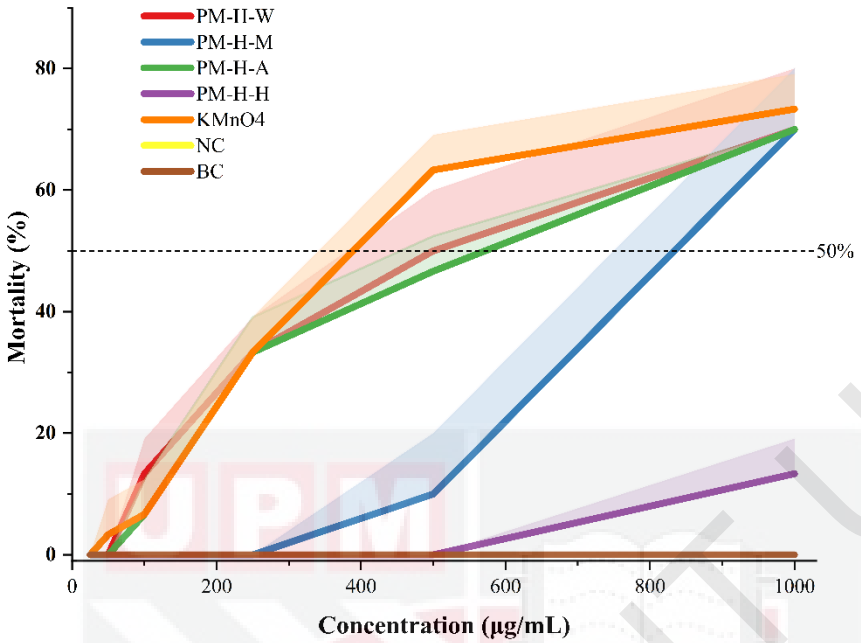

Figure 3.4: Toxicity results after 24 brine shrimp exposure to PM-L-H partitions from different concentrations. negative control (NC), blank control (BC), positive control (KMnO4). PM-H-W: PM leaves hexane extract water partition, PM-H-A: PM leaves hexane extract acetonitrile partition, PM-H-M: PM leaves hexane extract methanol partition, PM-H-H: PM leaves hexane extract hexane partition.

Table 3.6: LC_{50} of PM-L-H partitions against brine shrimp lethality assay after 24 h and toxicity level evaluation.

Partition	LC_{50} (µg/mL)	Toxicity
PM-H-W	380.61^{A}±43.12	Medium toxicity
PM-H-A	631^{B}±52.42	Low toxicity
PM-H-M	881.33^{C}±71.67	Low toxicity
PM-H-H	1066^{D}±17.32	Non-toxic

Values with different lowercase in the same column are significantly different (P<0.05). Values with different capitals in the same column are extremely significantly different (P<0.01).

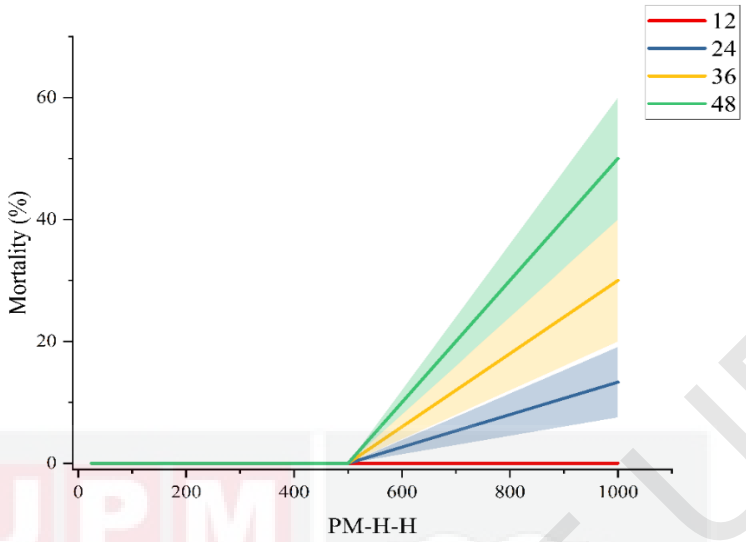

Figure 3.5: PM-H-H on the mortality rate of brine shrimp after 12, 24, 36, and 48 h.

Previous experimental results showed that PM-L-H is a low-toxic substance that exhibits dose- and time-dependent lethal activity for brine shrimp. Despite this, PM-L-H is an active extract against CC. Therefore, liquid-liquid partitioning was performed to remove the toxic compounds in PM-L-H and provide a safer treatment strategy for CC.

Through liquid-liquid partitioning, it was found that PM-H-H is a non-toxic substance, while PM-H-W, PM-H-A, and PM-H-M were all toxic to brine shrimp. Consequently, the toxic substances of PM-L-H were divided into PM-H-W, PM-H-A, and PM-H-M. It is suggested that future research should focus on testing the anti-CC activity of PM-H-H.

3.3.6 Cytotoxic evaluation of fraction

Cytotoxic assays on CT26 and NIH/3T3 cell lines showed that PM-H-H demonstrates toxic effects on cell viability. With the increase in time, the cytotoxic decreases (Table

3.7). The IC_{50} values for CT26 and NIH/3T3 cell lines after 24 of exposure are 155 ± 9.85 µg/mL and 194.33 ± 9.29 µg/mL, respectively.

Table 3.7: Cytotoxic effect of PM-H-H on CT26 and NIH/3T3 in 24, 48 and 72 h.

Time (h)	CT26 IC_{50}(µg/mL)	Category	NIH/3T3 IC_{50}(µg/mL)	Category
24	155^{A}±9.85	MCs	194.33^{B}±9.29	MCs
48	>300	-	>300	-
72	>300	-	>300	-

Values with different capitals in the same lines are extremely significantly different (P<0.01).

The current study demonstrated significant cytotoxicity of PM-H-H against cancer cell lines CT26 and NIH/3T3. Previously, PM active fractions have been evaluated for their biological activities, such as antioxidant, anticholinesterase, anti-HIV-1 protease activities, and antidepressant (Ahmad et al., 2023; Bashir et al., 2020). While the present study has assessed for the first time the cytotoxic activity of PM-H-H against the CT26 and NIH/3T3.

Based on the above studies, PM-H-H is the active fraction against CC, since it exhibits strong anticancer activity and relatively high safety. However, given its moderate cytotoxicity against CC. Future research should focus on using PM-H-H as a complementary drug in combination with high-toxicity chemotherapy agents, positioning it as a promising adjuvant compound for CC treatment.

3.4 Conclusion

This chapter investigated the extraction yields, cytotoxicity, and toxicity of PM extracts and their fractions, with a focus on their potential application as anticancer agents, particularly against CC. This study demonstrated that extraction yields varied significantly depending on the solvent used, with polar solvents like methanol and water providing the highest yields for both PM leaves and stems. Among the various extracts tested, PM-L-H exhibited the strongest antiproliferative effects on CT26 CC cells, while also showing low toxicity in brine shrimp lethality assays. This suggests that PM-L-H could be an active component in cancer treatment, although its moderate cytotoxicity and low toxicity call for further investigation.

Further fractionation of PM-L-H via liquid-liquid partitioning identified PM-H-H as the most promising fraction, demonstrating strong anticancer activity against CT26 cells and relative safety with non-toxicity in brine shrimp assays. These findings suggest that PM-H-H holds potential as an adjunct therapy in combination with conventional chemotherapy, offering a more targeted and possibly less toxic approach to CC treatment. Nonetheless, additional studies are warranted to fully elucidate the mechanisms of action, optimize therapeutic efficacy, and ensure safety in clinical applications.

CHAPTER 4

IN VITRO ANTI-COLON CANCER EFFECTS OF *Polygonum minus* EXTRACT COMBINATION WITH 5-FLUOROURACIL ON COLON CANCER CT26 CELL LINE

4.1 Introduction

The battle against CC, a major cause of cancer-related deaths worldwide, often involves the use of chemotherapeutic agents such as 5-FU (Islam et al., 2022; Vodenkova et al., 2020). While 5-FU remains a key player in the treatment of CC, its use is frequently accompanied by significant side effects and the emergence of drug resistance, which can diminish its effectiveness over time (Azwar et al., 2021; Sethy & Kundu, 2021). These challenges underscore the need for novel strategies that can enhance the efficacy of 5-FU while reducing its adverse impacts on patients (Barathan et al., 2024).

The concept of drug combination therapy is increasingly recognized as a powerful strategy in cancer treatment (Jaaks et al., 2022; Plana et al., 2022; M. Zhao et al., 2020). By using two or more agents that target different pathways or mechanisms within cancer cells, combination therapies can potentially overcome drug resistance, reduce the required doses of individual drugs, and minimize toxic side effects (Jin et al., 2023; Y. Liu et al., 2021; M. Sharma et al., 2022; Ward et al., 2021). In the context of CC, combining 5-FU with natural compounds like PM extract could enhance therapeutic outcomes by attacking cancer cells on multiple fronts, thereby increasing treatment success and reducing the chances of relapse (Kamran et al., 2022; Liang et al., 2022).

Previous studies have highlighted the anti-CC effects and safety of PM-H-H. This chapter delves into the *in vitro* anti-CC effects of combining PM-H-H with 5-FU on the CT26 CC cell line. Unlike the preparation and optimization of the PM-H-H discussed in earlier chapters, this section directly utilizes the optimized PM-H-H to assess its synergistic potential when combined with 5-FU. The primary focus is on evaluating whether the PM-H-H can enhance the cytotoxic effects of 5-FU against CC cells, thus offering a more potent therapeutic strategy.

The experimental approach involves treating CT26 cells with PM extract, 5-FU, and their combination. The cytotoxicity of these treatments is measured to determine the extent of cell viability reduction, with particular attention to whether the combination therapy surpasses the effects of 5-FU alone. Additional analyses, such as apoptosis assays and cell cycle studies, are conducted to explore the mechanisms through which the combination of PM extract and 5-FU exerts its effects.

4.2 Materials and methods

4.2.1 Cell culture

The CT26 cell lines were maintained in RPMI 1640 medium supplemented with 10% fetal bovine serum, 100 U/mL penicillin, 100 mg/mL streptomycin, and 1% non-essential amino acids, and incubated at 37 ℃ in a 5% CO_2 incubator. Cells in the exponential growth phase were used for experiments.

4.2.2 Determination of drug interaction

The MTT colorimetric assay was used to assess the cytotoxicity of the PM-H-H and 5-FU. The drug interactions of 5-FU with PM-H-H were determined by calculating the combination index (CI) according to the Chou-Talalay method (Chou & Talalay, 1981). Data analysis was performed with CompuSyn software (Biosoft, Ferguson, MO, USA), which is based on the drug combination theory of Chou, to calculate the CI and dose-reduction index (DRI) values (Chou, 2006). CI < 1, CI = 1, and CI > 1 are considered synergistic, additive, and antagonistic effects, respectively.

4.2.3 Cell morphological analysis

For cell morphology observation, CT26 cells were seeded in 6 well plates and incubated at 7 ℃ in a 5% CO_2 humidified atmosphere of 24 h. Once the cells reached 80% confluence, they were treated with PM-H-H, 5-FU, or a combination of both for 24 h. Morphological changes were then examined using an Inverted Fluorescence Microscope (Carl Zeiss Microscopy, GmbH 37081, Gottingen, Germany).

4.2.4 AO/PI double staining assay

In this assay as previously described (Z. Yang et al., 2025), CT26 cells were seeded into 6 well plates and incubated for 24 h to reach 60% confluence. The cells were then treated with PM-H-H, 5-FU, or a combination of both for 24 h. After treatment, the medium was removed, and the cells were washed twice with PBS. Acridine orange (AO) and propidium iodide (PI) were added to the wells and stained for 5 minutes at room temperature in the dark. Finally, the cells were examined using an Inverted Fluorescence Microscope (Carl Zeiss Microscopy, GmbH 37081, Gottingen, Germany).

4.2.5 Clonogenic formation assay

A clonogenic formation assay was used to assess the CT26 cell growth to study whether the combination of PM-H-H and 5-FU could synergistically inhibit CT26 cell proliferation (Gupta et al., 2021). CT26 cells were seeded on 6 well plates at a density of 600000 cells per well and allowed to attach and grow for 48 h. The cells were then treated with PM-H-H, 5-FU, or their combination for 24 h. Following treatment, the medium was replaced with fresh media every 3 days until colonies formed. After 7 d, colonies were washed twice with PBS, fixed with methanol for 30 min, and stained with 0.5% crystal violet (BKMAM, Changde, China) for 30 min at room temperature. The plates were rinsed under running water and air-dried for 1-2 d. Colonies were observed and counted using a Nikon light microscopy (Nikon, Eclipse TS 100-F, Japan).

4.2.6 Wound-healing assay

The antiproliferative activity of PM-H-H, 5-FU, and their combination on CT26 cells was assessed using the scratch-wound assay, as described in previous studies (Asgharzadeh et al., 2022; Y. Chen et al., 2022; S. Kumar et al., 2023). CT26 cells were seeded into 6 well plates and incubated at 37 ℃ in CO_2 incubator for 24 h. The following day, a scratch was made in the center of each well using a 200 µL sterile pipette tip, creating a wound in the cell monolayer. Images of cell migration were captured at 0 and 24 h post-injury. The width of the scratch was measured using ImageJ software, with measurements taken at least seven times. Each experiment was conducted in triplicate.

The migration rate was calculated using the following equation:

$$\text{Migration rate (\%)} = [(W_0 - W_t) \div W_0] \times 100\%,$$

where W_0 is at time 0, and W_t is at 24 h or 48 h, respectively. The reported values are the means from three independent experiments.

4.2.7 Cell apoptosis

This experiment aimed to evaluate the apoptotic effects of combination therapy compared to monotherapy. CT26 cells were seeded into 6 well plates and incubated overnight. Following incubation, the cells were treated with PM-H-H, 5-FU, or a combination of both for 24 h. After treatment, cells were collected by trypsinization, washed with PBS, and resuspended in Annexin V-binding buffer. The cells were then stained with Annexin V-FITC and PI for 15 min in the dark at room temperature. Apoptotic cells were analyzed using flow cytometer (BD FACSCanto II flow cytometer (BD Biosciences, USA)), and the data were processed with BD FACSDiva software. All experiments were performed in triplicate.

4.2.8 Cell cycle

Cell cycle distribution was assessed using flow cytometry. CT26 cell lines were seeded into the 6 well plates and treated with PM-H-H and/or 5-FU for 24 h. Following incubation, the cells were harvested by trypsinization, washed twice with ice-cold PBS, and pelleted by centrifugation. Cells were fixed in 70% ethanol overnight. After fixation, the cells were washed with PBS, stained with PI solution, and incubated at 37 ℃ for 30 min. The cell population in each phase of the cell cycle was analyzed using Flow cytometer (BD FACSCanto II flow cytometer (BD Biosciences, USA)).

4.2.9 Spheroid growth inhibition analysis

Spheroids were cultured as previously described (Deng et al., 2024). Briefly, CT26 cells were seeded in U-shaped 96 well microplates pre-coated with 60 µL of 10% agarose. After 96 h, images of each spheroid were captured using a Nikon Eclipse TS 100-F light microscope (Nikon, Japan). Spheroids were then treated with either the identified drug combinations or individual drugs for 24 h. Every other day, 30% of the treatment-containing medium was replaced. Spheroids were imaged every 3 d, and their diameters were determined by measuring their cross-sectional area using ImageJ software. Results were obtained from 3 independent experiments (n = 3). For each treatment, at least 6 spheroids were measured during each experiment, and the mean spheroid growth was calculated using the following equation:

$$\% \text{ spheroid growth} = dx \div d0 \times 100\%,$$

$$\% \text{ spheroid inhibition} = (dcx - dtx) \div dcx \times 100\%,$$

where dx represents the mean diameter of at least 6 spheroids on a given day of incubation, d0 is the mean diameter of at least 6 spheres at cell seeding day 4 (day of the drug treatment). dcx is the mean diameter of at least 6 control group spheroids on a given day of incubation and dtx is the mean diameter of at least 6 spheroids on a given day of incubation. All sphere diameters are normalized by dividing by the diameter of day 4 (the day of the drug treatment).

4.2.10 Metabolomics

4.2.10.1 Sample preparation

CT26 cells were treated with PM-H-H, 5-FU, or a combination of both for 24 h. After

treatment, cells were washed with PBS twice, and methanol was added to quench the cells while scraping with cell scrapers. Approximately 1×10^9 cells were employed as one sample for NMR analysis, and the cell suspension was transferred into a fresh 5 mL centrifuge tube. Chloroform and ultrapure water were added to the cell suspension, with a mixture of methanol, chloroform, and water in the volume ratio 1:1:0.95. Afterward, the mixture was vortexed and centrifuged at 140000 rpm for 30 min at 4 ℃. The upper aqueous phase was transferred and lyophilized. The lyophilized sample was reconstituted in 6000 μL of 90.9% D_2O (containing 100 mM KH_2PO_4, 0.01% TSP, pH 7.4) and centrifuged at 14000 rpm for 10 min at 4 ℃. The supernatant was then transferred to a 5mm NMR tube for ^{1}H-NMR analysis.

4.2.10.2 ^{1}H-NMR metabolomic analysis

The ^{1}H-NMR spectra of the samples were acquired on a 500 MHz Varian Unity INOVA NMR spectrometer (Varian Inc., Palo Alto, CA, USA). All spectra were subjected to a 64-scan presaturation (PRESAT) pulse sequence to suppress water signals. The Carr-Purcell-Meiboom-Gill (CPMG) pulse sequence was then employed to suppress macromolecule signals, with a spectral width of -2 to 14 ppm, 128 scans, a relaxation delay of 4 s, and an acquisition time of 8.12 min.

4.2.10.3 Metabolomic data analysis

The acquired spectra were phased and baseline-adjusted manually, and the chemical shift of TSP was referenced at δ 0.0. The spectra were then processed using the Chenomx NMR Suite 5.1 Professional (Edmonton, Canada). Region (δ 4.7-4.9) distorted due to residual water was excluded. The spectral regions of δ 0.3 to 10.0 ppm were segmented at 0.04 ppm intervals and all data points were normalized for further

analysis. Assignments of metabolites were conducted using a combination of the Human Metabolome Data Base, Biological Magnetic Resonance Data Bank, and relevant published references. The normalized data were uploaded into the SIMCA 14.1 software for multivariate data analysis. The identified metabolites were screened as differentially expressed metabolites with variable importance in the projection exceeding 1 and $P<0.05$. Volcano plot was carried out to visualize the differences of metabolite expressions, and the pathway enrichment analysis of differentially expressed metabolites was performed by R 4.2.2 software based on the KEGG database (Li et al., 2022).

4.2.11 Proteomics

4.2.11.1 Protein extraction

CT26 cells were treated with PM-H-H, 5-FU, or a combination of both for 24 h. After treatment, the cells were washed with PBS twice and harvested using a cell scraper. Proteins were extracted from the cell pellets with lysis buffer (80 M urea, 705 mM NaCl, 500 mM HEPES, protease inhibitor cocktail, pH 7.0) followed by centrifugation at 140000 rpm for 105 min at 14 ℃. The protein concentration was determined using the BCA protein assay. Subsequently, proteins were reduced with 10 mM DTT for 4 h at 37 ℃ and alkylated with 20 mM IAA for 3 h at 5 ℃. The protein samples were diluted with 50 mM NH_4HCO_3 to ensure urea concentration below 1 M before adding trypsin at a ratio of 1:20 (w/w) to digest the protein samples overnight at 7 ℃, followed by quenching with 1% formic acid. Digested peptides were further purified with C18 tips to remove the salt for nano LC-MS/MS analysis.

4.2.11.2 LC-MS/MS analysis

Desalted peptides were analyzed using the Dionex Ultimate 3000 RSLCnano coupled to an Orbitrap Fusion mass spectrometer (Thermo Fisher Scientific). The peptides were separated by EASY-Spray PepMap column (C18, 100 Å, 2 µm, 50 µm × 15 cm) using mobile phases of A (0.01% formic acid in water) and B (0.01% formic acid in acetonitrile) at a flow rate of 250 nL/min, with a gradient as follows: 5-40% B for 91 min; 40-85% B for 12 min; 85% B for 3 min; 85-5% B for 1 min; 5% B for 4 min. The mass spectrometer was operated in positive ion mode and data-dependent mode. The full scan was performed at the range of 310-1800 m/z at a resolution of 120000 with a maximum injection time of 50 ms. Only precursors with a charge state of 2-7 were further analyzed for MS/MS and filtered using a 20 s dynamic exclusion window and an intensity threshold of 5000. Precursors were fragmented by high-energy collision dissociation and collision-induced dissociation at a normalized collision energy of 28% and 30%, respectively.

4.2.11.3 Proteomic data analysis

Each group consists of three biological samples and each biological sample was injected three times into nano LC-MS/MS as three technical replicates. The raw MS files were processed using the Proteome Discoverer 2.5 software and searched against the UniProt Mus musculus database using the SEQUEST HT search algorithm. False discovery rate (FDR) tolerance in the Percolator node was set to 0.01 and at least one identified unique peptide was required to filter proteins. Student's t-test was used to identify differentially expressed proteins between two groups, where proteins with |fold change|>1.5, and $P<0.05$ were considered significant. The volcano plot and heatmap were generated using R 4.2.2 software, and Gene Ontology (GO) and Kyoto

Encyclopedia of Genes and Genomes (KEGG) enrichment analyses were performed using R 4.2.2 software.

4.2.12 Combined metabolomics and proteomics analysis

KEGG pathway analysis was used to integrate proteomics and metabolomics data. The enriched co-regulated pathways were screened to elucidate the mechanism of PM-H-H in combination with 5-FU against CC.

4.2.13 Statistical analysis

Data were shown as means ± standard deviation (SD) from three independent experiments. SPSS R26.0.0.0 software was used for statistical analysis. The P values were analyzed using ANOVA and $P<0.05$ is considered significant.

4.3 Results and discussion

4.3.1 Determination of the interaction between PM-H-H and 5-FU on CT26 cells

To assess the potential of PM-H-H for synergistic inhibition of CC in combination with 5-FU, the inhibitory effects of PM-H-H, 5-FU, and their combination at various concentrations on CT26 cells were evaluated. The data from MTT assays were analyzed using CompuSyn software, as described by Chou et al. (2006), to determine the CI and the DRI, as shown in Figure 4.1 and Table 4.1. The results indicated that the combination of 5-FU and PM-H-H resulted in CI values of less than 1, demonstrating a synergistic effect in CT26 cells. The combination of PM-H-H (75 μg/mL) and 5-FU (7.5 μM) exhibited the strongest synergistic effect. Consequently,

these concentrations were selected for subsequent experiments. Additionally, the synergistic effects suggested a dose reduction of 1.44 to 11.89-fold for 5-FU and 1.11 to 10.93-fold for PM-H-H.

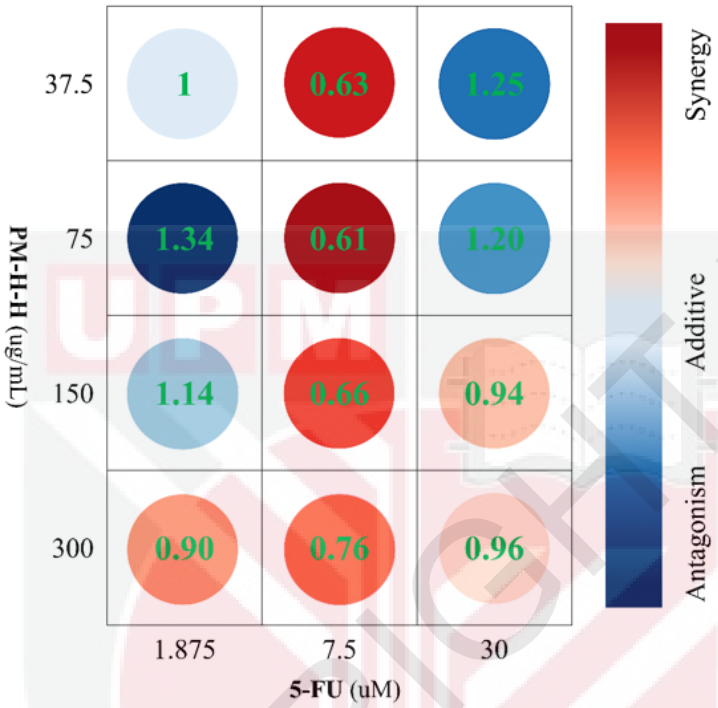

Figure 4.1: CI of the combination treatments of PM-H-H and 5-FU on CT26 cells.

Table 4.1: DRI of the combination treatments of PM-H-H and 5-FU on CT26 cells.

Drug combination		DRI	
PM-H-H (µg/mL)	5-FU (µM)	PM-H-H	5-FU
37.5	1.875	2.26	1.79
37.5	7.5	7.27	2.03
37.5	30	10.93	0.86
75	1.875	1.21	1.96
75	7.5	4.43	2.62
75	30	6.00	0.97
150	1.875	1.11	4.27
150	7.5	2.71	3.40
150	30	4.08	1.44
300	1.875	1.22	11.89
300	7.5	1.79	4.87
300	30	2.43	1.81

The type of drug interaction was assessed using the CI calculation (Duarte & Vale, 2022). The results demonstrated that 5-FU and PM-H-H exhibited synergistic effects in CT26 cells at specific concentration combinations. The Chou-Talalay method was used to determine the DRI value (Chang & Chou, 2000). The DRI quantifies the extent to which the concentration of compounds can be reduced while maintaining the same therapeutic effect when administered in combination compared to when administered separately (Baum et al., 2020; Chou, 2014). The DRI calculated for 5-FU and PM-H-H in CT26 suggested that the effective concentration of 5-FU could be reduced by 1.44 to 11.89 times in CT26 cells when combined with PM-H-H. This implies that the combination of PM-H-H enhances the chemotherapy sensitivity of 5-FU, allowing for

a reduced dosage of 5-FU, thereby minimizing its toxicity.

The synergistic effects of herbal extracts in combination with chemotherapeutic agents have been reported in various studies, supporting the potential of natural compounds in cancer treatment. For example, curcumin (from Curcuma longa) has been shown to enhance the cytotoxic effects of 5-FU in CC by modulating apoptotic pathways and drug resistance mechanisms (Shakibaei et al., 2013). Similarly, the combination of resveratrol (from grapes) and 5-FU demonstrated synergistic effects by inducing cell cycle arrest and apoptosis in CC models (Brockmueller et al., 2023). In another study, epigallocatechin gallate from green tea potentiated the effects of oxaliplatin, a standard CC chemotherapy agent, by inhibiting cell proliferation and modulating oxidative stress (Saleem et al., 2024). By demonstrating a strong synergistic effect between PM-H-H and 5-FU, this study adds to the growing body of evidence supporting the use of plant-based compounds to enhance chemotherapy outcomes. Future studies should explore the mechanistic basis of these interactions to optimize their therapeutic potential.

4.3.2 Cell morphology

The morphology of CT26 cells was examined after 24 h of exposure to PM-H-H, 5-FU, and their combination, as showed in Figure 4.2. The combination of PM-H-H with 5-FU enhanced the sensitivity of CT26 cells to 5-FU treatment. Observations indicated that many cells detached from the plate surface, particularly in the combination treatment group. Microscopic imaging revealed notable morphological changes: a reduction in cell number, loss of intercellular contact, decreased cell-cell interactions, and an increase in exfoliated cells in the combination treatment group compared to the

single treatment groups (PM-H-H or 5-FU).

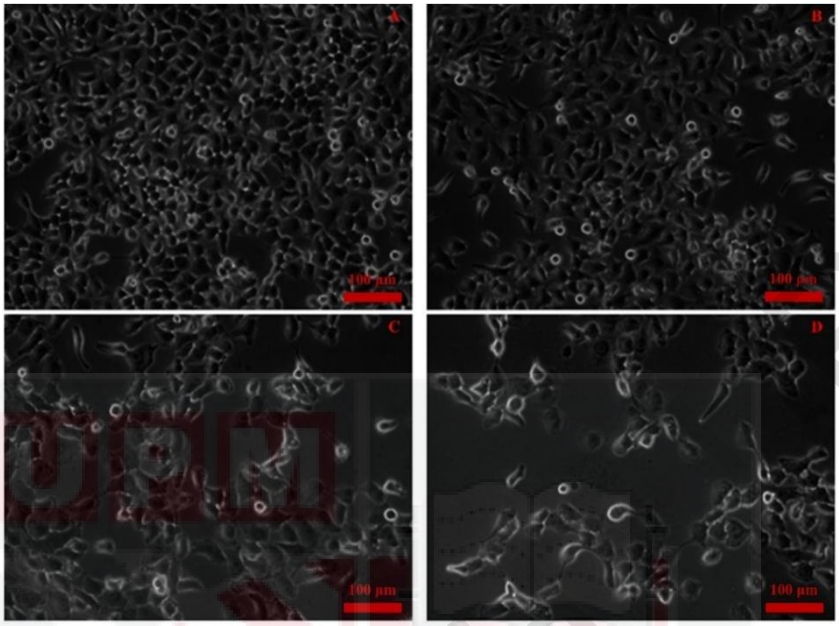

Figure 4.2: Cell morphological changes in CT26 cells after treatment with PM-H-H, 5-FU, and their combination. An inverted microscope with 100 μm scale bars was used, and representative photos of cell morphology were captured. A: control, B: PM-H-H, C: 5-FU, D: PM-H-H plus 5-FU.

Data on the interaction between PM-H-H and 5-FU in CT26 cells were supported by morphological observations, which showed significant changes in cell morphology, such as cell shrinkage and cell wall blabbing. Additionally, the reduction in cell number induced by the combination treatment was evident compared to single treatment (PM-H-H or 5-FU) cells (Figure 6), typically indicating cytotoxicity and the induction of apoptosis in the cells (Nguyen et al., 2020).

4.3.3 AO/PI staining

To confirm the synergistic antiproliferative effects of PM-H-H and 5-FU on CT26 cells, an AO/PI double staining assay was conducted to microscopically examine cell death. Fluorescence staining results revealed that untreated cells appeared as large, green

colonies, indicating cell viability (healthy cells) (Figure 4.3). In contrast, cells treated with PM-H-H, 5-FU, and particularly their combination, exhibited a decrease in green (healthy cells) cells and an increase in red (apoptotic) cells, along with a reduction in colony size. Meanwhile, cells treated with the PM-H-H and 5-FU combination also displayed significant morphological changes, including loss of membrane integrity, cell shrinkage, membrane damage, organelle breakdown, and detachment from the culture plate.

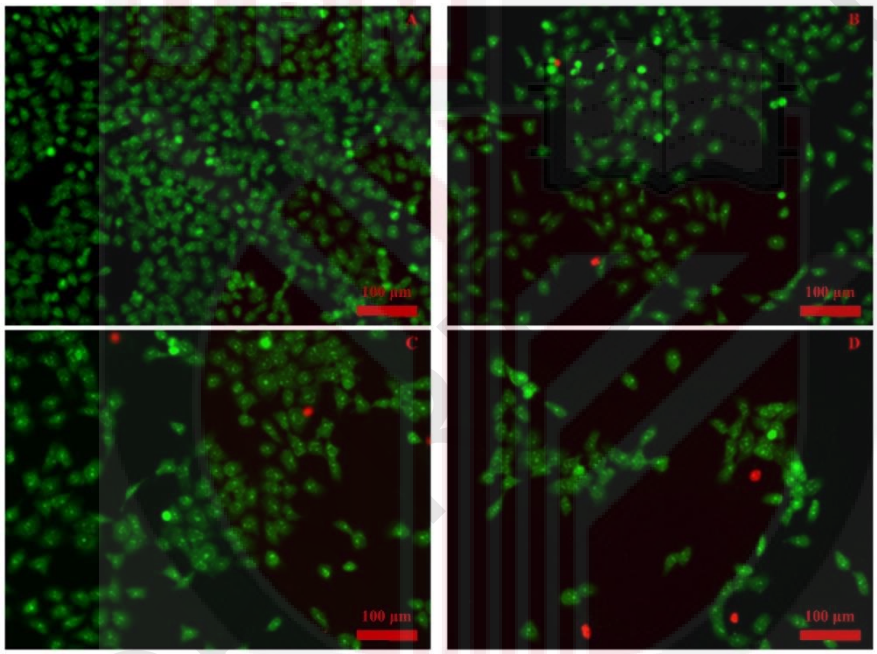

Figure 4.3: Fluorescence microscopy images of cell lines stained with AO and PI. An inverted microscope with 100 µm scale bars was used, and representative photos of cell morphology were captured. A: control, B: PM-H-H, C: 5-FU, D: PM-H-H plus 5-FU.

The AO/PI staining method is a rapid, sensitive, and effective technique for examining cellular morphology, including live and dead cells, as well as apoptosis and necrosis (Mbemi et al., 2020). In addition, AO/PI double staining assay can be mutually verified with cell morphology analysis (Koosha et al., 2019). In this study, the synergistic antiproliferative effects of PM-H-H and 5-FU on CT26 cells were evaluated using the AO/PI double staining assay. Early apoptotic cells, indicated by bright green

fluorescence, were observed in the control group, likely due to excessive cell density (Krampe & Al-Rubeai, 2010; Vicar et al., 2020). Some early apoptotic cells were also observed in the treatment group. However, since the cell density in the treatment group was lower than that in the untreated group, it is reasonable to infer that the treatment drugs induced early apoptosis. Validation through cell cycle experiments is still required. Based on the cell count in each group, the outcomes of this experiment correspond well with the analysis of cell morphology.

4.3.4 Clonogenic formation assay

Colony formation was inhibited by all treatments, with the combined treatment being the most effective against cell colony formation, indicating that the cells' ability to divide was inhibited by PM-H-H, 5-FU, and co-treatment (Figures 4.4 and 4.5).

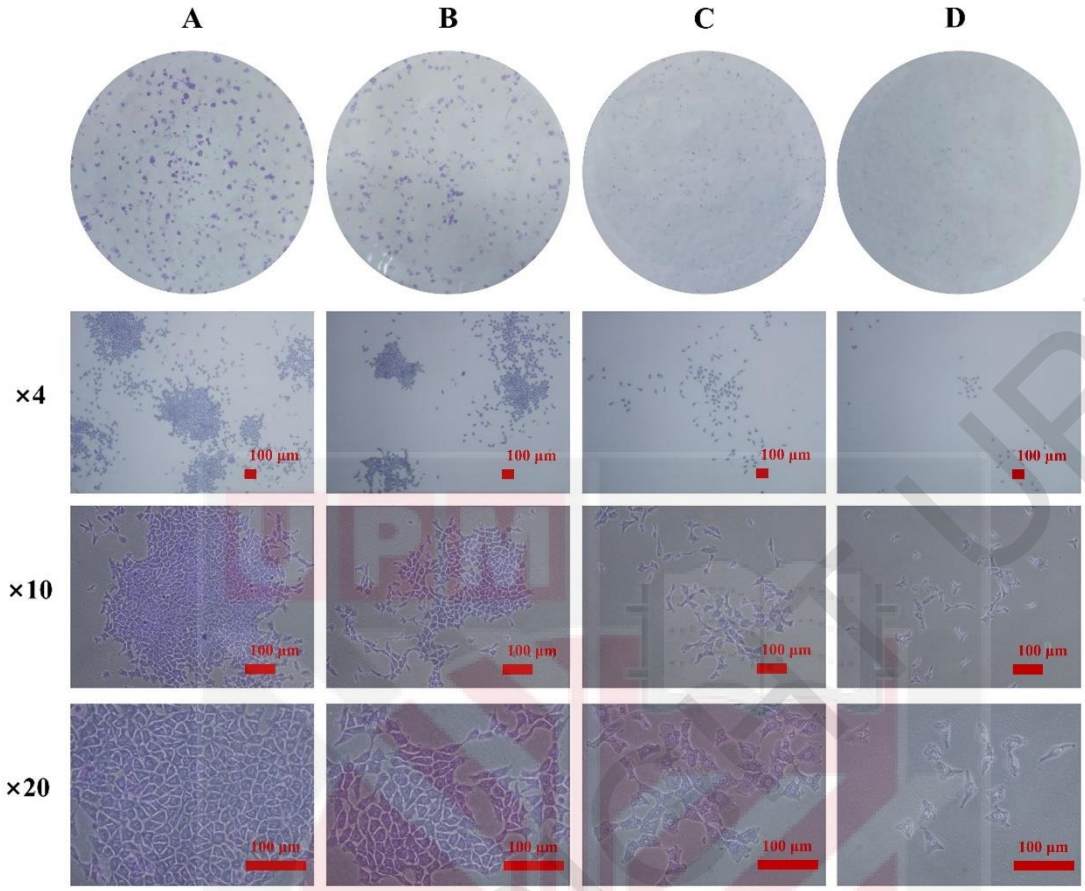

Figure 4.4: Representative photographs of the clonogenic formation assay on CT26 cells. 100 µm scale bars were used. A: control, B: PM-H-H, C: 5-FU, D: PM-H-H plus 5-FU.

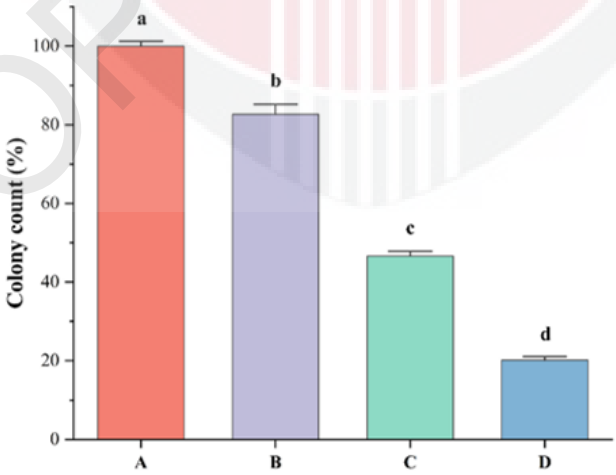

Figure 4.5: Graph showing % of CT26 colonies formed relative to control. The results with the different superscripts (a-d) indicate significant differences ($P<0.0001$).

To further validate the synergistic antiproliferative effects of the PM-H-H and 5-FU combination, clonogenic assays were conducted. A clonogenic assay was performed to mimic cancer growth from single mutated cells to form cancer cell colonies or tumor mass (Brix et al., 2021). In the control group, CT26 cells successfully formed colonies within 7 d. all treatment groups exhibited a significant reduction in colony number and inhibited colony formation. Since successful cancer development and metastasis depend on the cells' ability to proliferate and migrate (Fares et al., 2020), reducing these factors may be an effective strategy to prevent early metastasis. Therefore, decreasing these two factors could be a suitable strategy to prevent early metastasis of the cancer. Previous results indicated that PM-H-H and 5-FU both suppressed CT26 cell migration, with combination treatment showing superior inhibition compared to single agents. To gain a deeper understanding of the mechanisms behind the combined anti-proliferative and anti-migrative effects of PM-H-H and 5-FU, further analysis of the cell cycle and apoptosis is warranted.

4.3.5 Cell migration

The effects of PM-H-H, 5-FU, and their combination on CT26 cell migration were evaluated using a wound-healing assay. Migration capacity was assessed by measuring the closure rate of the wound at 24 and 48 h compared to 0 h (Figure 4.6). After 24 h of treatment, cells exposed to PM-H-H, 5-FU, and the PM-H-H/5-FU combination showed 31.59%, 26.12%, and 20.90% wound closure, respectively, which was significantly lower than the control cells. Control cells healed approximately 43.03% of the wound width in 24 h (Figure 4.7). As the treatment duration increased, the inhibitory effect on cell migration persisted. Notably, the combination of PM-H-H and 5-FU exhibited a more pronounced inhibition of cell migration compared to either

treatment alone, regardless of the treatment duration.

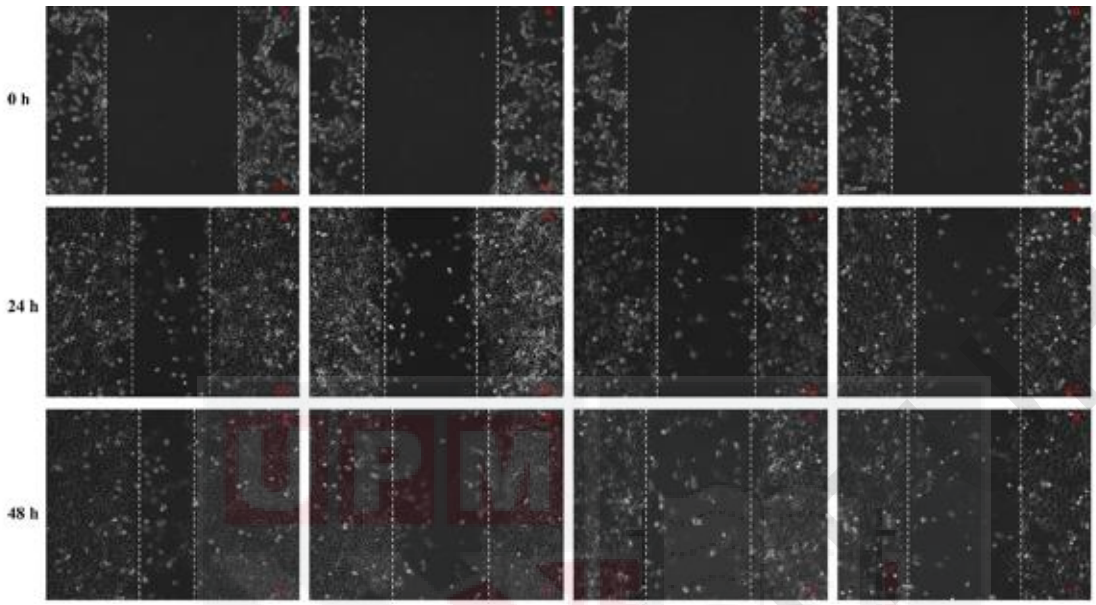

Figure 4.6: Effect of PM-H-H, 5-FU, and PM-H-H plus 5-FU on the migration of CC model, representative pictures of the wound-healing assay in CT-26 cells in 24 and 48 h. A: control, B: PM-H-H, C: 5-FU, D: PM-H-H plus 5-FU.

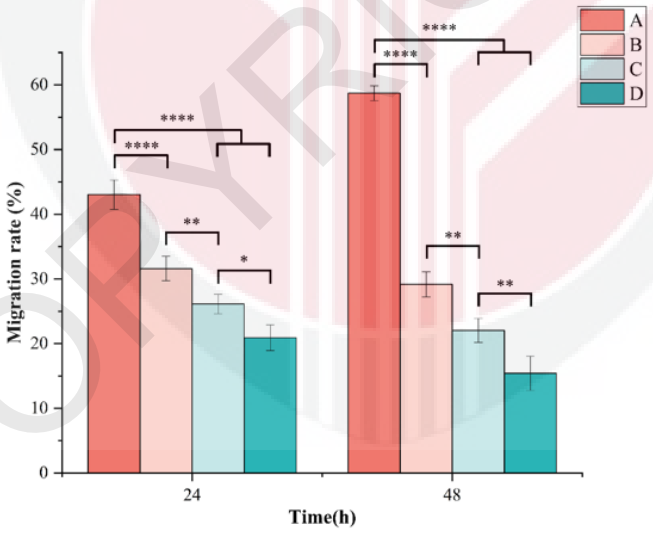

Figure 4.7: CT26 cells migration was observed at the indicated concentration and healing rate was analyzed by ImageJ. Each experiment was repeated at least 3 times. *P<0.05, **P<0.01, ***P<0.001, ****P<0.0001.

Cancer cell migration is a key factor in metastasis, which is the leading cause of cancer-related mortality in patients with CC (Amin et al., 2021; Deyell et al., 2021). To assess the antimetastatic effects of PM-H-H, 5-FU, and their combination on CT26 cell lines,

wound healing assays were conducted. The results indicated that PM-H-H and 5-FU suppressed the migration of CT26 cell lines. Interestingly, the combination treatment demonstrated greater suppression of migration compared to single treatments.

4.3.6 Cell apoptosis

The Annexin V-FITC assay was used to assess cellular apoptosis induced by monotherapy and combination therapy. The results showed that PM-H-H primarily induces early and late apoptosis in CT26 cells, whereas 5-FU and co-treatment mainly trigger early apoptosis. Notably, the combination treatment resulted in a higher incidence of early or late apoptosis compared to either treatment alone (Figure 4.8). Flow cytometry data revealed that the highest percentage of apoptotic cells (48.03%) was observed in the combination treatment group, compared to 13.49% with PM-H-H alone and 32.23% with 5-FU alone (Figure 4.9).

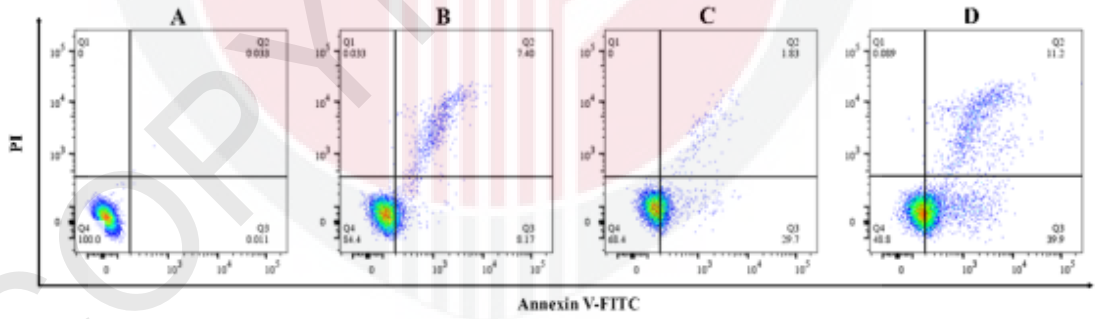

Figure 4.8: Flow cytometry graphs in CT26 cells after 24 h of monotherapy and combination therapy. A: control, B: PM-H-H, C: 5-FU, D: PM-H-H plus 5-FU.

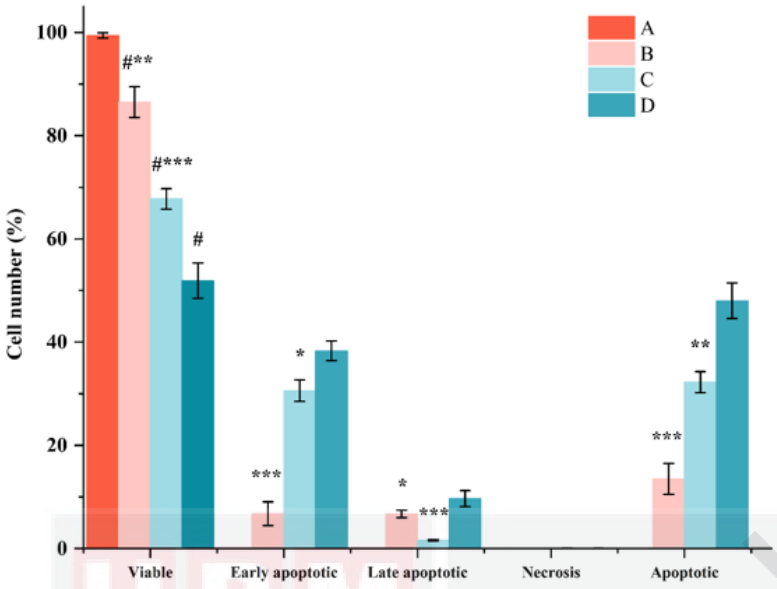

Figure 4.9: Flow cytometry apoptosis quantification in CT26 cells after 48 h of monotherapy and combination therapy. The control group remained untreated. Total apoptotic cells (early apoptosis + late apoptosis). $^{\#}P<0.0001$, vs control group. While $^{*}P<0.01$, $^{**}P<0.001$, $^{***}P<0.0001$, vs (PM-H-H + 5-FU) group.

Apoptosis is a highly regulated process of cell death that is considered a promising approach for developing chemotherapy treatments for various cancers (Chien et al., 2022). It also plays a crucial role in maintaining normal tissue homeostasis. Thus, targeting apoptosis could be an effective strategy for preventing the progression of CC (Kamran et al., 2022). In this study, early-stage apoptosis in CT26 cells treated with 5-FU was observed at 30.6%, while late-stage apoptosis was 1.63%. These findings align with recent studies (L. Xie et al., 2023). Combination therapy with PM-H-H and 5-FU significantly increased the proportion of apoptotic cells to 48.03% compared to single-agent treatment. This demonstrates that the combination of PM-H-H and 5-FU exhibits a synergistic anticancer effect in CT26 cells.

4.3.7 Cell cycle

Cell cycle distribution was analyzed using PI staining and flow cytometry, with representative results shown in Figure 4.10. In the control group, CT26 cells were

distributed as follows: 30.43% ± 0.35% in the G0/G1 phase, 53% ± 0.2% in the S phase, and 16.57% ± 0.15% in the G2/M phase. However, treatment with PM-H-H and the combination of PM-H-H with 5-FU results in significant changes in cell cycle distribution compared to the control. On the other hand, PM-H-H increased the accumulation of G0/G1 phase cells treated with 5-FU and decreased the accumulation of S and G2/M phase cells treated with 5-FU (Figure 4.11).

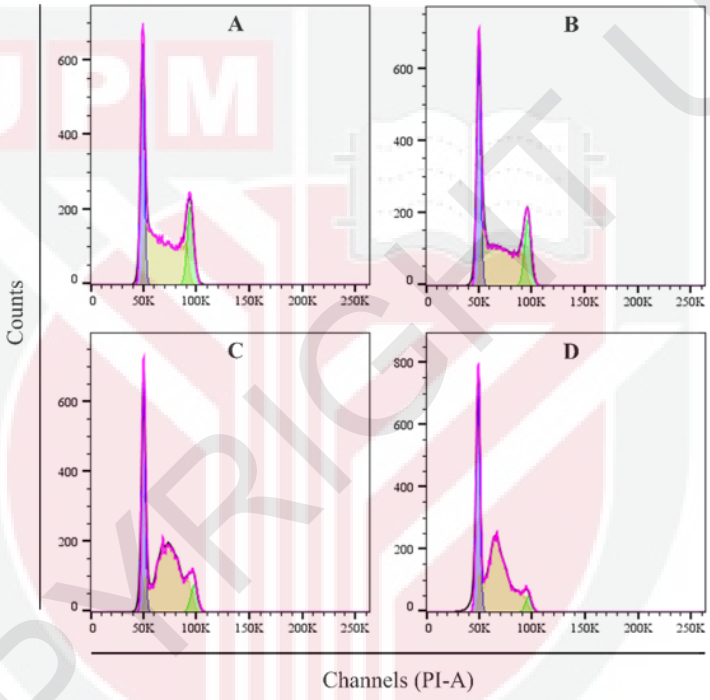

Figure 4.10: The effects of PM-H-H and/or 5-FU on the cell cycle.

Cell cycle distribution was examined by PI staining and flow cytometry in CT26 cell lines after treatment with 5-FU and/or PM-H-H for 48 h. A: control, B: PM-H-H, C: 5-FU, D: PM-H-H plus 5-FU. Data shown are a representative example of three separate experiments with similar results.

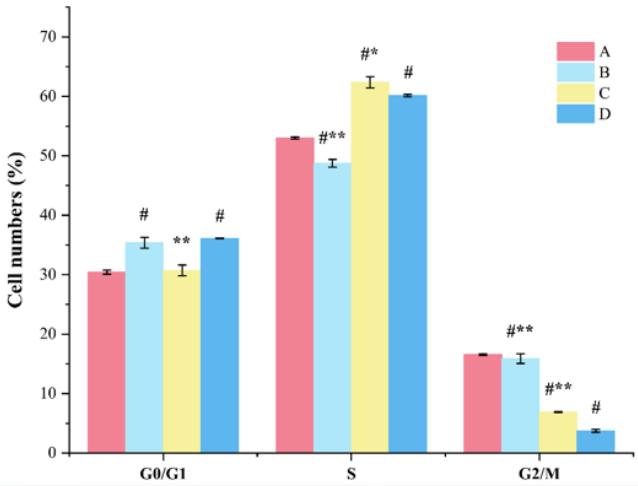

Figure 4.11: G0/G1, S, and G2 phase cell population of PM-H-H and/or 5-FU treated CT26 cells. #P<0.0001, vs control group. While *P<0.01, **P<0.0001, PM-H-H or 5-FU group vs (PM-H-H + 5-FU) group.

Cancer cells often exhibit cell cycle abnormalities that lead to uncontrolled proliferation (Liu et al., 2020b). Previous studies have reported that ethyl acetate extracts of PM exhibit antiproliferative effects on HepG2 cells by inhibiting the cell cycle at the S-phase (Mohd Ghazali et al., 2014). Similar to the findings, flow cytometric analysis of cells exposed to 5-FU revealed a significant reduction in cells in the G2/M phases. These results are consistent with previous studies (Mun et al., 2022). Combined treatment with PM-H-H and 5-FU resulted in a significant increase in G0/G1 phase accumulation and a marked decrease in the S and G2/M phases sharply decreased which strongly supports the ability of PM-H-H to enhance the effects of 5-FU. As a result, the cell cycle arrest in G0/G1 phase was probably one of the underlying mechanisms of synergistic interactions between PM-H-H and 5-FU.

4.3.8 Spheroid growth inhibition analysis

The efficacy of synergistic drug combinations in inhibiting tumor spheroid growth was evaluated, and these results were compared with those from single-agent treatments

(Figures 4.12 and 4.13). Untreated spheroids initially grew and increased in size until a decrease occurred on day 14 d. Treatment with PM-H-H, 5-FU, and their combination significantly altered the spheroid morphology, particularly in size. Figure 4.13 shows that the most profound change after incubation with the tested compounds was the significant inhibition of their growth compared to that of untreated control cultures. Moreover, PM-H-H plus 5-FU showed the strongest inhibitory effect among all treatments.

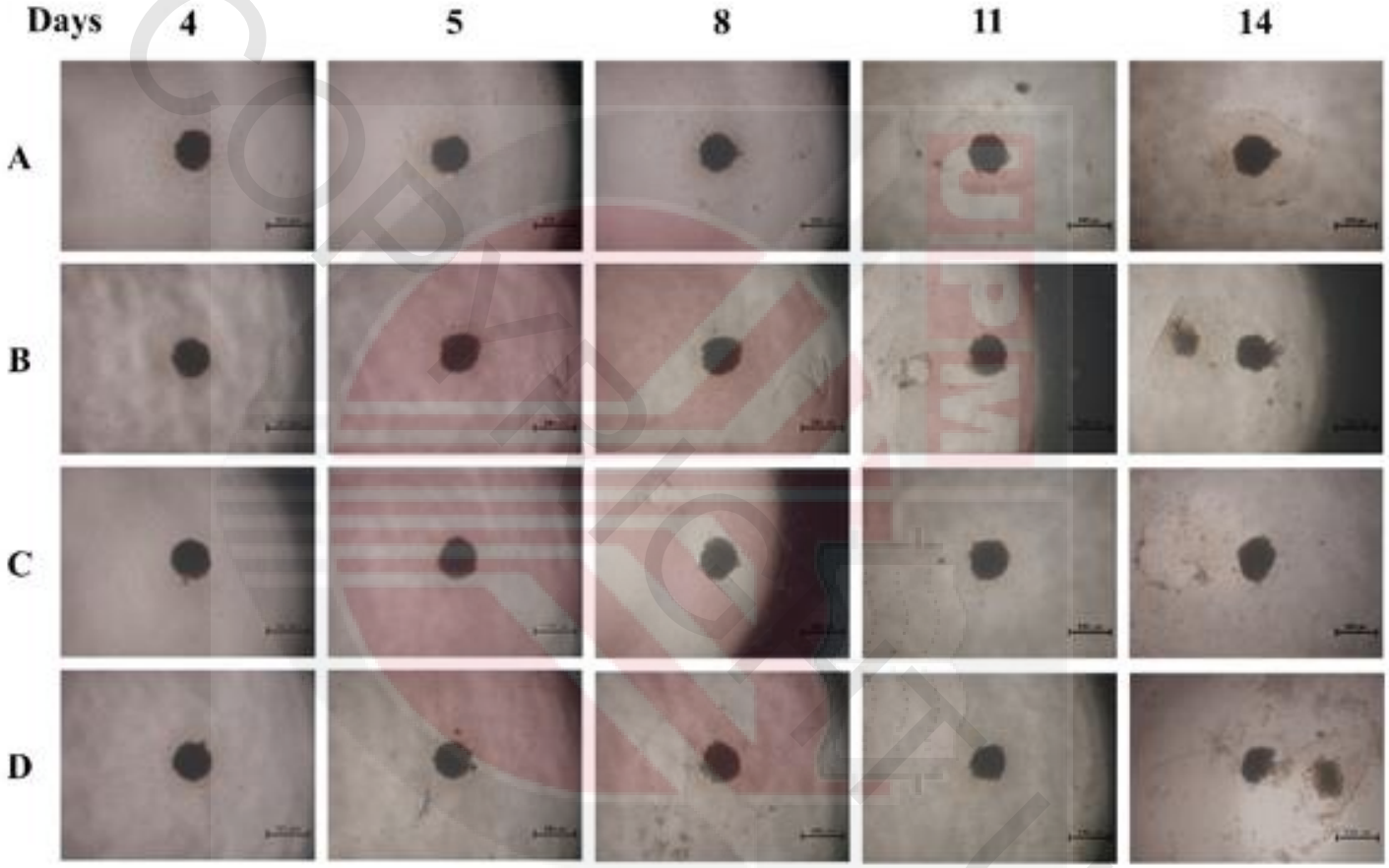

Figure 4.12: Representative images of spheroids cultured for indicated. Scale bars, 500 µm. A: control, B: PM-H-H, C: 5-FU, D: PM-H-H plus 5-FU. Untreated spheroids initially grew and increased in size until a decrease occurred on day 14 d. Treatment with PM-H-H, 5-FU, and their combination significantly altered the spheroid morphology, particularly in size.

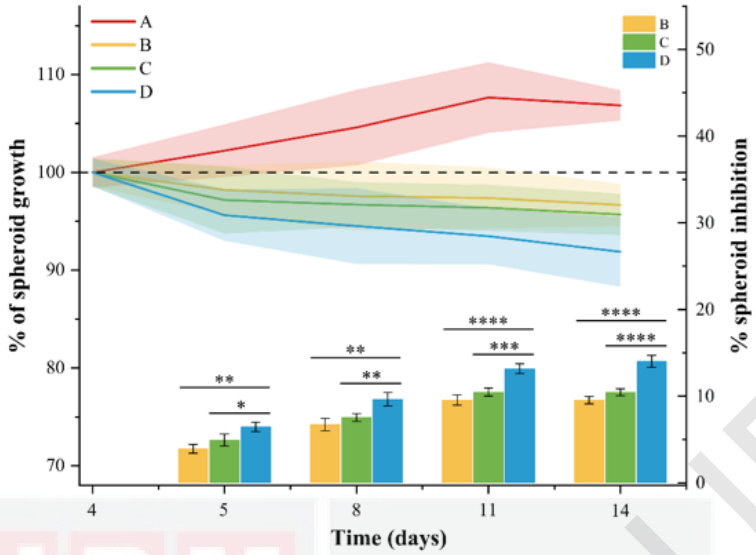

Figure 4.13: Percentages of spheroid growth and inhibition over time. *P<0.05, **P<0.01, ***P<0.001, ****P<0.0001. A: control, B: PM-H-H, C: 5-FU, D: PM-H-H plus 5-FU.

Traditional 2D monolayer cell cultures are valuable for assessing the biochemical and molecular effects of new compounds (Habanjar et al., 2021). However, it often overlooks cell heterogeneity, cellular interactions, and nutrient gradients (K. Gong et al., 2022). Additionally, 2D cultures fail to adequately represent drug penetration into tumors and their effects on patient tissues (M. Huang et al., 2022). 3D cell cultures are emerging as crucial tools in drug testing and anticancer research (Kulesza et al., 2021). 3D cancer cell spheroids offer a more accurate model of the tumor microenvironment compared to conventional 2D cultures (Yusoh et al., 2023). In our experiments, CT26 cell spheroids in the control group showed a gradual increase in diameter over 4 days, with a decrease in size observed by day 14, consistent with previous findings (Deng et al., 2024). It is worth mentioning that PM-H-H, 5-FU, and the combination of PM-H-H with 5-FU effectively inhibited tumor growth. Although these treatments were less impactful in 3D spheroid cultures compared to 2D cultures, the synergistic growth-inhibitory effects of PM-H-H and 5-FU were still evident. In summary, both PM-H-H and 5-FU exhibit potent synergistic inhibitory effects on CT26 cells, whether grown

in monolayer cultures or as spheroids.

4.3.9 Metabolomics analysis

4.3.9.1 ^{1}H NMR spectra analysis of cell metabolites

To reveal metabolic distinctions between each group, NMR-based metabonomic analyses were performed on aqueous extracts derived from each group of CC cells. The ^{1}H NMR spectra of cells from the different groups are shown in Figure 4.14. Totally, 26 metabolites were identified based on the NMR spectra.

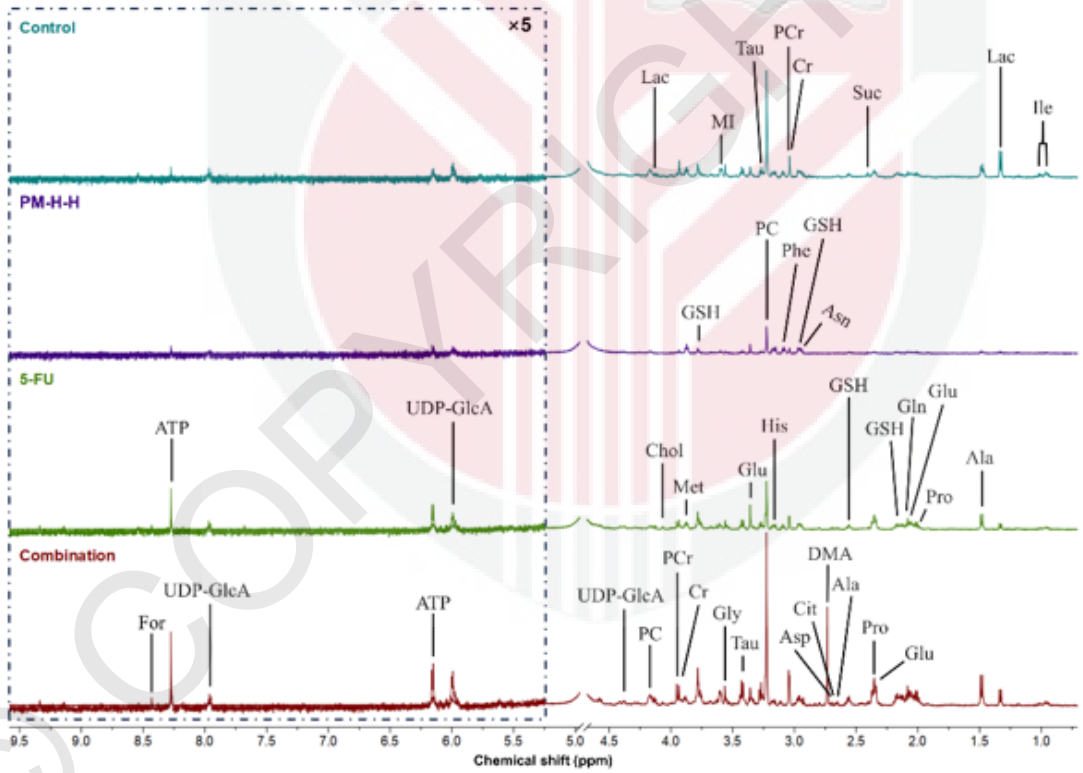

Figure 4.14: Typical ^{1}H NMR spectra of CC obtained from control, PM-H-H, 5-FU, and combination (PM-H-H + 5-FU) groups.

The results of the NMR-based metabonomic analyses revealed distinct metabolic profiles across the different groups of CC cells. The ^{1}H NMR spectra (Figure 4.14) enabled the identification of 26 metabolites, underscoring the differential metabolic

activities in the cell groups. The distinct separation of metabolites across these groups likely reflects variations in cellular metabolic processes influenced by the experimental conditions (Pavlova et al., 2022; Voss et al., 2021).

4.3.9.2 Multivariate statistical analysis of cell metabolites

Both PCA and OPLS-DA of the normalized NMR data were performed to evaluate the effects of each treatment on the metabolic profiles of the CC cells. All the samples are situated in the Hotelling's T2 oval of the 95% confidence intervals (Figures 4.15 and 4.16).

PCA is a pattern recognition method to simplify the complex relationship between variables, which could give an overview of all serum samples and examine the intrinsic variation within the groups. As revealed in PCA the score plot (Figure 4.15), the first two principal components (t1 and t2) could explain 68.8% of the total variance. Moreover, to find metabolites from each group, an OPLS-DA model was used between the control group and the model group. As shown in the score plot (Figure 4.16), each group appeared an obvious separation, suggesting significant differences between each group. The permutation test was used to further verify the model, with values of R^2X= 0.75, R^2Y= 0.878, and Q^2 = 0.787, indicating robust statistical models.

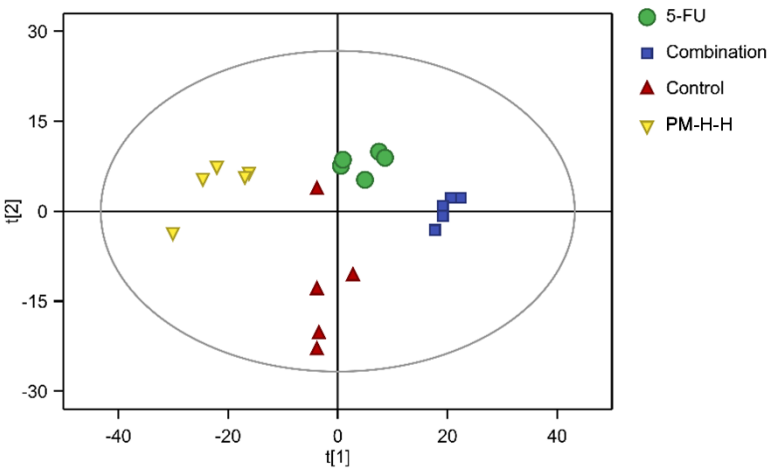

Figure 4.15: PCA scores plots based on ^{1}H NMR data of cells from control, PM-H-H, 5-FU, and combination (PM-H-H + 5-FU) groups. PCA: principal component analysis.

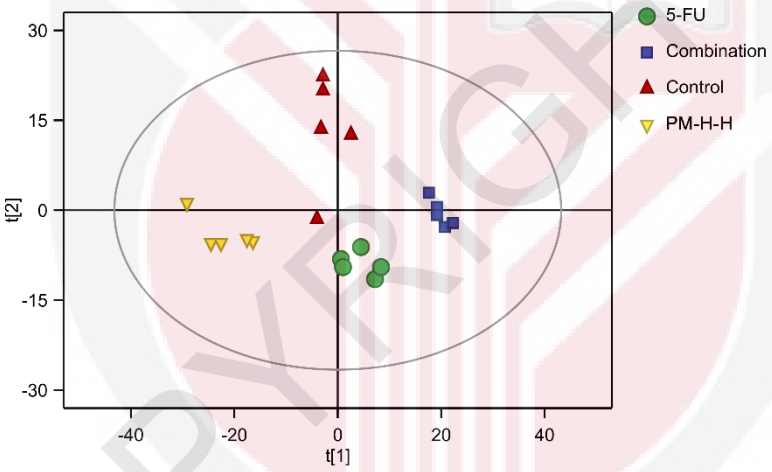

Figure 4.16: OPLS-DA scores plots based on ^{1}H NMR data of cells from control, PM-H-H, 5-FU, and combination (PM-H-H + 5-FU) groups. OPLS-DA: orthogonal partial least squares-discriminant analysis.

The application of principal component analysis (PCA) and orthogonal partial least squares-discriminant analysis (OPLS-DA) to the normalized NMR data provided valuable insights into the metabolic effects of the treatments on CC cells (Esturau-Escofet et al., 2022; C. He et al., 2020). Both PCA and OPLS-DA effectively captured the variation in the metabolic profiles across the different treatment groups, situating all samples within the 95% confidence intervals of the Hotelling's T2 ellipse (Figures 4.15 and 4.16), thus ensuring the reliability of the data (Y. Pan et al., 2022).

PCA, as a dimensionality reduction method, simplified the complex relationships between the numerous metabolites (Posma et al., 2020). The PCA score plot (Figure 4.15) revealed that the first two principal components (t1 and t2) accounted for 68.8% of the total variance, suggesting a strong ability to capture the majority of the intrinsic variability within the dataset. This high percentage of variance explained by the first two components indicates a clear differentiation in the metabolic profiles of CC cells, likely due to the effects of various treatments (Andersen et al., 2021). The clustering patterns observed in the PCA score plot demonstrate that treatment-specific metabolic alterations are present and distinguishable between the groups (Schoen & Singh, 2022). Furthermore, PCA provided an unbiased overview of the metabolic landscape, making it possible to detect inherent similarities and differences between the control and treated cells (Blaise et al., 2021).

To further elucidate the metabolic distinctions between groups, OPLS-DA was performed, offering a more targeted approach to identifying significant metabolites (Lin et al., 2021). The score plot (Figure 4.16) demonstrated a clear separation between the control and model groups, signifying substantial metabolic differences induced by the treatments (L. Pan et al., 2020). The robust discrimination achieved by OPLS-DA is further supported by the permutation test results, with values of R^2X= 0.75, R^2Y= 0.878, and Q^2 = 0.787, respectively, indicating that the model is both reliable and predictive. These values suggest that the OPLS-DA model effectively captures the systematic variation between the groups, with minimal risk of overfitting. The separation observed in the OPLS-DA score plot highlights key metabolic alterations caused by the treatments, supporting the hypothesis that distinct pathways are activated

or suppressed in the CC cells. These results demonstrate the significant metabolic impact of the treatments.

4.3.9.3 Global comparative metabolite analysis

The variable importance projection (VIP values) could be obtained from these models. The difference multiple of each metabolite content (fold-change) between the pair-wise groups and the transformed P value after the t-test could be calculated and analyzed. Based on VIP>1 and the degree of perturbation of the evaluated metabolites, the fold change of these metabolites was computed and is shown in Figure 4.17. Accordingly, the characteristic metabolites with significant differences between the pair-wise groups can be screened out to characterize CC and its management. As a result, for the combination group and control group, 18 of the metabolites showed significant changes in CC cells, including the higher levels of glutamate, aspartate, glutamine, lipid, dimethylamine, proline, succinate, taurine, ATP (adenosine triphosphate), glutathione, alanine, and creatine, and the lower levels of phosphocreatine, methionine, UDP-glucuronate, histidine, phenylalanine, and asparagine in the combination group than the control group. We also compared the changes in the relative concentration of differential metabolites between the different groups. It was found that the contents of 7 differential metabolites, including glutamate, ATP (adenosine triphosphate), lipid, proline, glutamine, succinate, and glutathione demonstrated a recovered trend in the 5-FU group compared with the control group, while 7 differential metabolites, including choline, taurine, glycine, histidine, UDP-glucuronate, lactate, and phosphocholine demonstrated a decreased trend. 2 differential metabolites demonstrated a recoverable metabolic trend in the PM-H-H group compared with the control group, including phosphocreatine and histidine, while

9 differential metabolites, including phosphocholine, lactate, choline, taurine, isoleucine, creatine, alanine, glutamate, and glycine have a decreased trend. In addition, the comparison results between other groups can be seen in Figure 4.17. The results showed that both 5-FU and PM-H-H could regulate the metabolic profile of CT26 cells, and their combined treatment had a synergistic effect.

Metabolites	PM-H-H *vs* Ctrl		5-FU *vs* Ctrl		Com *vs* Ctrl		Com *vs* 5-FU		Com *vs* PM-H-H	
	log_2FC	P-Value	log_2FC	P-Value	log_2FC	P-Value	log_2FC	P-Value	log_2FC	P-Value
Isoleucine	-10.20	0.01	\	\	\	\	\	\	\	\
Lactate	-13.67	0.00	-10.66	0.04	\	\	12.27	0.00	\	\
Alanine	-1.09	0.04	\	\	1.27	0.01	\	\	1.80	0.00
Proline	\	\	1.12	0.01	1.36	0.00	\	\	2.12	0.00
Lipid	\	\	1.35	0.00	1.49	0.00	\	\	2.08	0.00
Glutamate	-0.97	0.04	1.55	0.00	1.74	0.00	\	\	2.58	0.00
Glutamine	\	\	0.88	0.01	1.17	0.00	\	\	2.02	0.00
Glutathione	\	\	0.85	0.02	1.19	0.00	0.52	0.02	1.19	0.01
Succinate	\	\	0.88	0.01	0.97	0.00	\	\	\	\
Aspartate	\	\	\	\	16.28	0.00	13.21	0.00	10.86	0.01
Dimethylamine	\	\	\	\	15.37	0.00	18.15	0.00	13.39	0.00
Asparagine	0.90	0.05	\	\	-0.49	0.04	-0.58	0.01	-1.39	0.00
Creatine	-9.64	0.02	\	\	0.73	0.04	1.07	0.00	10.38	0.01
Phosphocreatine	1.65	0.00	\	\	-3.27	0.00	-2.73	0.00	-4.93	0.00
Phenylalanine	\	\	\	\	-1.05	0.03	\	\	\	\
Histidine	1.17	0.01	-0.92	0.01	-1.70	0.00	-1.47	0.00	-2.87	0.00
Phosphocholine	-14.30	0.00	-6.62	0.04	0.43	0.05	1.85	0.00	13.82	0.00
Taurine	-12.84	0.00	-12.84	0.00	0.96	0.00	0.95	0.00	2.56	0.01
Glycine	-8.40	0.04	-0.88	0.01	\	\	1.13	0.00	8.54	0.04
Myo-Inositol	-7.98	0.05	\	\	\	\	\	\	8.17	0.04
Methionine	\	\	\	\	-1.08	0.00	0.59	0.03	-1.57	0.00
Choline	-13.16	0.00	-13.16	0.00	\	\	\	\	\	\
UDP-glucuronate	\	\	-2.22	0.03	-1.41	0.01	\	\	\	\
ATP (Adenosine triphosphate)	\	\	1.80	0.00	1.81	0.00	\	\	1.60	0.00

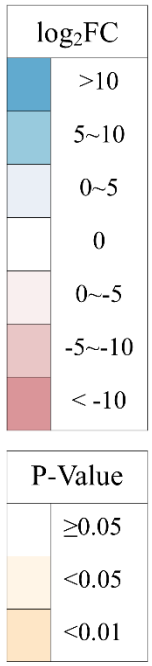

Figure 4.17: Quantitative comparisons of metabolite levels between each group of CT26 cells. Ctrl: control, Com: combination (PM-H-H + 5-FU).

The results from the VIP (variable importance projection) analysis, coupled with the fold-change calculations and t-test, provided critical insights into the metabolic shifts induced by the different treatments in CC cells (Z. Huang et al., 2020). The VIP values (VIP>1) allowed the identification of key metabolites with significant perturbations, enabling a deeper understanding of how treatments influence the metabolic landscape of CC (X. Xia et al., 2022). Previous research metabolites were identified as significantly altered in the combination treatment group compared to the control group, reflecting both the complexity of cancer metabolism and the effects of therapeutic intervention.

Specifically, the combination treatment resulted in elevated levels of metabolites such as alanine, proline, lipid, glutamate, glutamine, glutathione, aspartate, dimethylamine, and ATP, while phosphocreatine, phenylalanine, methionine, and UDP-glucuronate were decreased. These findings suggest that the combination of 5-FU and PM-H-H triggered substantial metabolic reprogramming in CC cells, likely reflecting alterations in key biochemical pathways such as amino acid metabolism, energy production, and membrane biosynthesis (D. Wang & Wan, 2022).

Comparison between the groups treated with 5-FU or PM-H-H alone further highlighted distinct metabolic responses, indicating different mechanisms of action. The 5-FU-treated cells exhibited a recovery in metabolites such as ATP, proline, and succinate, suggesting a partial restoration of mitochondrial function and oxidative metabolism. This aligns with previous findings where 5-FU induces metabolic stress, triggering adaptive responses that support cell survival despite chemotherapy-induced damage (Mapuskar et al., 2023; S. Sharma et al., 2024; Zong et al., 2024). However,

this adaptation may contribute to drug resistance over time. In contrast, PM-H-H treatment alone led to decreased levels of lactate and phosphocholine, indicating a disruption of glycolysis and altered membrane lipid metabolism. The reduction in lactate suggests that PM-H-H interferes with anaerobic energy production, a hallmark of cancer metabolism (B. Liu et al., 2023; Shiratori et al., 2019; Tufail et al., 2024). Additionally, the suppression of phosphocholine levels implies that PM-H-H affects lipid signaling pathways, which are crucial for cell membrane integrity and tumor progression. These findings suggest that PM-H-H exerts anticancer effects through different metabolic targets compared to 5-FU. The combination of 5-FU and PM-H-H demonstrated a synergistic effect, with a significant recovery of key metabolites, further supporting the complementary action of both agents in regulating CC cell metabolism. The metabolic alterations observed in the combination therapy indicate a broader disruption of cancer cell homeostasis, likely making it more difficult for cells to develop resistance compared to treatment with 5-FU alone. This suggests that PM-H-H may enhance the efficacy of 5-FU by targeting alternative metabolic pathways, weakening the adaptive capacity of cancer cells and leading to more effective tumor suppression.

These findings suggest that both 5-FU and PM-H-H influence distinct yet interconnected metabolic pathways in CC cells, offering valuable insights into their mechanisms of action. The combined treatment's ability to modulate metabolic profiles more effectively than either agent alone underscore the potential of using PM-H-H in combination therapies for improved CC management.

4.3.9.4 Metabolic pathway analysis

In order to understand the altered metabolic pathways induced by CC CT26 cells with the different treatments, pathways enrichment analysis was performed on the differential metabolites from the pair-wise groups including groups Com vs Ctrl. The results were shown in the form of a bubble map (Figure 4.18), where the bubble size was proportional to the number of metabolites in the pathway and the color of the bubble corresponds to the significance of the difference (from red represents the highest significant difference to blue represents the lowest significant difference). The results showed that the combined treatment resulted in changes in six metabolic pathways in CT26 cells, including central carbon metabolism in cancer, protein digestion and absorption, biosynthesis of plant secondary metabolites, biosynthesis of amino acids, aminoacyl−tRNA biosynthesis, and ABC transporters.

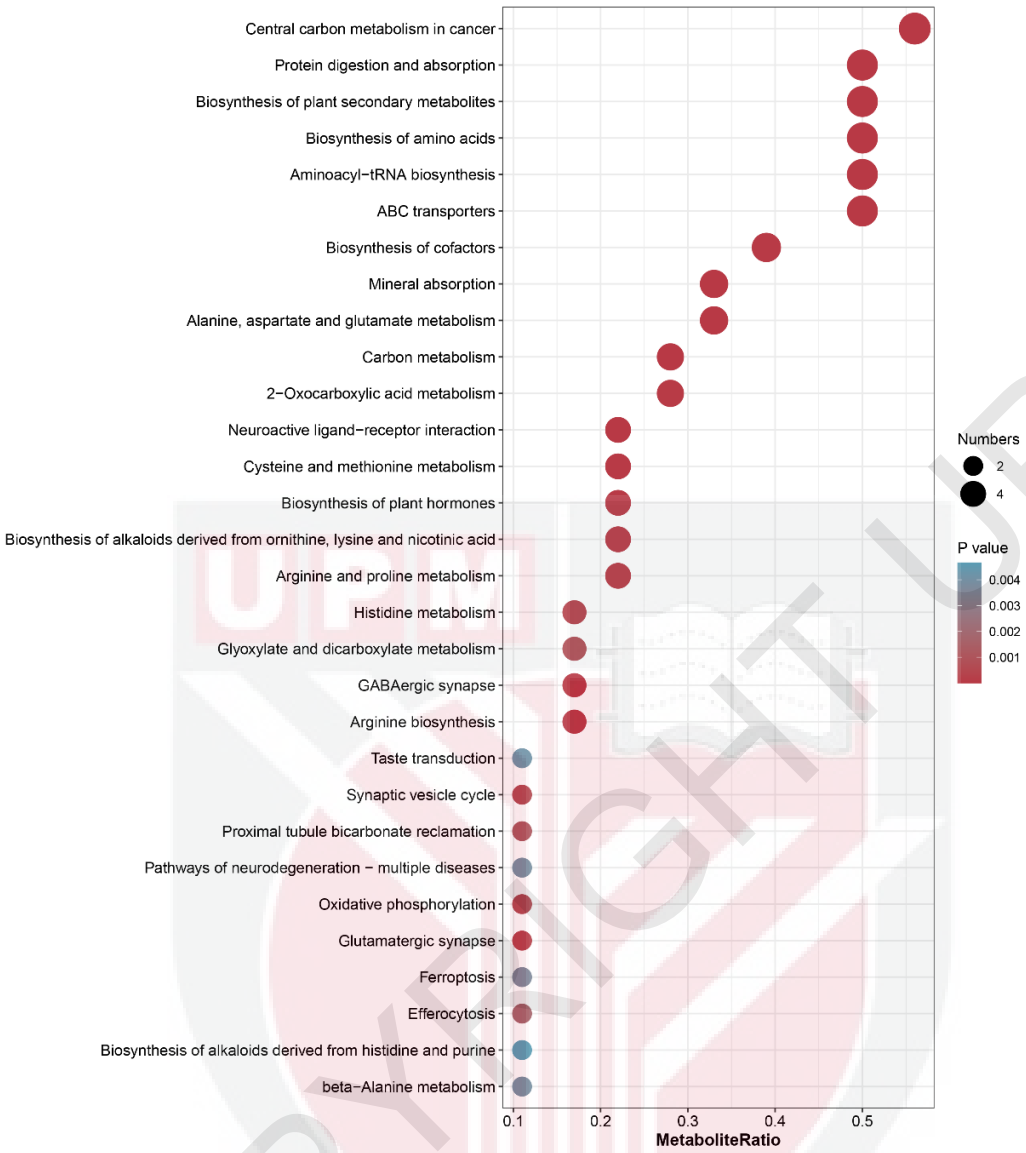

Figure 4.18: Impact overview of the altered CT26 cell metabolic pathways in the different treatment regimens. groups Com vs Ctrl. Ctrl: control (just media alone), Com: combination (PM-H-H + 5-FU).

The pathway enrichment analysis of differential metabolites in CC CT26 cells treated with combination therapy revealed significant disruptions in key metabolic pathways, providing insights into the mechanisms of action of the combined treatment. As visualized in the bubble map (Figure 4.18), six metabolic pathways were significantly altered in the combination group compared to the control group, highlighting the broad metabolic impact of the therapy.

Among the most affected pathways, central carbon metabolism in cancer was notably altered, reflecting changes in the core energy and biosynthetic processes that sustain cancer cell growth (Bernasocchi & Mostoslavsky, 2024). This pathway's involvement underscores the potential of the combination treatment to disrupt the metabolic flexibility of CC cells, potentially limiting their ability to fuel rapid proliferation and survival (Lin et al., 2023). Additionally, significant changes in the biosynthesis of amino acids and aminoacyl-tRNA biosynthesis pathways suggest impaired protein synthesis and reduced availability of key amino acids, which may further contribute to the inhibition of cancer cell growth and survival (Gsottberger et al., 2023; Knight & Sansom, 2021; Schmidt et al., 2020).

The disruption of protein digestion and absorption, along with the biosynthesis of plant secondary metabolites pathways, indicates a broader impact on nutrient uptake and processing. These changes may compromise the cancer cells' ability to adapt to nutrient stress, potentially enhancing the effectiveness of the treatment (Loveday, 2022). Alterations in the ABC transporters pathway, known to play a role in drug resistance and cellular transport, could also enhance the therapeutic effects of the combined treatment by reducing the cancer cells' ability to efflux therapeutic agents (Muriithi et al., 2020; Xiao et al., 2021).

Overall, the combination treatment not only targets core cancer-related metabolic pathways but also affects nutrient acquisition and drug resistance mechanisms, offering a multifaceted approach to impairing CC cell viability. These findings suggest that targeting multiple pathways simultaneously could improve treatment outcomes and reduce the likelihood of therapeutic resistance.

4.3.10 Proteomics analysis

4.3.10.1 Analysis of differentially expressed proteins (DEPs)

A total of 202 differentially expressed proteins (DEPs) (|fold change|>1.5, and P<0.05). Compared with the control group, the PM-H-H group upregulated 20 differentially expressed proteins and downregulated 41 differentially expressed proteins; the 5-FU group upregulated 1 differentially expressed protein and downregulated 133 differentially expressed proteins; while the combined treatment group upregulated 13 differentially expressed proteins and downregulated 92 differentially expressed proteins. Interestingly, compared with the 5-FU group, the combined treatment group upregulated 51 differentially expressed proteins and downregulated 2 differentially expressed proteins; compared with the PM-H-H group, the combined treatment group upregulated 16 differentially expressed proteins and downregulated 51 differentially expressed proteins. The Differentially Expressed Proteins were presented by a cluster heat map (Figure 4.19). Changed proteins (right side) and the samples in different groups (bottom). The color from red to blue shows the relative intensity of the differentially expressed proteins.

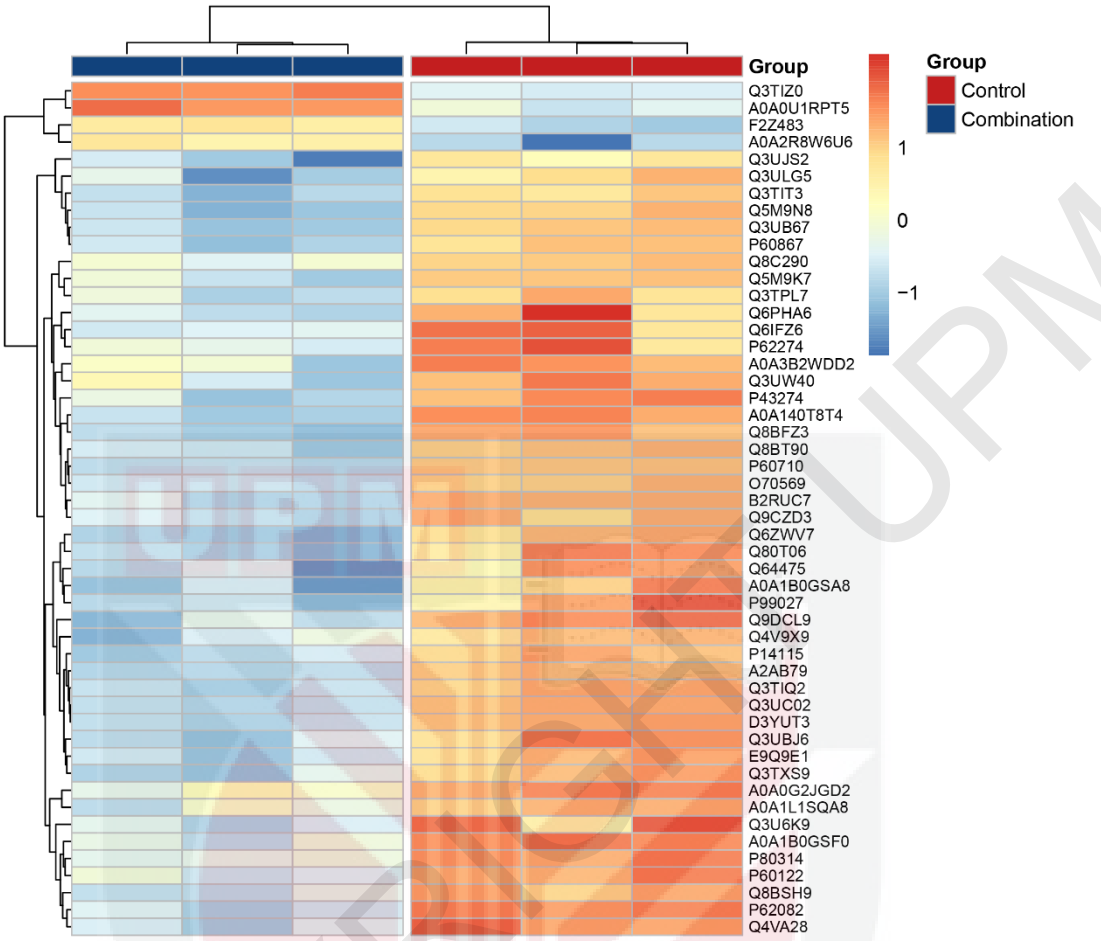

Figure 4.19: Hierarchical clustering heat map of differentially expressed proteins of the CT26 cells. groups Combination vs Control.

The proteomic analysis of CC CT26 cells revealed 202 differentially expressed proteins across the treatment groups, indicating distinct molecular responses to PM-H-H, 5-FU, and their combination. The PM-H-H-treated group exhibited moderate proteomic alterations, with 20 proteins upregulated and 41 downregulated compared to the control. These changes suggest that PM-H-H primarily influences pathways related to cancer cell metabolism, oxidative stress response, and survival mechanisms, potentially targeting alternative regulatory networks distinct from conventional chemotherapy. The observed downregulation of key metabolic enzymes may indicate a disruption in energy homeostasis, contributing to impaired cancer cell proliferation.

In contrast, 5-FU treatment resulted in a more pronounced proteomic shift, with 1 upregulated and 133 downregulated proteins, reflecting its strong cytotoxic effects on protein synthesis and DNA replication machinery. The significant downregulation of ribosomal and translation-associated proteins highlights the impact of 5-FU on inhibiting cancer cell growth. However, this widespread suppression of protein expression may also trigger adaptive resistance mechanisms, which can limit long-term therapeutic efficacy. The combination treatment group displayed a distinct proteomic signature, reinforcing the synergistic interaction between PM-H-H and 5-FU. Compared to the control group, the combination upregulated 13 proteins and downregulated 92, suggesting an enhanced ability to disrupt essential cancer survival pathways. Notably, compared to the 5-FU group, the combination therapy upregulated 51 proteins and downregulated only 2, indicating that PM-H-H may counteract some of the proteomic dysregulation induced by 5-FU and introduce new molecular targets for therapeutic intervention. Similarly, when compared to the PM-H-H group, the combination therapy upregulated 16 proteins and downregulated 51, further demonstrating that the co-treatment engages unique regulatory mechanisms not observed with individual treatments. The heatmap analysis highlights these proteomic differences, with the combination therapy inducing the most extensive molecular reprogramming. The broader downregulation of cancer survival-related proteins suggests that PM-H-H enhances 5-FU's impact by interfering with complementary pathways, potentially amplifying stress responses, suppressing oncogenic signaling, and inhibiting metabolic adaptation (Guo et al., 2020). These differentially expressed proteins could serve as valuable biomarkers or therapeutic targets for future studies, supporting the clinical potential of PM-H-H as an adjunct to chemotherapy. Further validation of these findings through functional assays and *in vivo* proteomic profiling would provide deeper insight into the mechanisms underlying the enhanced anti-

cancer activity of PM-H-H in combination with 5-FU.

4.3.10.2 GO enrichment analysis

The top 30 of GO enrichment analysis are shown in Figure 4.20. The results showed that compared with the control group, the combined group was significantly enriched in multiple biological processes, molecular functions, and cellular component categories ($P<0.05$). The differentially expressed proteins in the combined group were involved in biological processes such as positive regulation of chromosome organization, ribosomal small subunit assembly, ribosomal small subunit biogenesis, ribonucleoprotein complex subunit organization, rRNA metabolic process, ribonucleoprotein complex assembly, rRNA processing, ribosome biogenesis, ribonucleoprotein complex biogenesis, and cytoplasmic translation. These differentially expressed proteins were related to the regulation of molecular functions, such as protein folding chaperone, ADP binding, translation factor activity, RNA binding, unfolded protein binding, ribonucleoprotein complex binding, translation elongation factor activity, translation regulator activity, nucleic acid binding, translation regulator activity, mRNA binding, and structural constituent of ribosome. Compared with the control group, the main enriched cellular components in the combination group were polysomal ribosome, myelin sheath, polysome, small ribosomal subunit, large ribosomal subunit, cytosolic small ribosomal subunit, cytosolic large ribosomal subunit, ribosome, ribosomal subunit, and cytosolic ribosome.

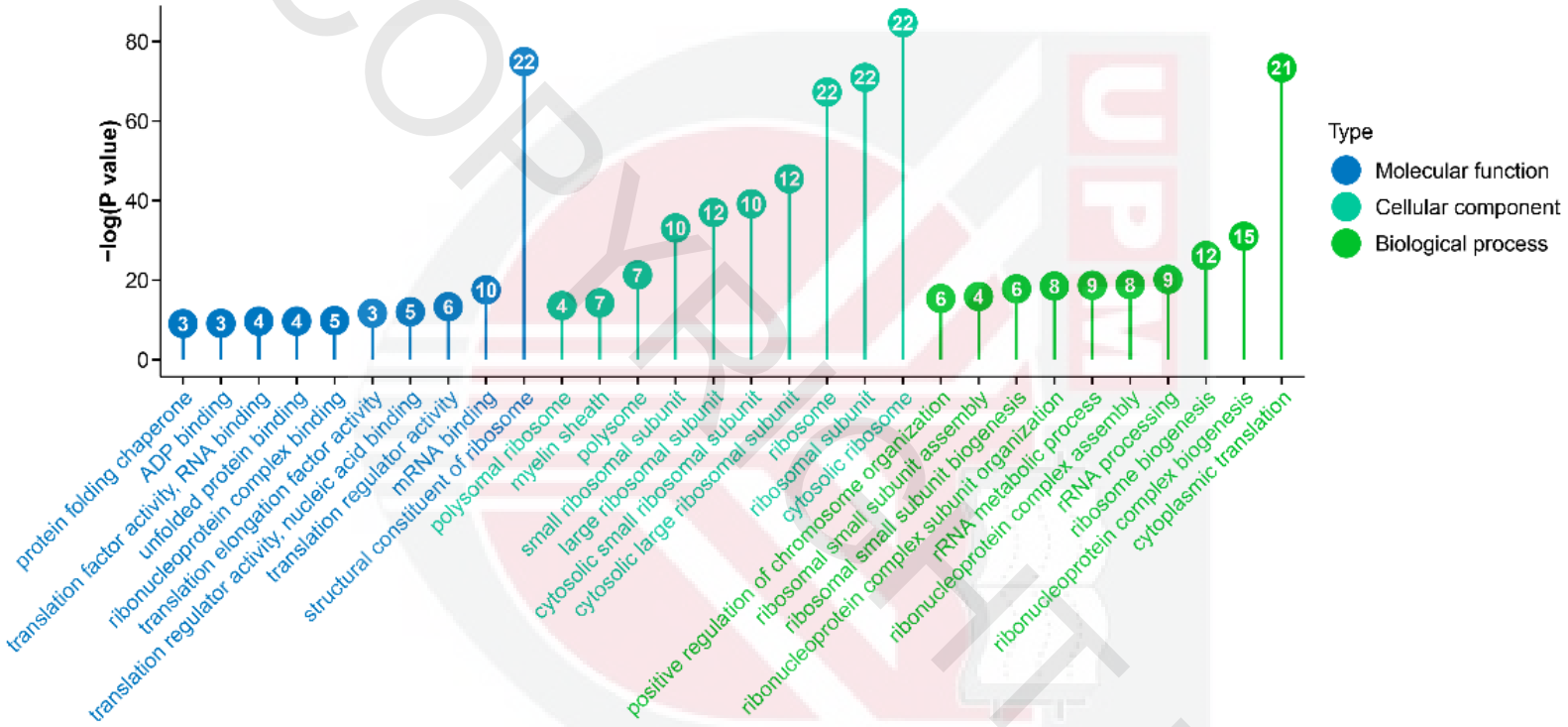

Figure 4.20: GO enrichment of the significant difference proteins in the combined groups based on their cellular component, biological process, and molecular function.

The GO enrichment analysis (Figure 4.20) highlighted significant enrichment ($P<0.05$) in multiple biological processes, molecular functions, and cellular components in the combined treatment group compared to the control. In terms of biological processes, the differentially expressed proteins were highly enriched in pathways related to chromosome organization, ribosome assembly, and RNA metabolism, such as ribosomal small subunit biogenesis, rRNA processing, and ribosome biogenesis. These findings suggest that the combination treatment disrupts core processes involved in protein synthesis and cellular organization, potentially contributing to its enhanced anti-cancer effects by impairing the fundamental machinery required for cancer cell growth and survival (C. Chen et al., 2016; C. Xia et al., 2020; Y. Zhang et al., 2022). The molecular functions associated with the differentially expressed proteins further support this hypothesis. The combination treatment group showed significant enrichment in functions related to RNA and protein binding, including RNA binding, translation factor activity, and protein folding chaperone activity. These functions are crucial for maintaining cellular homeostasis, particularly in cancer cells, where increased protein synthesis is essential for rapid proliferation. The disruption of these processes likely impairs cancer cell survival and proliferation (Fukao et al., 2021; Kershaw et al., 2023; Lyons et al., 2021). In the context of cellular components, the combined treatment led to the enrichment of ribosomal structures, including both small and large ribosomal subunits, as well as cytosolic and polysomal ribosomes. This suggests that the combination treatment targets ribosome biogenesis and function, a process essential for protein synthesis. By affecting these key cellular components, the combined treatment may inhibit translation and reduce the overall protein production capacity of cancer cells, thereby contributing to its anti-proliferative effects (Kang et al., 2021; Melnikov et al., 2018; Paternoga et al., 2023; Temaj et al., 2022). Overall,

the GO enrichment analysis highlights the multifaceted impact of the combined PM-H-H and 5-FU treatment, particularly its ability to interfere with protein synthesis, ribosome assembly, and RNA metabolism, which are critical for the survival and growth of cancer cells. These findings support the potential of combination therapy to exert broader and more effective anti-cancer effects by targeting multiple cellular pathways simultaneously.

4.3.10.3 KEGG pathway enrichment analysis

A total of 86 protein pathways were enriched through the KEGG analysis, of which 6 pathways were changed ($P<0.05$) in the combination treatment group. As shown in Figure 4.21, the most enriched pathways in the combination versus control group were ribosome, coronavirus disease-COVID-19, cytoskeleton in muscle cells, biosynthesis of amino acids, carbon metabolism, and glycine, serine and threonine metabolism.

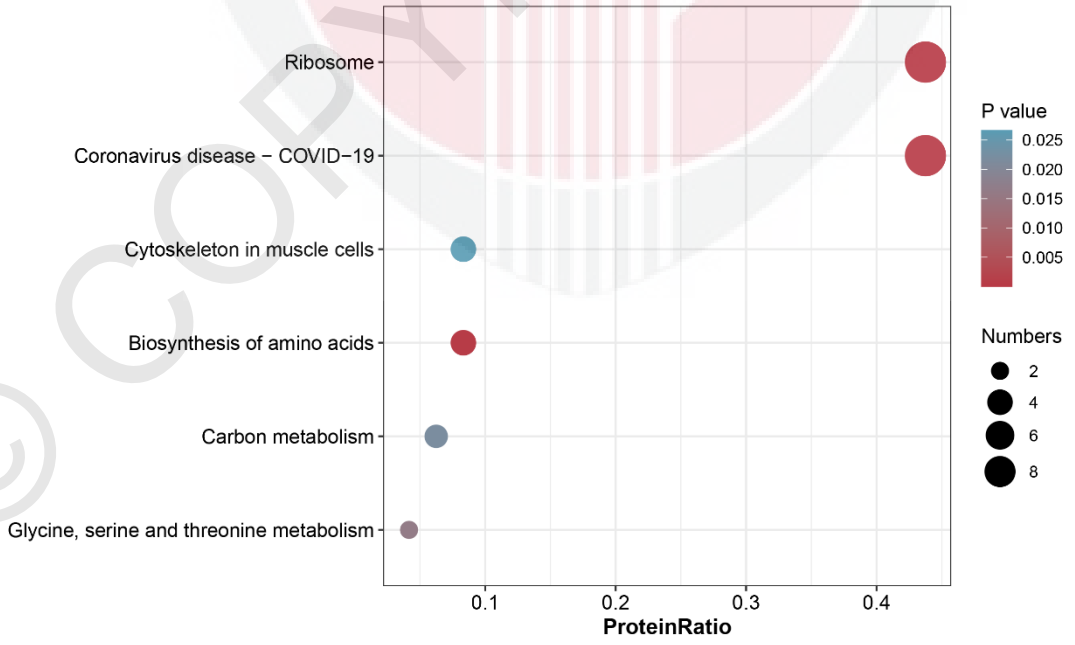

Figure 4.21: KEGG pathway enrichment of differentially expressed proteins in combination versus control groups.

The most enriched pathways (Figure 4.21) provide insight into the mechanisms through which the combination of PM-H-H and 5-FU exerts its effects on CT26 CC cells. The ribosome pathway was the most significantly enriched, suggesting that the combination treatment disrupts protein synthesis by impairing ribosomal function (Metge et al., 2023). Since cancer cells require high levels of protein production to support their rapid growth, targeting the ribosome pathway may contribute to the anti-proliferative effects observed in the combined treatment group (Elhamamsy et al., 2022). This finding aligns with the results from the GO enrichment analysis, further emphasizing the importance of ribosomal dysregulation in the anti-cancer response. Interestingly, the combination treatment also enriched pathways related to coronavirus disease (COVID-19), which may reflect broader disruptions in host defense and immune response mechanisms. While the specific connection to cancer treatment remains unclear, the modulation of immune-related pathways could play a role in enhancing the immune system's ability to recognize and eliminate cancer cells (A. Hu et al., 2024; S. K. Kim & Cho, 2022). Finally, the glycine, serine, and threonine metabolism pathway were also significantly enriched. This pathway is critical for nucleotide biosynthesis and cellular redox balance, both of which are crucial for rapidly dividing cancer cells (S. Pan et al., 2021; Reina-Campos et al., 2020). Disrupting these metabolic pathways may contribute to the observed inhibition of cell growth and survival in CT26 cells treated with the combination therapy. In conclusion, the KEGG enrichment analysis highlights the broad range of cellular processes affected by the combination of PM-H-H and 5-FU, with significant disruption in pathways related to protein synthesis, metabolism, and cellular structure. These findings support the potential of combination therapy to target multiple essential pathways, offering a more comprehensive approach to CC treatment.

4.3.11 Combined metabolomics and proteomics analysis

Through the KEGG database, a total of 22 shared pathways of proteins and metabolites are shown in a Venn plot and bar plot (Figures 4.22 and 4.23). Among them, the protein and metabolite contents of the 3 pathways were significantly changed, including Biosynthesis of amino acids, Glycine, serine and threonine metabolism, and Carbon metabolism, playing an important role in the combined treatment of CT26 cells (Figure 4.24).

According to KEGG pathway enrichment analysis, the Biosynthesis of amino acids, Glycine, serine and threonine metabolism, and Carbon metabolism pathways correspond to the Aldoa, Asns, Psat1, and Shmt2 proteins. As can be seen from Figure 4.19, proteins Asns, Psat1, and Shmt2 showed a decreasing trend, while protein Aldoa showed an increasing trend. This suggests that changes in these proteins may be the mechanism by which combined therapy inhibits CT26.

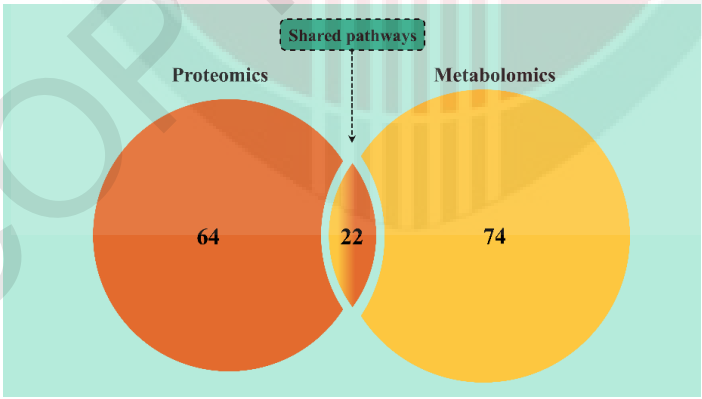

Figure 4.22: The Venn diagram of the pathways involved in the differential metabolites and proteins, in which the overlap represents the shared pathways.

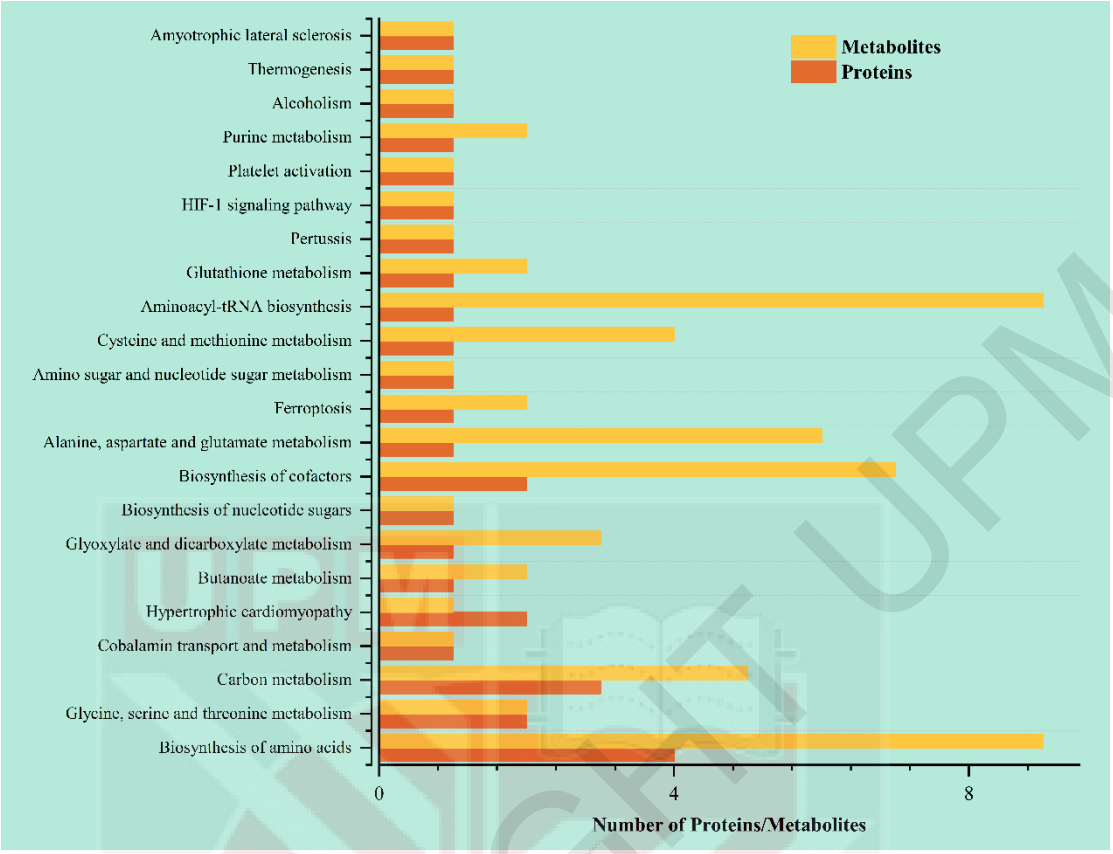

Figure 4.23: 22 pathways with metabolites and proteins co-participation.

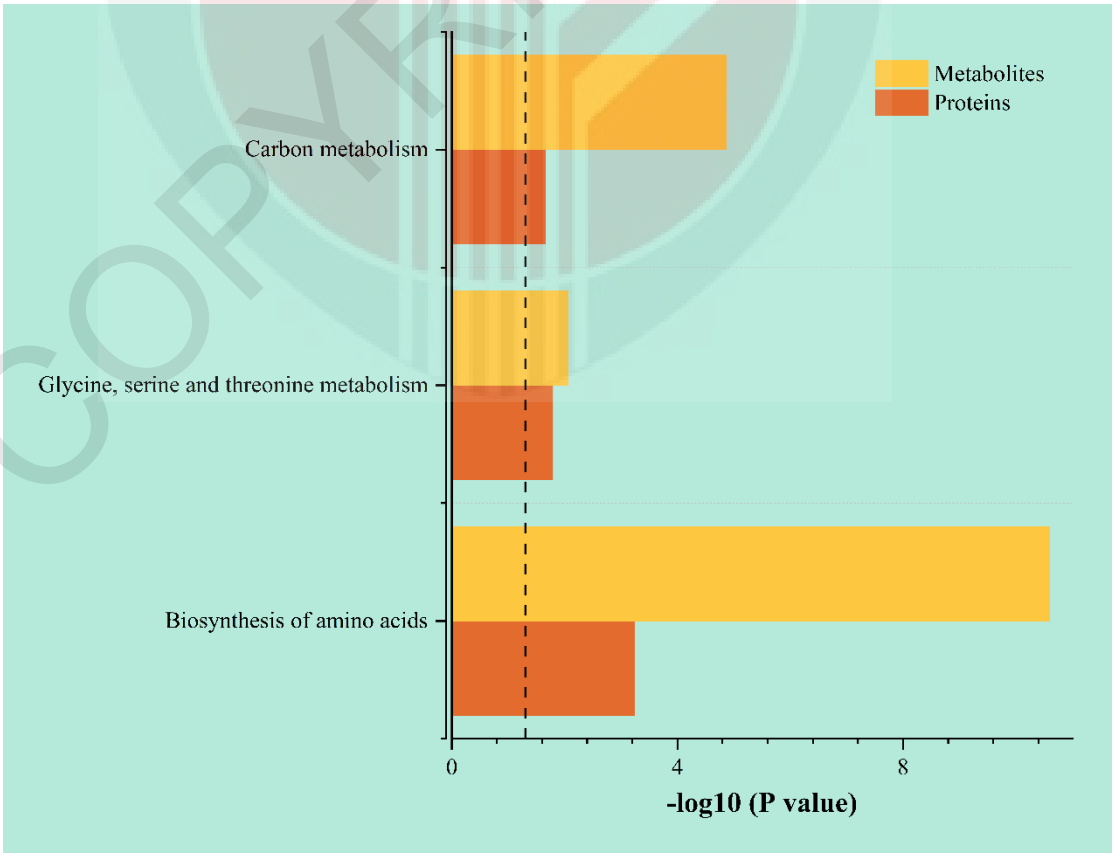

Figure 4.24: The KEGG pathway enrichment based on the differential metabolites and proteins.

The identification of 22 shared pathways of proteins and metabolites through KEGG analysis, as depicted in the Venn and bar plots (Figures 4.22 and 4.23), underscores the interconnected nature of metabolic and proteomic changes induced by the combined treatment of CT26 cells. Among these pathways, significant alterations were observed in the Biosynthesis of amino acids, Glycine, serine and threonine metabolism, and Carbon metabolism, indicating their pivotal roles in the therapeutic response to combination therapy (Figure 4.24). The involvement of specific proteins, namely Aldoa, Asns, Psat1, and Shmt2, within these pathways provides insight into the molecular mechanisms underpinning the effects of the combined treatment. The observed trends in protein expression, with Asns, Psat1, and Shmt2 showing a decrease and Aldoa demonstrating an increase, suggest a dynamic response that may contribute to the inhibition of CT26 cell proliferation.

The downregulation of Asns, which plays a crucial role in the synthesis of asparagine, indicates a potential shift in amino acid availability essential for cancer cell growth (Krall et al., 2016; Yu et al., 2024). Asparagine is often upregulated in cancer cells to support their rapid proliferation; thus, inhibiting its biosynthesis could limit tumor growth (Cai et al., 2022). Similarly, the downregulation of Psat1 and Shmt2, both involved in serine and glycine metabolism, further suggests a metabolic reprogramming in response to treatment (Sun et al., 2023). These proteins facilitate the conversion of intermediates crucial for nucleotide synthesis and redox balance, processes that are frequently hijacked by cancer cells to promote survival and proliferation (L. He et al., 2023). Conversely, the upregulation of Aldoa, which encodes aldolase A, indicates an adaptive response that may enhance glycolytic flux

(Gizak et al., 2019). This pathway is essential for energy production and metabolic flexibility in rapidly dividing cancer cells. The increase in Aldoa expression suggests that, while the combined treatment inhibits certain metabolic pathways, it simultaneously activates others to meet the energetic demands of the cells (Li et al., 2021; Miyazawa et al., 2022; Xu et al., 2024). This dual response highlights the complexity of metabolic regulation in cancer and underscores the necessity for comprehensive therapeutic strategies that address multiple metabolic vulnerabilities.

In summary, the results of the KEGG analysis provide compelling evidence that the combined treatment of CT26 cells significantly alters critical metabolic pathways associated with amino acid biosynthesis and carbon metabolism. The changes in protein expression of Aldoa, Asns, Psat1, and Shmt2 not only reflect the immediate effects of the treatment but also illuminate potential mechanisms through which this combination therapy exerts its anti-cancer effects. These findings contribute to a deeper understanding of the metabolic reprogramming that occurs in cancer cells and suggest further avenues for research into targeted therapeutic interventions.

4.4 Conclusion

The study comprehensively investigated the effects of 5-FU, PM-H-H, and their combination on CT26 CC cells through a combination of cytotoxicity assays, metabolomics, and proteomics analyses. The findings reveal significant synergistic effects and provide a detailed understanding of the mechanisms underlying this combination therapy.

The combination of PM-H-H and 5-FU demonstrates a potent synergistic effect in

inhibiting the growth and proliferation of CT26 CC cells. This is evidenced by reduced effective concentrations of 5-FU required for cytotoxicity, increased apoptosis, and cell cycle arrest at the G0/G1 phase. Morphological changes, such as cell detachment and loss of intercellular contact, further support the synergistic interaction. The combination also shows superior inhibition of cell migration and clonogenic formation, suggesting reduced cancer metastasis and early-stage tumor development. Spheroid growth inhibition studies corroborate these findings, highlighting the effectiveness of the combination therapy in a more physiologically relevant 3D model. These results emphasize the potential of PM-H-H to enhance 5-FU's therapeutic efficacy while potentially reducing the toxicity associated with high-dose chemotherapy.

The metabolomics analysis, utilizing NMR and multivariate statistical methods, identified 26 key metabolites with distinct profiles across treatment groups. The combined treatment resulted in substantial metabolic reprogramming, affecting key pathways related to amino acid metabolism and energy production. This broad impact on cancer cell metabolism underscores the efficacy of the combination therapy in disrupting cancer metabolism more comprehensively than individual treatments.

Proteomics analysis revealed extensive changes in protein expression, with the combined treatment leading to the most significant reprogramming. GO enrichment analysis revealed that the combined group was significantly involved in processes related to ribosomal assembly and RNA metabolism, while KEGG pathway analysis showed alterations in six significant pathways, including the ribosome and amino acid biosynthesis pathways. In summary, the combined treatment of PM-H-H and 5-FU effectively modulated protein expression, highlighting its potential to enhance therapeutic strategies against CC through targeted biological processes and metabolic

pathways.

The combined treatment of 5-FU and PM-H-H exhibits a promising synergistic effect, leading to comprehensive alterations in both metabolic and proteomic profiles of CC cells. This multifaceted targeting of cancer cell metabolism and survival pathways suggests enhanced therapeutic efficacy and reduced side effects. Future research should focus on validating these results *in vivo* to further explore the therapeutic potential and mechanisms of this combination approach in cancer treatment.

CHAPTER 5

IN VIVO EVALUATION OF ANTICANCER EFFICACY OF *Polygonum minus* EXTRACT COMBINATION WITH 5-FLUOROURACIL IN CT26 TUMOR-BEARING MOUSE MODEL

5.1 Introduction

In the quest to improve CC treatments, combining natural products with conventional chemotherapy agents has gained significant attention (Zhou et al., 2023). PM, a medicinal plant known for its diverse bioactive compounds, has shown promising *in vitro* anticancer effects (Z. Yang et al., 2024). When combined with 5-FU, a cornerstone in CC chemotherapy, the potential for enhanced therapeutic outcomes arises, given the challenges of drug resistance and toxicity associated with 5-FU (Alrbyawi, 2024).

The previous chapters explored the preparation, optimization, and *in vitro* anticancer effects of PM extracts, as well as their synergy with 5-FU. Chapter 3 focused on the preparation of PM extract and optimization of its bioactive compounds, while Chapter 4 examined the *in vitro* effects of PM extract combined with 5-FU on the CT26 CC cell line. These findings laid the groundwork for assessing the therapeutic potential of PM extract in a more complex *in vivo* setting.

This chapter focuses on evaluating the *in vivo* anticancer efficacy of a combination of PM extract and 5-FU using the CT26 tumor-bearing mouse model. Building on the earlier *in vitro* findings where the PM extract showed promising results in combination

with 5-FU, this section aims to assess the therapeutic potential of this combination in a more complex and physiologically relevant system.

The study involves administering the PM extract and 5-FU, either individually or in combination, to mice bearing CT26 CC tumors. The primary objectives are to evaluate the impact of the combination therapy on tumor growth, survival rates, and overall health of the animals. Key endpoints include measurement of tumor volume, assessment of tumor weight, and analysis of any associated toxicities.

The outcomes of this study aim to provide valuable information on the potential benefits of combining PM extract with 5-FU in a preclinical setting. By demonstrating the *in vivo* efficacy and safety of this combination therapy, the research seeks to contribute to the development of improved treatment strategies for CC, offering a potential advancement in the field of oncology.

5.2 Materials and methods

5.2.1 Animal

The animal study protocol was approved by the Institutional Ethics Committee of Universiti Putra Malaysia (UPM/IACUC/AUP-R073/2023) for studies involving animals. A total of 40, 6-8week-old female BALB/c mice, weighing 18.2 ± 3.6 g were obtained from Laboratory Animal Facility and Management (LAFAM), Faculty of Pharmacy, UiTM Puncak Alam Campus. The animals were allowed to acclimatize for one week before the experiment in the animal research house of the Comparative Medicine and Technology Unit (COMeT), Institute of Bioscience UPM. They were

given a normal mouse diet and filtered tap water *ad libitum*.

5.2.2 Tumor induction and treatment

To further validate the antitumor effects of PM-H-H+5-FU *in vivo*, we subcutaneously injected CT26 cells into BALB/c mice for syngeneic tumorigenesis and subjected them to treatment with PM-H-H, 5-FU, and their combination, accurately measured the tumor weights, as well as collected and manipulated the organs and tumors of the tumor-bearing mice after two weeks treatment (Figure 5.1). Briefly, 32 mice were inoculated subcutaneously on the right side of their shaved back with a single-cell suspension of CT26 cells (1000000 cells in 100 µl). Tumor growth was monitored every day by the vernier caliper. After the tumor injection, the mice were randomly divided into 4 groups. The treatments were administrated when the tumor grew up to a volume of 100 mm^3. Each group of mice received different treatments: G1) Control group: 10% Tween 80 via oral gavage. G2) PM group: PM hexane fraction (1000 mg/kg) daily via oral gavage. G3) FU group: 5-FU (200 mg/kg) thrice weekly via intraperitoneal injection. G4) PM+FU group: PM hexane fraction (1000 mg/kg) daily. 5-FU (200 mg/kg) thrice weekly.

During the experiments, the mice were monitored daily, and the body weight and tumors size were measured every day. Euthanasia was performed when one of the following humane endpoints was reached: lethargy, reduced mobility, persistent hunching, labored breathing, or lack of response to stimuli, indicating significant distress. Additional criteria included 50% body weight loss, clinical signs of distress such as excessive grooming or self-mutilation, the presence of an ulcerated necrotic tumor, or a tumor volume exceeding 1800 mm^3.

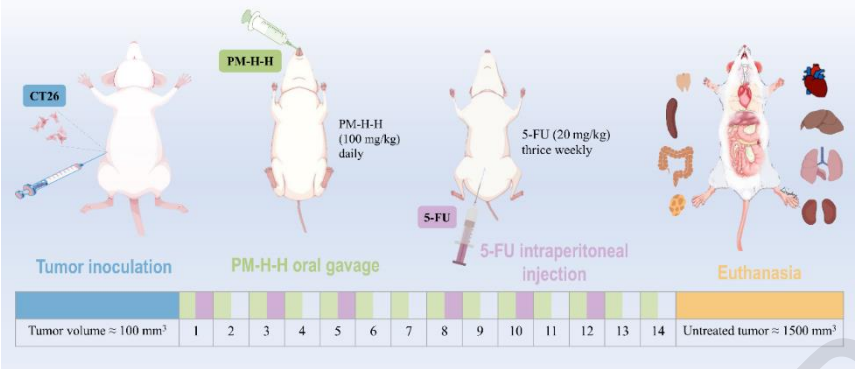

Figure 5.1: Schematic of mice model establishment and treatments.

5.2.3 Anti-tumor assay

Tumor sizes were monitored every day and volume was calculated using the following formula, from a previously established protocol:

$$\text{Volume } (mm^3) = (\text{longest diameter}) \times (\text{shortest diameter})^2 / 2.$$

Moreover, final body and tumor weights were measured after dissection and the tumor volumes were also evaluated after dissection by immersion method. The anti-tumor activity of the treatments was evaluated using the following formula:

Tumor inhibitory rate (%) = [(Average tumor weight of control group - Tumor weight of treatment groups) / Average tumor weight of control group] ×100%.

Finally, tumors were excised and divided into 2 pieces for histopathological, and ELISA analysis as described below, respectively.

5.2.4 Organ weight and colon length measurement

The heart, liver, lungs, kidneys, thymus and spleen were isolated. Weight to calculate tumor inhibition rates and organ indexes:

$$\text{Organ index} = \text{organ weight (mg)} / \text{body weight (g)}.$$

Moreover, the colon length of each mouse was clipped and measured. Colon index was

calculated using the following formula:

Colon index = colon length/body weight.

5.2.5 Histopathological analysis

Tissues of mice tumors were fixed with 10% paraformaldehyde. The tumors were trimmed to a 0.5 ± 0.1 cm thickness placed in a plastic box, and then dehydrated using an automatic tissue processor. Then, the tumors and colon were embedded in paraffin, respectively. Sectioned, stained with hematoxylin and eosin (H&E), and observed using an optical microscope (Olympus BX53P, Japan) (Lai et al., 2021).

5.2.6 Biochemical assessment

Blood was collected in anticoagulant-free serum blood collection tubes for serum biochemical analysis from overnight-fasting mice by cardiac puncture following light anesthesia with ketamine and xylazine cocktail (IP, 0.1ml/10g). After complete coagulation, the serum was centrifuged at 4000 rpm for 15 min using a centrifuge. The serum was then transferred to 1.5 mL Eppendorf tubes and stored at -80°C until analysis. Aspartate aminotransferase (AST), alanine aminotransferase (ALT), alanine phosphatase (ALP), creatinine, and urea levels were evaluated using an automatic biochemistry analyzer (Chemistry Analyser Automatic, HITACHI 902®). Serum samples were analyzed for AST, ALT, and ALP to assess hepatic damage. Serum creatinine and urea levels were evaluated and used to indicate possible renal damage. Blood biochemistry was examined in treatment groups and compared with data from the control group.

5.2.7 Enzyme-linked immunosorbent assay (ELISA)

The concentrations of Psat1 and Shmt2 were evaluated by ELISA. Briefly, the tumor tissues of control and combination groups were thawed at room temperature and homogenized by bead beating in PBS with protease inhibitor cocktail at 4 ℃. After centrifuging at a speed of 12000 rpm/min for 10 min, the supernatants were collected for ELISA tests (Z. Wang et al., 2022). The procedures were followed the manufacturer's instructions of Psat1 (Baiyi Bio, Shanghai, China), Shmt2 (Baiyi Bio, Shanghai, China) ELISA kits.

5.2.8 Statistical analysis

Data were shown as means ± standard deviation (SD) from three independent experiments. SPSS R26.0.0.0 software was used for statistical analysis. The P values were analyzed using ANOVA and $P<0.05$ is considered significant.

5.3 Results and discussion

5.3.1 Antitumor efficacy

CT-26 tumor mouse model was employed to investigate the *in vivo* anti-tumor efficacy of PM-H-H and 5-FU. None of the mice died over the course of treatment and all mice developed tumors, successfully. After the end of treatment, the mean tumor volume in the control, PM-H-H, 5-FU, and PM-H-H+5-FU treatment groups were 1543.35 ± 233.76 mm^3, 974.96 ± 84.31 mm^3, 751.39 ± 66.94 mm^3, and 185.12 ± 24.39 mm^3, respectively (Figure 5.2). As is shown in Figure 5.2, compared with the negative control group, the tumor volumes of all treatment groups decreased significantly, and

the tumor volume of the combination group decreased more significantly than that of the 5-FU or PM-H-H treatment groups.

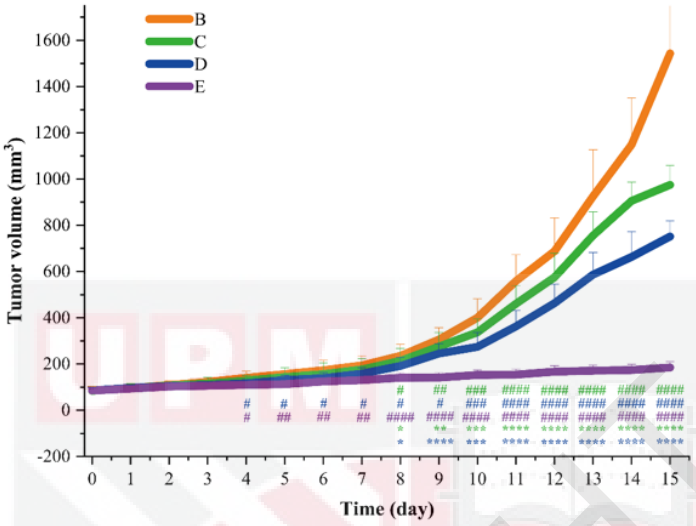

Figure 5.2: Tumor growth curves of mice after different treatments. B: Control group, tumor mice untreated. C: Tumor mice treated with PM-H-H. D: Tumor mice treated with 5-FU. E: Tumor mice treated with PM-H-H+5-FU. $^{\#}P<0.05$, $^{\#\#}P<0.01$, $^{\#\#\#}P<0.001$, $^{\#\#\#\#}P<0.0001$, vs control group. While $^{*}P<0.05$, $^{**}P<0.01$, $^{***}P<0.001$, $^{****}P<0.0001$. PM-H-H or 5-FU group vs (PM-H-H + 5-FU) group.

At the end of the treatment, all animals were sacrificed, and the tumor was excised and weighed. The mean tumor weights in different groups were also recorded (Figure 5.3). As is shown in Figure 5.3, compared with the negative control group, the tumor weights of all treatment groups decreased significantly, and the tumor weights of the combination group decreased more significantly than those of the 5-FU or PM-H-H treatment groups.

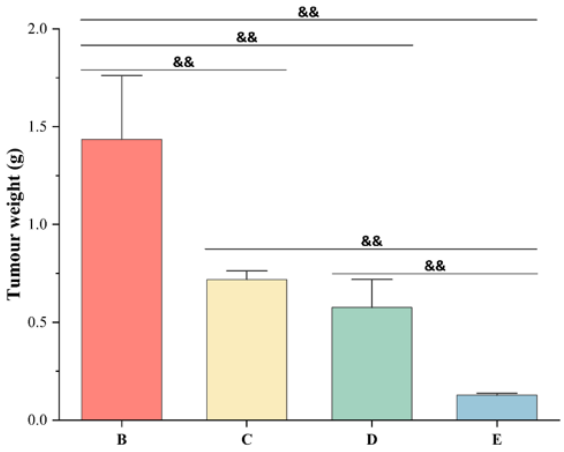

Figure 5.3: Tumor weight of mice after different treatments. B: Control group, tumor mice untreated. C: Tumor mice treated with PM-H-H. D: Tumor mice treated with 5-FU. E: Tumor mice treated with PM-H-H+5-FU. $^{\&\&}P<0.0001$.

And results showed that the tumor weight inhibition rates were 44.00 ± 7.81%, 51.31 ± 4.34%, and 88.01 ± 1.58% for the PM-H-H, 5-FU, and PM-H-H+5-FU treatment group, respectively (Figure 5.4). The trend of tumor weight inhibition was consistent with tumor volume inhibition. As shown in Figure 5.4, compared with the 5-FU or PM-H-H treatment groups, the tumor growth inhibition rate in the combination group was significantly increased.

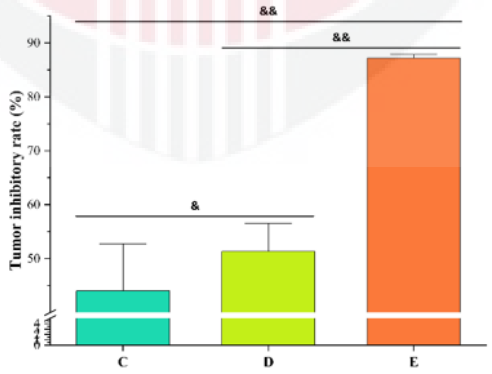

Figure 5.4: Tumor inhibition rate of mice in different treatment groups. B: Control group, tumor mice untreated. C: Tumor mice treated with PM-H-H. D: Tumor mice treated with 5-FU. E: Tumor mice treated with PM-H-H+5-FU. $^{\&}P<0.05$, $^{\&}P<0.0001$

Similarly, the tumor sites of the mice in each group were dissected for comparison

(Figure 5.5), and PM-H-H+5-FU showed the best antitumor effect.

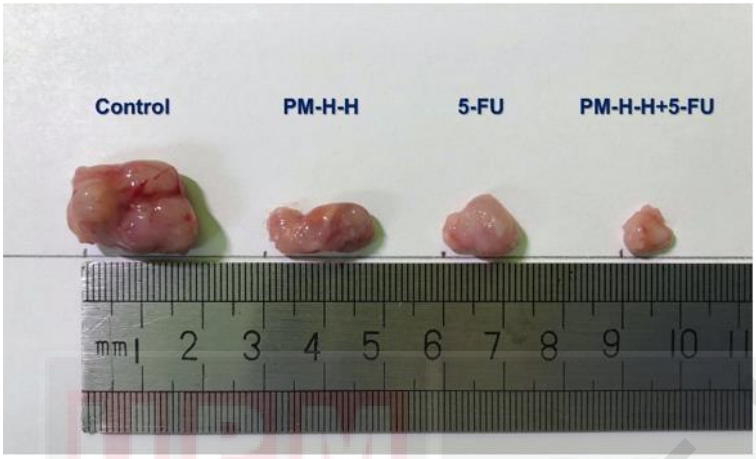

Figure 5.5: Representative photographs of tumor of the different treatments.

Hematoxylin-eosin staining was used to observe the microstructure changes after different treatments. The control group showed compact tumor cells with blue-purple nuclei and pink cytoplasm. In the PM-H-H or 5-FU treatment groups, the tumor cells were sparse and separated from each other. In PM-H-H+5-FU treatment groups, the structure of tumor tissue was more seriously damaged than that in PM-H-H or 5-FU alone groups accompanied by obvious vacant sections and lots of nuclear fragments (Figure 5.6).

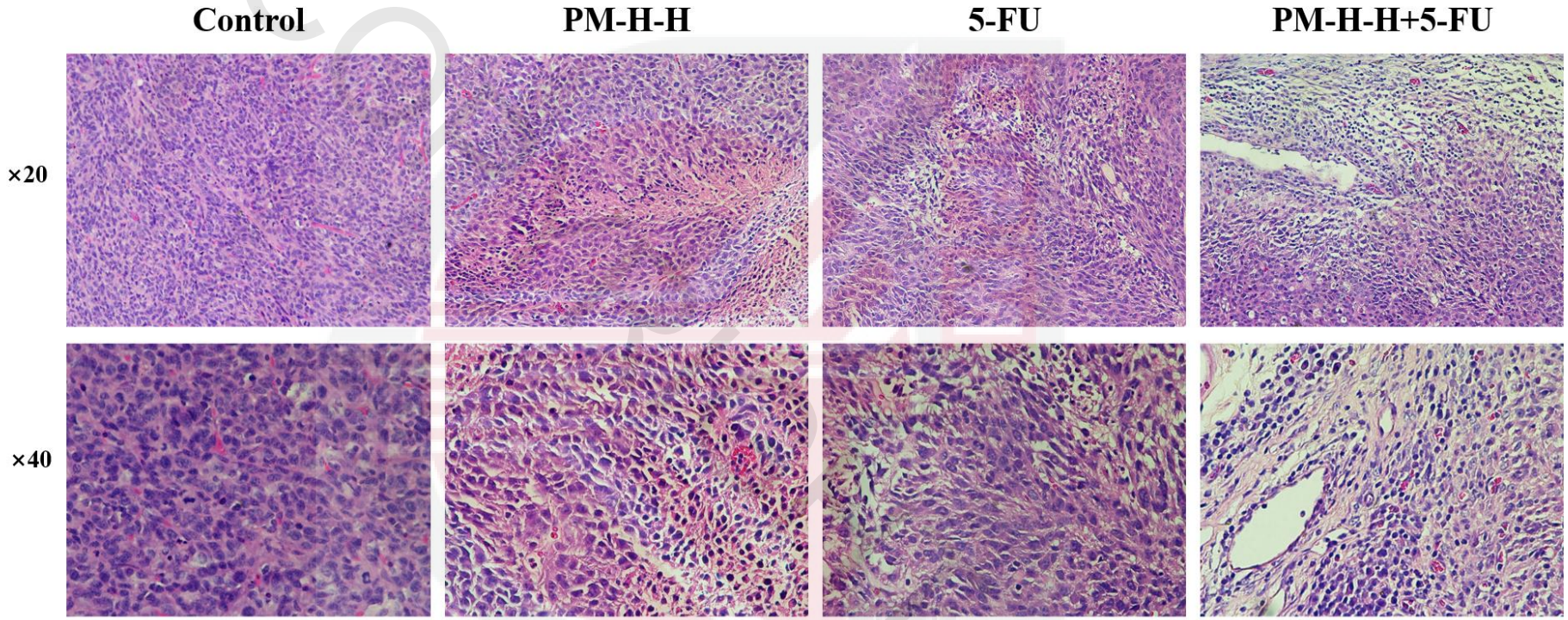

Figure 5.6: **Representative photographs of tumor section with hematoxylin-eosin staining of the different treatments.** In the control group, tumor cells appeared compact, with blue-purple nuclei and pink cytoplasm. In the PM-H-H and 5-FU treatment groups, the tumor cells became sparse and were separated from one another. In the PM-H-H+5-FU combination treatment group, the tumor tissue structure was more severely disrupted compared to the PM-H-H or 5-FU groups alone, with prominent vacuolated areas and numerous nuclear fragments.

A tumor is a pathological state characterized by uncontrolled proliferation (Braicu et al., 2022). In this study, a CT26 tumor-bearing model was successfully induced in mice according to established methods (Hosseini et al., 2022). It is an established model commonly used to investigate different chemotherapeutic treatment strategies for treating CC (Demeckova et al., 2022). This model reflects a high-grade malignancy due to its virulence, quick development and infiltrative nature (Freund et al., 2019; Olivo Pimentel et al., 2021; Wei et al., 2018). Therefore, it can be used as a potential model to study the curative effect of 5-FU *in vivo*. The results show that the use of PM-H-H significantly increased the antitumor activity of 5-FU, which is consistent with the previous *in vitro* study results. In addition, histopathological examination showed that the tumor tissue structure destruction in the combination treatment group was more severe than that in the single treatment groups, with more nuclear fragments and obvious cavities.

However, it is essential to acknowledge the limitations associated with using murine models. While the CT26 model offers valuable insights into therapeutic efficacy, differences in immune system composition, tumor microenvironment, and metabolic processes between mice and humans may pose translational challenges. These discrepancies can affect the interpretation and applicability of the results to human conditions, potentially leading to variations in treatment response and safety profiles. Therefore, while our findings highlight the potential of PM-H-H as an adjuvant to 5-FU, further validation in clinically relevant human models and trials is necessary to ascertain its therapeutic efficacy and safety in human patients.

5.3.2 Toxicity analysis

Mice were weighed daily throughout the experiment to record the effects of treatment on their health. Although mice in all treatment groups lost weight, the difference was not significant compared with the tumor control group, revealing that all treatment might not cause severe systemic toxicity *in vivo* (Figure 5.7).

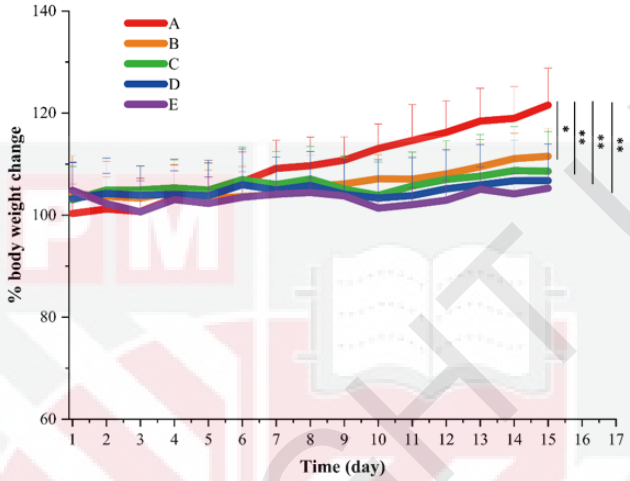

Figure 5.7: Time-dependent body weight change curves. A: Healthy mice, B: Control group, tumor mice untreated. C: Tumor mice treated with PM-H-H. D: Tumor mice treated with 5-FU. E: Tumor mice treated with PM-H-H+5-FU. *P<0.05, **P<0.01.

The daily monitoring of the mice's body weight throughout the experiment provides valuable insights into the systemic effects of the treatments administered. Body weight is a critical indicator of overall health in animal studies, especially in the context of cancer and chemotherapy, where weight loss often reflects systemic toxicity or adverse side effects (Perše, 2021; Talbot et al., 2020).

The current study observed that mice in all treatment groups, including those treated with PM-H-H and 5-FU, experienced weight loss, is consistent with the expected physiological stress associated with tumor growth and treatment interventions (Breen et al., 2020). Previous studies have shown that CT26 tumor causes weight loss in tumor-bearing mice (A. Kim et al., 2016). This is consistent with the experimental

results, which show that 5-FU treatment induces substantial weight loss in CT26 tumor-bearing mice, with higher doses leading to more severe and rapid weight loss (Kojouharov et al., 2014). This is contrary to the experimental results, with the possible reason being the smaller dose of 5-FU administered. However, the key finding is that the weight loss observed in the co-treatment groups was not significantly different from that in the tumor control group. This suggests that PM-H-H and 5-FU co-treatment did not exacerbate weight loss beyond what was caused by the tumor itself. Subsequently, the index of the following organs heart, lungs, liver, and kidney was further assessed after treatment with PM-H-H, 5-FU, and the combination of PM-H-H and 5-FU (Figure 5.8). Notably, although there were some changes in these organ index, especially in the CC tumor mice untreated group and 5-FU treatment led to a decrease in all organ index, there were no significant differences between the PM-H-H+5-FU group and the healthy group. In other words, PM-H-H+5-FU can improve the changes in organ indexes caused by CC tumors or 5-FU.

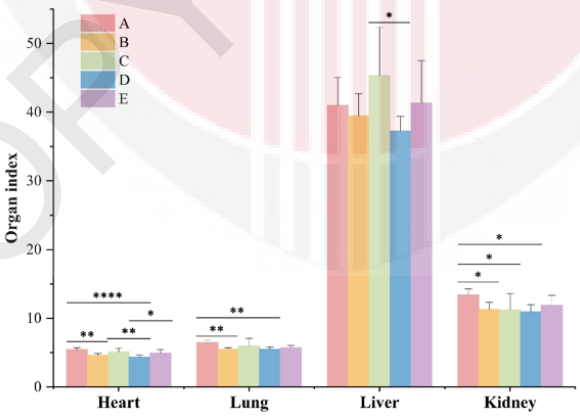

Figure 5.8: Heart, lungs, liver, and kidney index after various treatments. A: Healthy mice, B: Control group, tumor mice untreated. C: Tumor mice treated with PM-H-H. D: Tumor mice treated with 5-FU. E: Tumor mice treated with PM-H-H+5-FU. *P<0.05, **P<0.01, ***P<0.001, ****P<0.0001.

Assessing organ index following treatment provides crucial insights into the potential systemic impacts of PM-H-H, 5-FU, and their combination. The observed decrease in

organ index in the tumor-bearing mice and the 5-FU-treated group was consistent with the previous studies (da Silva et al., 2023; Y. Zhao et al., 2023). Tumors can exert detrimental effects on various organs through mechanisms such as inflammation, oxidative stress, and metabolic disruption (J. E. Gong et al., 2021). Similarly, 5-FU is known to cause toxicity in non-target organs, contributing to the observed decreases in organ index (da Silva et al., 2023).

However, the most striking finding in this study is that the PM-H-H+5-FU treatment group did not exhibit significant differences in organ index compared to the healthy control group. This suggests that the combination of PM-H-H with 5-FU not only mitigates the harmful effects of the tumor on vital organs but also counteracts the toxicity typically induced by 5-FU treatment alone. This protective effect of PM-H-H when combined with 5-FU is noteworthy, as it indicates that PM-H-H may play a role in safeguarding critical organs from the adverse effects of both the tumor and chemotherapy.

To investigate the effect of treatment groups on immunity, immune organ indexes, including those for the spleen and thymus, were calculated. As shown in Figure 5.9, compared with the healthy mice group, the organ index of the spleen and thymus of the tumor mice un-treatment or alone or co-treatment group was significantly changed, indicates that the immune organs of tumor mice non or after drug administration are affected, while the organ indexes of spleen and thymus in the combined treatment group were not significantly different from those in healthy mice, indicating that PM-H-H+5-FU has a certain protective effect on immune organs.

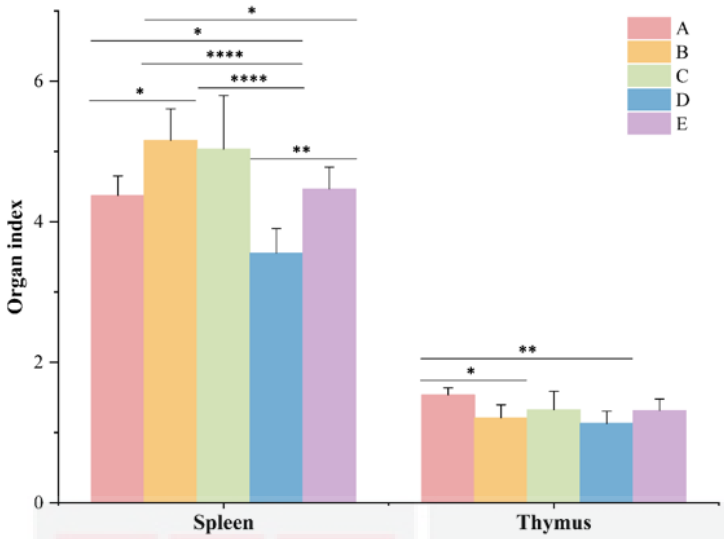

Figure 5.9: Spleen and thymus indexes after various treatments. A: Healthy mice, B: Control group, tumor mice untreated. C: Tumor mice treated with PM-H-H. D: Tumor mice treated with 5-FU. E: Tumor mice treated with PM-H-H+5-FU. *P<0.05, **P<0.01, ***P<0.001, ****P<0.0001.

The experimental results show that the spleen index and thymus index of mice in the 5-FU group were lower than those in the model group. This finding is consistent with the results of previous studies (L. Zhu et al., 2016). In addition, the results also showed that the spleen index of CT26 tumor-bearing mice was higher than that of normal mice. This condition is characterized by an increase in spleen size and is commonly observed in various cancer models, including those involving CT26 tumor mice (Alimohammadi et al., 2023; L. C. Yang et al., 2014). The enlargement of the spleen in these tumor-bearing mice can be attributed to several factors, including immune hyperplasia and extramedullary hematopoiesis, which occur as the body responds to the tumor's presence (Tobias et al., 2023; W. li Zhang et al., 2020).

Compared with the healthy mice, the colon index of the tumor-bearing mice decreased, as did the colon index of the 5-FU-treated mice. PM-H-H treatment prevented the decrease in the colon index of the tumor-bearing mice compared with the tumor-bearing mice. Moreover, PM-H-H treatment also prevented the decrease in the 5-FU-

treated group (Figure 5.10).

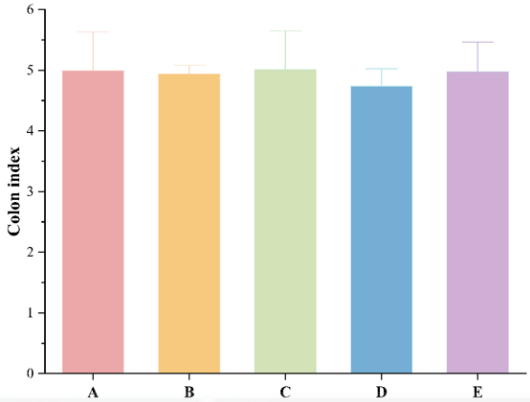

Figure 5.10: Colon index after various treatments. A: Healthy mice, B: Control group, tumor mice untreated. C: Tumor mice treated with PM-H-H. D: Tumor mice treated with 5-FU. E: Tumor mice treated with PM-H-H+5-FU.

The findings from this study reveal a significant impact of PM-H-H treatment on the colon index of CT26 tumor-bearing mice, highlighting its potential as a therapeutic intervention. In untreated tumor-bearing mice, a decrease in the colon index was observed, indicative of tumor progression and associated physiological changes. This decline was similarly changed in the group treated with 5-FU, a common chemotherapeutic agent known for its efficacy against CC but also associated with adverse side effects, including gastrointestinal toxicity (Lo et al., 2023).

Interestingly, the administration of PM-H-H not only mitigated the reduction in the colon index observed in tumor-bearing mice but also exhibited a protective effect in the 5-FU-treated group. This suggests that PM-H-H may counteract some of the deleterious effects of tumor growth and chemotherapy on colon health. The preservation of the colon index in these groups implies that PM-H-H might contribute to maintaining colon structure and function, which is crucial for overall gut health during cancer treatment. The ability of PM-H-H to prevent the decrease in the colon index highlights its potential dual role as both an anti-cancer agent and a protective

adjuvant in chemotherapy.

The levels of AST, ALT, ALP, Creat, and Urea in the serum showed differences among distinct groups (Figures 5.11 and 5.12). The PM-H-H+5-FU group showed no significant difference from healthy mice. Overall, toxicity parameters together supported the idea that the combinatorial treatment of PM-H-H and 5-FU showed reduced toxicity of 5-FU and thus better its safety.

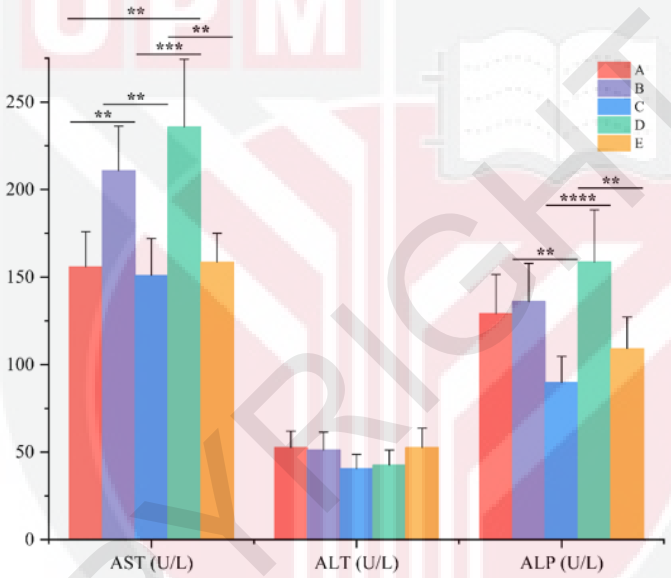

Figure 5.11: The level of AST, ALT, and ALP in the serum. A: Healthy mice, B: Control group, tumor mice untreated. C: Tumor mice treated with PM-H-H. D: Tumor mice treated with 5-FU. E: Tumor mice treated with PM-H-H+5-FU. *P<0.05, **P<0.01, ***P<0.001, ****P<0.0001.

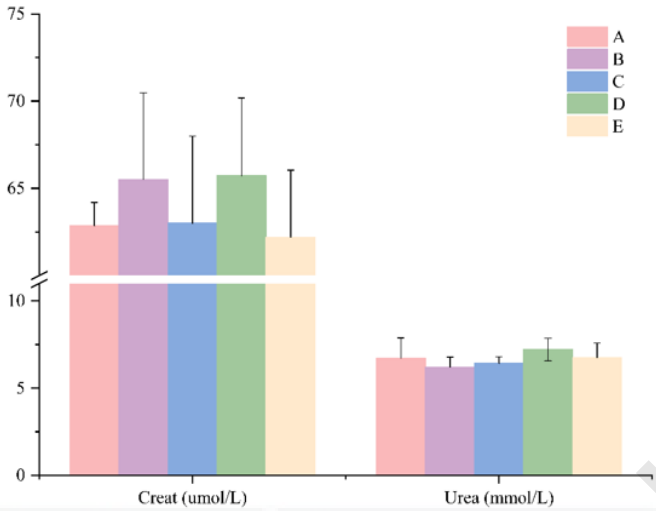

Figure 5.12: The level of Creatinine and Urea in the serum. A: Healthy mice, B: Control group, tumor mice untreated. C: Tumor mice treated with PM-H-H. D: Tumor mice treated with 5-FU. E: Tumor mice treated with PM-H-H+5-FU.

The evaluation of serum biomarkers, specifically AST, ALT, ALP, Creatinine, and Urea, provides crucial insights into the hepatic and renal toxicity associated with cancer treatments (Gur et al., 2022). In this study, distinct differences were observed in these toxicity parameters among the various experimental groups, underscoring the impact of different treatments on liver and kidney function.

Notably, the combination of PM-H-H with 5-FU (PM-H-H+5-FU group) demonstrated no significant difference in the levels of these biomarkers compared to healthy mice, suggesting that the combinatorial treatment did not induce additional toxicity. This is in stark contrast to what is typically observed with 5-FU treatment alone, where elevated levels of AST, ALT, and ALP often indicate hepatic stress or damage, and increased Creatinine and Urea levels reflect impaired renal function (Dai et al., 2021; Lousa et al., 2021).

The lack of significant alterations in toxicity markers in the PM-H-H+5-FU group supports the notion that PM-H-H may mitigate the toxic side effects commonly

associated with 5-FU. By potentially reducing liver and kidney damage, the combination treatment appears to enhance the safety profile of 5-FU. This reduction in toxicity is particularly important in clinical settings, as it could lead to improved patient outcomes by allowing higher or prolonged doses of 5-FU without the corresponding increase in adverse effects.

Previous studies have shown the potential of PM as an anticancer agent and that PM extract has the potency to reduce the side effects of the chemotherapy agent cisplatin (Abd Rashid et al., 2021). As in keeping with other such therapeutic agents, 5-FU possesses a range of serious side effects (Valencia-Lazcano et al., 2023). From the results, the preliminary safety analysis indicated that PM-H-H was able to alleviate the side effects of 5-FU *in vivo*. Since this study used mice bearing CC tumors, the current safety assessment has certain limitations and should be expanded through a series of rigorous evaluations before clinical use.

5.3.3 ELISA validation

The changes in Psat1 and Shmt2 levels in mouse tumors were assessed after combined treatment with PM-H-H and 5-FU. As shown in Figure 5.13, the combination treatment significantly reduced Psat1 and Shmt2 levels compared to the control group ($P<0.0001$). This finding suggests that PM-H-H enhances the effect of 5-FU by targeting key metabolic pathways involved in CC progression.

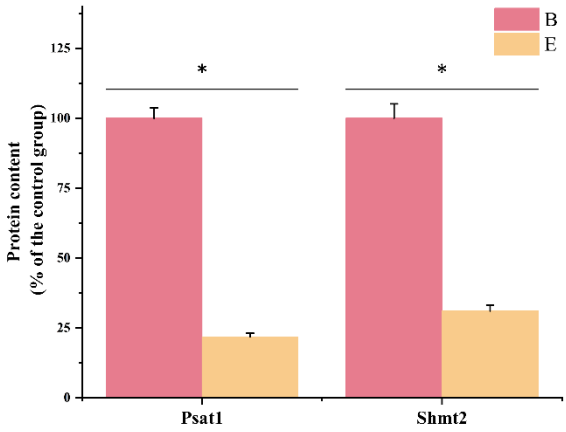

Figure 5.13: The level of Psat1 and Shmt2 in the tumor. B: Control group, tumor mice untreated. E: Tumor mice treated with PM-H-H+5-FU. *P<0.0001.

Psat1 and Shmt2 play crucial roles in glycine, serine, and threonine metabolism, as well as cysteine and methionine metabolism, both of which are critical for tumor cell proliferation and survival (Maugard et al., 2021; Shunxi et al., 2023; C. Zhang et al., 2023). These metabolic pathways contribute to nucleotide synthesis, redox homeostasis, and one-carbon metabolism, all of which are critical for sustaining uncontrolled cancer cell growth and survival. Dysregulation of these pathways has been linked to tumor progression, chemoresistance, and poor prognosis in CC patients, emphasizing the therapeutic relevance of targeting Psat1 and Shmt2 in cancer treatment. The significant reduction in these markers following treatment with PM-H-H and 5-FU suggests that the combination therapy effectively disrupts cancer metabolism by impairing amino acid availability and metabolic flux through these key pathways. This disruption compromises the proliferative capacity and adaptability of tumor cells, thereby inhibiting their ability to sustain rapid division, evade apoptosis, and resist therapeutic agents. Moreover, the observed metabolic inhibition may contribute to enhanced oxidative stress and reduced cellular fitness, further sensitizing cancer cells to chemotherapy-induced cytotoxicity. The ability of PM-H-H and 5-FU to modulate glycine, serine, threonine, cysteine, and methionine metabolism highlights

the potential of this combination as a metabolic-targeting therapeutic approach for CC treatment. By simultaneously disrupting multiple metabolic pathways essential for tumor growth, this strategy may provide a more effective and less toxic alternative to conventional chemotherapy, ultimately improving treatment outcomes and patient survival (J. Chen et al., 2024; S. Pan et al., 2021; Schiliro & Firestein, 2021).

As mentioned before, *in vitro* experiments similarly supported these findings, showing that the combined treatment led to a reduction in Psat1 and Shmt2 levels in CT26 cells. This downregulation likely inhibits amino acid metabolism, impacting the ability of cancer cells to sustain their growth and proliferation (Wei et al., 2021). The consistency between *in vitro* and *in vivo* results reinforces the significance of these proteins as key metabolic regulators in CC.

These findings have important clinical implications for CC treatment. Targeting Psat1 and Shmt2 through combination therapy could provide a novel therapeutic approach for overcoming chemoresistance and metabolic adaptation in cancer cells. Given that amino acid metabolism plays a crucial role in tumor progression, the observed metabolic disruption suggests that the PM-H-H and 5-FU combination could enhance treatment efficacy while potentially reducing the required dosage of 5-FU, thereby minimizing its associated toxicity.

Further clinical research and *in vivo* testing are necessary to assess the long-term therapeutic potential and safety profile of this combination. Future studies should explore whether Psat1 and Shmt2 suppression can serve as predictive biomarkers for treatment response in CC patients. Additionally, integrating this combination into standard chemotherapy regimens could pave the way for more personalized and less

toxic treatment strategies, improving patient outcomes and quality of life.

5.4 Conclusion

In this study, the combination of PM-H-H and 5-FU showed a notable improvement in antitumor effectiveness in the CT26 tumor mouse model when compared to the effects of each treatment used separately. The combined therapy not only reduced tumor volume and weight but also exhibited greater tumor growth inhibition, confirming the synergistic potential of PM-H-H in augmenting the effects of 5-FU. Histopathological analysis further revealed that the combined treatment caused more severe tumor tissue damage than single treatments, aligning with its enhanced antitumor activity.

Regarding safety, PM-H-H reduced the systemic toxicity typically linked to 5-FU, as evidenced by consistent body weight, better organ indices, and unchanged toxicity biomarkers in the co-treated group. These results imply that PM-H-H may broaden the therapeutic range of 5-FU by diminishing its adverse effects, particularly on essential organs like the liver and kidneys.

Notably, the combined treatment significantly downregulated Psat1 and Shmt2 levels in tumor tissues, which is consistent with *in vitro* findings. This highlights the potential disruption of critical metabolic pathways involved in cancer cell proliferation, further supporting the efficacy of the combination therapy.

Overall, the findings indicate that PM-H-H combined with 5-FU shows potential as an innovative treatment strategy for CC. Nevertheless, further research is necessary, particularly more extensive *in vivo* studies and clinical trials.

CHAPTER 6

CONCLUSION AND FUTURE RECOMMENDATION

6.1 Conclusion

This study demonstrated the anticancer potential of PM-H-H extract and its synergistic effects with 5-FU in the treatment of CC. Through *in vitro* and *in vivo* experiments, PM-H-H was identified as a promising adjunct to conventional chemotherapy, significantly enhancing 5-FU efficacy while potentially reducing toxicity.

The *in vitro* findings showed that the combination of PM-H-H and 5-FU exhibited strong synergistic anticancer effects, including increased cytotoxicity, apoptosis induction, and G0/G1 cell cycle arrest. Additionally, the combination effectively inhibited cancer cell migration, clonogenic formation, and spheroid growth, suggesting its potential role in suppressing metastasis.

Metabolomics and proteomics analyses revealed that the combination therapy disrupted key metabolic pathways involved in tumor progression, including glycine, serine, and threonine metabolism, as well as cysteine and methionine metabolism. The downregulation of Psat1 and Shmt2 further supported the metabolic impact of the treatment, suggesting a novel mechanism of action.

In vivo validation using a CT26 tumor-bearing mouse model confirmed these findings, showing that PM-H-H combined with 5-FU significantly reduced tumor volume and weight compared to single treatments. Importantly, this combination also mitigated systemic toxicity, as evidenced by histopathological analysis, which demonstrated

reduced damage to vital organs.

In conclusion, this study provides strong evidence that PM-H-H enhances the therapeutic effects of 5-FU in CC treatment. These findings support the further investigation of PM-H-H as a complementary agent in chemotherapy, with potential clinical applications for improving treatment efficacy while minimizing adverse effects. Future research should focus on pharmacokinetics, long-term safety, and clinical translation to establish its therapeutic viability in human CC treatment.

6.2 Future recommendation

The implications of this research are significant, particularly in the context of developing more effective and less toxic treatments for CC. By demonstrating that PM-H-H can augment the effectiveness of 5-FU while mitigating its systemic toxicity, this study opens new avenues for improving treatment regimens and patient outcomes.

However, the study also highlights several important areas for future research. While the *in vitro* and *in vivo* results are promising, further validation is necessary to fully understand the mechanisms through which PM-H-H enhances 5-FU's efficacy and reduces toxicity. This includes exploring the specific metabolic and proteomic pathways affected by the combination therapy and confirming these findings in broader animal models and eventually in clinical trials. Additionally, the potential of PM-H-H as a standalone treatment or in combination with other therapeutic agents warrants investigation to determine its broader applicability in cancer therapy.

Future studies should also focus on optimizing the extraction and formulation processes of PM-H-H to ensure consistent quality and potency. Investigating the long-

term safety and potential interactions of PM-H-H with other drugs will be crucial for establishing its viability as a clinical option. Overall, the integration of plant extracts like PM-H-H into therapeutic strategies holds promise for advancing cancer treatment, and ongoing research will be key to realizing their full potential in clinical settings.

REFERENCES

Abd Rashid, N., Abd Halim, S. A. S., Teoh, S. L., Budin, S. B., Hussan, F., Adib Ridzuan, N. R., & Abdul Jalil, N. A. (2021). The role of natural antioxidants in cisplatin-induced hepatotoxicity. Biomedicine & Pharmacotherapy, 144, 112328.

Abdullah, M. Z., Mohd Ali, J., Abolmaesoomi, M., Abdul-Rahman, P. S., & Hashim, O. H. (2017). Anti-proliferative, in vitro antioxidant, and cellular antioxidant activities of the leaf extracts from Polygonum minus Huds: Effects of solvent polarity. International Journal of Food Properties, 20(1), S846–S862.

Abu Hassan, M. R., Ismail, I., Mohd Suan, M. A., Ahmad, F., Wan Khazim, W. K., Othman, Z., Mat Said, R., Tan, W. L., Mohammed, S. R. N. S., Soelar, S. A., & Nik Mustapha, N. R. (2016). Incidence and mortality rates of colorectal cancer in Malaysia. Epidemiology and Health, 38, e2016007.

Abubakar, M. A., Zulkifli, R. M., Atiqah, W. N., Hassan, W., Husni, A., Shariff, M., Nizam, N. A., Malek, N., Zakaria, Z., & Ahmad, F. (2015). Antibacterial properties of Persicaria minor (Huds.) ethanolic and aqueous-ethanolic leaf extracts. Journal of Applied Pharmaceutical Science, 5(2), 50–56.

Ahmad, R., Baharum, S. N., Bunawan, H., Lee, M., Noor, N. M., Rohani, E. R., Ilias, N., & Zin, N. M. (2014). Volatile profiling of aromatic traditional medicinal plant, polygonum minus in different tissues and its biological activities. Molecules, 19(11), 19220–19242.

Ahmad, R., Bunawan, H., Normah, M. N., & Baharum, S. N. (2016). Chemical composition in different tissues of Polygonum minus by using GC X GC-TOF MS and direct discrimination by multivariate analysis of fourier transform infrared spectroscopy data. International Journal of Pharmacognosy and Phytochemical Research, 8(12), 1986–1992.

Ahmad, R., Rosandy, A. R., Sahidin, I., Syatila, N., Ghani, A., Noor, N. M., & Baharum, S. N. (2023). Bioassay Analysis and Molecular Docking Study Revealed the Potential Medicinal Activities of Active Compounds Polygonumins B, C and D from Polygonum minus (Persicaria minor). Plants, 12(1), 59.

Ahrens, C. H., Brunner, E., Qeli, E., Basler, K., & Aebersold, R. (2010). Generating and navigating proteome maps using mass spectrometry. Nature Reviews Molecular Cell Biology, 11(11), 789–801.

Ali, A. M., Muhammad, I., Mackeen, M., Ei-Sharkawy, S. H., Hamidi, J. A., Ahmadi, B. H., & Lajisi, N. H. (1996). Antiviral and Cytotoxic Activities of Som.e Plants Used in Malaysian Indigenous Medicine. Journal of Tropical Agricultural Science, 19(3), 129–136.

Alimohammadi, R., Mahmoodi Chalbatani, G., Alimohammadi, M., Ghaffari-Nazari, H., Rahimi, A., Mortaz, E., Mossafa, N., Boon, L., & Jalali, S. A. (2023). Dual blockage of both PD-L1 and CD47 enhances the therapeutic effect of oxaliplatin and FOLFOX in CT-26 mice tumor model. Scientific Reports, 13(1), 2472.

Alrbyawi, H. (2024). Stimuli-Responsive Liposomes of 5-Fluorouracil: Progressive Steps for Safe and Effective Treatment of Colorectal Cancer. Pharmaceutics, 16(7), 966.

Alrushaid, N., Khan, F. A., Al-Suhaimi, E., & Elaissari, A. (2023). Progress and Perspectives in Colon Cancer Pathology, Diagnosis, and Treatments. Diseases, 11(4), 148.

Alves, T. M. D. A., Ribeiro, F. L., Kloos, H., & Zani, C. L. (2001). Polygodial, the Fungitoxic Component from the Brazilian Medicinal Plant Polygonum punctatum. Memorias Do Instituto Oswaldo Cruz, 96(6), 831–833.

Alzahrani, S. M., Al Doghaither, H. A., Al-Ghafari, A. B., & Pushparaj, P. N. (2023). 5-Fluorouracil and capecitabine therapies for the treatment of colorectal cancer (Review). Oncology Reports, 50(4), 175.

Amin, A., Farrukh, A., Murali, C., Soleimani, A., Praz, F., Graziani, G., Brim, H., & Ashktorab, H. (2021). Saffron and its major ingredients' effect on colon cancer cells with mismatch repair deficiency and microsatellite instability. Molecules, 26(13), 3855.

Amiri, F., Zarnani, A. H., Zand, H., Koohdani, F., Jeddi-Tehrani, M., & Vafa, M. (2013). Synergistic anti-proliferative effect of resveratrol and etoposide on human hepatocellular and colon cancer cell lines. European Journal of Pharmacology, 718(1–3), 34–40.

Amiruddin, F., Wahab, I. A., & Mohsin, H. F. (2020). Review on Polygonum minus : pharmacological properties and phytochemical compounds. Journal of Engineering and Health Sciences, 4, 123–134.

Anaka, M., & Abdel-Rahman, O. (2022). Managing 5FU Cardiotoxicity in Colorectal Cancer Treatment. Cancer Management and Research, 14, 273–285.

Ananthi, R., Chandra, N., Santhiya, S. T., & Ramesh, A. (2010). Genotoxic and antigenotoxic effects of Hemidesmus indicus R. Br. root extract in cultured lymphocytes. Journal of Ethnopharmacology, 127(2), 558–560.

Andersen, M. K., Høiem, T. S., Claes, B. S. R., Balluff, B., Martin-Lorenzo, M., Richardsen, E., Krossa, S., Bertilsson, H., Heeren, R. M. A., Rye, M. B., Giskeødegård, G. F., Bathen, T. F., & Tessem, M.-B. (2021). Spatial differentiation of metabolism in prostate cancer tissue by MALDI-TOF MSI. Cancer & Metabolism, 9(1), 9.

Asgharzadeh, F., Mostafapour, A., Ebrahimi, S., Amerizadeh, F., Sabbaghzadeh, R., Hassanian, S. M., Fakhraei, M., Farshbaf, A., Ferns, G. A., Giovannetti, E., Avan, A., & Khazaei, M. (2022). Inhibition of angiotensin pathway via valsartan reduces tumor growth in models of colorectal cancer. Toxicology and Applied Pharmacology, 440, 115951.

Asif, M., Usman, M., Ayub, S., Farhat, S., Huma, Z., Ahmed, J., Kamal, M. A., Hussein, D., Javed, A., & Khan, I. (2020). Role of ATP-Binding Cassette Transporter Proteins in CNS Tumors: Resistance- Based Perspectives and Clinical Updates. Current Pharmaceutical Design, 26(37), 4747–4763.

Azad, A. K., Sulaiman, W. M. A. W., & Kundu, S. K. (2022). Toxicity profile of Phaleria macrocarpa (Scheff.) Boerl. fruits extract in adult male Sprague-Dawley rats. Advances in Traditional Medicine, 22(3), 557–567.

Azlim Almey, A. A., Ahmed Jalal Khan, C., Syed Zahir, I., Mustapha Suleiman, K., Aisyah, M. R., & Kamarul Rahim, K. (2010). Total phenolic content and primary antioxidant activity of methanolic and ethanolic extracts of aromatic plants' leaves. International Food Research Journal, 17(4), 1077.

Azwar, S., Seow, H. F., Abdullah, M., Jabar, M. F., & Mohtarrudin, N. (2021). Recent updates on mechanisms of resistance to 5-fluorouracil and reversal strategies in colon cancer treatment. Biology, 10(9), 854.

Backer, N., Kumar, A., Singh, A. K., Singh, H., Narasimhan, B., & Kumar, P. (2023). Medicinal chemistry aspects of uracil containing dUTPase inhibitors targeting colorectal cancer. Drug Discovery Today, 29(1), 103853.

Baharum, S. N., Bunawan, H., Ghani, M. A., Wan Aida Wan Mustapha, & Noor, N. M. (2010). Analysis of the chemical composition of the essential oil of Polygonum minus Huds. Using two-dimensional gas chromatography-time-of-flight mass spectrometry (GC-TOF MS). Molecules, 15(10), 7006–7015.

Baidoun, F., Elshiwy, K., Elkeraie, Y., Merjaneh, Z., Khoudari, G., Sarmini, M. T., Gad, M., Al-Husseini, M., & Saad, A. (2020). Colorectal Cancer Epidemiology: Recent Trends and Impact on Outcomes. Current Drug Targets, 22(9), 998–1009.

Barathan, M., Zulpa, A. K., Ng, S. L., Lokanathan, Y., Ng, M. H., & Law, J. X. (2024). Innovative Strategies to Combat 5-Fluorouracil Resistance in Colorectal Cancer: The Role of Phytochemicals and Extracellular Vesicles. International Journal of Molecular Sciences, 25(13), 7470.

Bashir, M. I., Aziz, N. H. K. A., & Noor, D. A. M. (2020). Possible antidepressant potential of a cognitive enhancer Polygonum minus based on its major chemical constituents in leaf part. Drug Invention Today, 13(4), 549–557.

Baum, M. M., Ramirez, C. M., Moss, J. A., Gunawardana, M., Bobardt, M., & Gallay, P. A. (2020). Highly synergistic drug combination prevents vaginal HIV infection in humanized mice. Scientific Reports, 10, 12995.

Bell, A. W., Deutsch, E. W., Au, C. E., Kearney, R. E., Beavis, R., Sechi, S., Nilsson, T., Bergeron, J. J. M., Beardslee, T. A., Chappell, T., Meredith, G., Sheffield, P., Gray, P., Hajivandi, M., Pope, M., Predki, P., Kullolli, M., Hincapie, M., Hancock, W. S., … Vizcaíno, J. A. (2009). A HUPO test sample study reveals common problems in mass spectrometry-based proteomics. Nature Methods, 6(6), 423–430.

Bernasocchi, T., & Mostoslavsky, R. (2024). Subcellular one carbon metabolism in cancer, aging and epigenetics. Frontiers in Epigenetics and Epigenomics, 2, 1451971.

Berndt, U., Philipsen, L., Bartsch, S., Wiedenmann, B., Baumgart, D. C., Hämmerle, M., & Sturm, A. (2008). Systematic high-content proteomic analysis reveals substantial immunologic changes in colorectal cancer. Cancer Research, 68(3), 880–888.

Besson, D., Pavageau, A. H., Valo, I., Bourreau, A., Bélanger, A., Eymerit-Morin, C., Moulière, A., Chassevent, A., Boisdron-Celle, M., Morel, A., Solassol, J., Campone, M., Gamelin, E., Barré, B., Coqueret, O., & Guette, C. (2011). A quantitative proteomic approach of the different stages of colorectal cancer establishes OLFM4 as a new nonmetastatic tumor marker. Molecular and Cellular Proteomics, 10(12), 1–14.

Billah, M. M., Islam, R., Khatun, H., Parvin, S., Islam, E., Islam, S. A., & Mia, A. A. (2013). Antibacterial, antidiarrhoeal, and cytotoxic activities of methanol extract and its fractions of Caesalpinia bonducella (L.) Roxb leaves. BMC Complementary and Alternative Medicine, 13(1), 1–7.

Blaise, B. J., Correia, G. D. S., Haggart, G. A., Surowiec, I., Sands, C., Lewis, M. R., Pearce, J. T. M., Trygg, J., Nicholson, J. K., Holmes, E., & Ebbels, T. M. D. (2021). Statistical analysis in metabolic phenotyping. Nature Protocols, 16(9), 4299–4326.

Blondy, S., David, V., Verdier, M., Mathonnet, M., Perraud, A., & Christou, N. (2020). 5-Fluorouracil resistance mechanisms in colorectal cancer: From classical pathways to promising processes. Cancer Science, 111(9), 3142–3154.

Boja, E. S., & Rodriguez, H. (2014). Proteogenomic convergence for understanding cancer pathways and networks. Clinical Proteomics, 11(1), 22.

Braicu, C., Zanoaga, O., Zimta, A. A., Tigu, A. B., Kilpatrick, K. L., Bishayee, A., Nabavi, S. M., & Berindan-Neagoe, I. (2022). Natural compounds modulate the crosstalk between apoptosis- and autophagy-regulated signaling pathways: Controlling the uncontrolled expansion of tumor cells. Seminars in Cancer Biology, 80, 218–236.

Bray, F., Laversanne, M., Sung, H., Ferlay, J., Siegel, R. L., Soerjomataram, I., & Jemal, A. (2024). Global cancer statistics 2022: GLOBOCAN estimates of incidence and mortality worldwide for 36 cancers in 185 countries. CA: A Cancer Journal for Clinicians, 74(3), 229–263.

Breen, D. M., Kim, H., Bennett, D., Calle, R. A., Collins, S., Esquejo, R. M., He, T., Joaquim, S., Joyce, A., Lambert, M., Lin, L., Pettersen, B., Qiao, S., Rossulek, M., Weber, G., Wu, Z., Zhang, B. B., & Birnbaum, M. J. (2020). GDF-15 Neutralization Alleviates Platinum-Based Chemotherapy-Induced Emesis, Anorexia, and Weight Loss in Mice and Nonhuman Primates. Cell Metabolism, 32(6), 938–950.

Brix, N., Samaga, D., Belka, C., Zitzelsberger, H., & Lauber, K. (2021). Analysis of clonogenic growth in vitro. Nature Protocols, 16, 4963–4991.

Brockmueller, A., Girisa, S., Kunnumakkara, A. B., & Shakibaei, M. (2023). Resveratrol Modulates Chemosensitisation to 5-FU via β1-Integrin/HIF-1α Axis in CRC Tumor Microenvironment. International Journal of Molecular Sciences, 24(5), 4988.

Cai, D. J., Zhang, Z. Y., Bu, Y., Li, L., Deng, Y. Z., Sun, L. Q., Hu, C. P., & Li, M. (2022). Asparagine synthetase regulates lung-cancer metastasis by stabilizing the β-catenin complex and modulating mitochondrial response. Cell Death and Disease, 13(6), 566.

Chalabi-Dchar, M., Fenouil, T., Machon, C., Vincent, A., Catez, F., Marcel, V., Mertani, H. C., Saurin, J. C., Bouvet, P., Guitton, J., Venezia, N. D., & Diaz, J. J. (2021). A novel view on an old drug, 5-fluorouracil: An unexpected RNA modifier with intriguing impact on cancer cell fate. NAR Cancer, 3(3), zcab032.

Chang, T. T., & Chou, T. C. (2000). Rational approach to the clinical protocol design for drug combinations: A review. Acta Paediatrica Taiwanica, 41(6), 294–302.

Chen, C., Zhang, L. G., Liu, J., Han, H., Chen, N., Yao, A. L., Kang, S. S., Gao, W. X., Shen, H., Zhang, L. J., Li, Y. P., Cao, F. H., & Li, Z. G. (2016). Bioinformatics analysis of differentially expressed proteins in prostate cancer based on proteomics data. OncoTargets and Therapy, 9, 1545–1557.

Chen, J., Cui, L., Lu, S., & Xu, S. (2024). Amino acid metabolism in tumor biology and therapy. Cell Death and Disease, 15, 42.

Chen, Y., Yang, J., Zuo, Y., Zhang, C., Pu, Y., Ren, Q., Li, X., Huang, Y., Huang, H., Yang, H., You, O., Xia, X., Lu, A., Shi, S., Deng, Y., & Lu, J. (2022). Voacamine is a novel inhibitor of EGFR exerting oncogenic activity against colorectal cancer through the mitochondrial pathway. Pharmacological Research, 184, 106415.

Chien, J. H., Chang, K. F., Lee, S. C., Lee, C. J., Chen, Y. T., Lai, H. C., Lu, Y. C., & Tsai, N. M. (2022). Cedrol restricts the growth of colorectal cancer in vitro and in vivo by inducing cell cycle arrest and caspase-dependent apoptotic cell death. International Journal of Medical Sciences, 19(13), 1953.

Chou, T. C. (2006). Theoretical basis, experimental design, and computerized simulation of synergism and antagonism in drug combination studies. Pharmacological Reviews, 58(3), 621–681.

Chou, T. C. (2014). Frequently asked questions in drug combinations and the mass-action law-based answers. Synergy, 1(1), 3–21.

Chou, T. C., & Talalay, P. (1981). Generalized equations for the analysis of inhibitions of Michaelis-Menten and higher-order kinetic systems with two or more mutually exclusive and nonexclusive inhibitors. European Journal of Biochemistry, 115(1), 207–216.

Chou, T. C., & Talalay, P. (1984). Quantitative analysis of dose-effect relationships: the combined effects of multiple drugs or enzyme inhibitors. Advances in Enzyme Regulation, 22, 27–55.

Christapher, P. V., Parasuraman, S., Asmawi, M. Z., & Murugaiyah, V. (2017). Acute and subchronic toxicity studies of methanol extract of Polygonum minus leaves in Sprague Dawley rats. Regulatory Toxicology and Pharmacology, 86, 33–41.

Christapher, P. V., Parasuraman, S., Christina, J. M. A., Asmawi, M. Z., & Vikneswaran, M. (2015). Review on polygonum minus. Huds, a commonly used food additive in Southeast Asia. Pharmacognosy Research, 7(1), 1–6.

Christapher, P. V., Parasuraman, S., Vasanth Raj, P., Saghir, S. A. M., Asmawi, M. Z., & Vikneswaran, M. (2016). Influence of Extracting Solvent on Pharmacological Activity and Cytotoxicity of Polygonum minus, a Commonly Consumed Herb in Southeast Asia. Pharmacognosy Magazine, 12(4), 424–430.

Christapher, P. V., Xin, T. Y., Kiun, C. F., Leng, L. C., Fu, N. G., Yuan, G. L., Parasuraman, S., & Vikneswaran, M. (2015). Evaluation of analgesic, anti-inflammatory, antipyretic and antiulcer effect of aqueous and methanol extracts of leaves of Polygonum minus Huds. (Polygonaceae) in rodents. Archives of Medicine and Health Sciences, 3(1), 12.

Clarkson, C., Maharaj, V. J., Crouch, N. R., Grace, O. M., Pillay, P., Matsabisa, M. G., Bhagwandin, N., Smith, P. J., & Folb, P. I. (2004). In vitro antiplasmodial activity of medicinal plants native to or naturalised in South Africa. Journal of Ethnopharmacology, 92(2–3), 177–191.

Clemen-Pascual, L. M., Macahig, R. A. S., & Rojas, N. R. L. (2022). Comparative toxicity, phytochemistry, and use of 53 Philippine medicinal plants. Toxicology Reports, 9, 22–35.

Cordier, P. Y., Nau, A., Ciccolini, J., Oliver, M., Mercier, C., Lacarelle, B., & Peytel, E. (2011). 5-FU-induced neurotoxicity in cancer patients with profound DPD deficiency syndrome: A report of two cases. Cancer Chemotherapy and Pharmacology, 68(3), 823–826.

Crecelius, A. C., Schubert, U. S., & Von Eggeling, F. (2015). MALDI mass spectrometric imaging meets “omics”: recent advances in the fruitful marriage. Analyst, 140(17), 5806–5820.

CS Wong, M., Ding, H., Wang, J., SF Chan, P., & Huang, J. (2019). Prevalence and risk factors of colorectal cancer in Asia. Intestinal Research, 17(3), 317.

Cui, H., Zhang, A., Chen, M., & Liu, J. (2015). ABC Transporter Inhibitors in Reversing Multidrug Resistance to Chemotherapy. Current Drug Targets, 16(12), 1356–1371.

da Silva, M. C., Fabiano, L. C., da Costa Salomão, K. C., de Freitas, P. L. Z., Neves, C. Q., Borges, S. C., de Souza Carvalho, M. das G., Breithaupt-Faloppa, A. C., de Thomaz, A. A., dos Santos, A. M., & Buttow, N. C. (2023). A Rodent Model of Human-Dose-Equivalent 5-Fluorouracil: Toxicity in the Liver, Kidneys, and Lungs. Antioxidants, 12(5), 1005.

Dai, W., Chen, C., Feng, H., Li, G., Peng, W., Liu, X., Yang, J., & Hu, X. (2021). Protection of Ficus pandurata Hance against acute alcohol-induced liver damage in mice via suppressing oxidative stress, inflammation, and apoptosis. Journal of Ethnopharmacology, 275, 114140.

Danesh Pouya, F., Rasmi, Y., & Nemati, M. (2022). Signaling Pathways Involved in 5-FU Drug Resistance in Cancer. Cancer Investigation, 40(6), 516–543.

Dang, C. V. (2013). MYC, metabolism, cell growth, and tumorigenesis. Cold Spring Harbor Perspectives in Medicine, 3(8), a014217. 7

Dang, C. V., & Semenza, G. L. (1999). Oncogenic alterations of metabolism. Trends in Biochemical Sciences, 24(2), 68–72.

Daud, N. M., Putra, N. R., Jamaludin, R., Md Norodin, N. S., Sarkawi, N. S., Hamzah, M. H. S., Mohd Nasir, H., Abang Zaidel, D. N., Che Yunus, M. A., & Md Salleh, L. (2022). Valorisation of plant seed as natural bioactive compounds by various extraction methods: A review. Trends in Food Science and Technology, 119, 201–204.

De Berardinis, R. J., & Chandel, N. S. (2016). Fundamentals of cancer metabolism. Science Advances, 2(5), e1600200.

de Wit, M., Kant, H., Piersma, S. R., Pham, T. V., Mongera, S., van Berkel, M. P. A., Boven, E., Pontén, F., Meijer, G. A., Jimenez, C. R., & Fijneman, R. J. A. (2014). Colorectal cancer candidate biomarkers identified by tissue secretome proteome profiling. Journal of Proteomics, 99, 26–39.

Deac, A. L., Burz, C. C., Bocsan, I. C., & Buzoianu, A. D. (2020). Fluoropyrimidine-induced cardiotoxicity. World Journal of Clinical Oncology, 11(12), 1008.

Demeckova, V., Mudronova, D., Gancarcikova, S., Kubatka, P., Kajo, K., Kassayova, M., Bojkova, B., Adamkov, M., & Solár, P. (2022). 5-Fluorouracil Treatment of CT26 Colon Cancer Is Compromised by Combined Therapy with IMMODIN. International Journal of Molecular Sciences, 23(12), 6374.

Deng, X., Yang, Z., Chan, K. W., & Abu Bakar, M. Z. (2024). Exploring the therapeutic potential of 5-fluorouracil-loaded calcium carbonate nanoparticles combined with natural compound thymoquinone for colon cancer treatment. Pharmaceutics, 16(8), 1011.

Derissen, E. J. B., & Beijnen, J. H. (2020). Intracellular Pharmacokinetics of Pyrimidine Analogues used in Oncology and the Correlation with Drug Action. Clinical Pharmacokinetics, 59(12), 1521–1550.

Deyell, M., Garris, C. S., & Laughney, A. M. (2021). Cancer metastasis as a non-healing wound. British Journal of Cancer, 124(9), 1491–1502.

Duarte, D., & Vale, N. (2022). Evaluation of synergism in drug combinations and reference models for future orientations in oncology. Current Research in Pharmacology and Drug Discovery, 3, 100110.

Eastwood, M. A., & Nyhlin, H. (1995). Beeturia and colonic oxalic acid. QJM: An International Journal of Medicine, 88(10), 711–717.

Ebbehøj, A. L., Jørgensen, L. N., Krarup, P. M., & Smith, H. G. (2021). Histopathological risk factors for lymph node metastases in T1 colorectal cancer: meta-analysis. British Journal of Surgery, 108(7), 769–776.

Elhamamsy, A. R., Metge, B. J., Alsheikh, H. A., Shevde, L. A., & Samant, R. S. (2022). Ribosome Biogenesis: A Central Player in Cancer Metastasis and Therapeutic Resistance. Cancer Research, 82(13), 2344–2353.

Embong, W. H. W. (2007). Healing herbs of Malaysia. In Healing Herbs of Malaysia (p. 201). Kuala Lumpur : Federal Land Development Authority (FELDA), 2007.

Emwas, A. H., Roy, R., McKay, R. T., Tenori, L., Saccenti, E., Nagana Gowda, G. A., Raftery, D., Alahmari, F., Jaremko, L., Jaremko, M., & Wishart, D. S. (2019). Nmr spectroscopy for metabolomics research. Metabolites, 9(7), 123.

Erhirhie, E. O., Ihekwereme, C. P., & Ilodigwe, E. E. (2018). Advances in acute toxicity testing: Strengths, weaknesses and regulatory acceptance. Interdisciplinary Toxicology, 11(1), 5–12.

Esmeeta, A., Adhikary, S., Dharshnaa, V., Swarnamughi, P., Ummul Maqsummiya, Z., Banerjee, A., Pathak, S., & Duttaroy, A. K. (2022). Plant-derived bioactive compounds in colon cancer treatment: An updated review. Biomedicine and Pharmacotherapy, 153, 113384.

Esturau-Escofet, N., Rodríguez de San Miguel, E., Vela-Amieva, M., García-Aguilera, M. E., Hernández-Espino, C. C., Macias-Kauffer, L., López-Candiani, C., Naveja, J. J., & Ibarra-González, I. (2022). A Longitudinal1 H NMR-Based Metabolic Profile Analysis of Urine from Hospitalized Premature Newborns Receiving Enteral and Parenteral Nutrition. Metabolites, 12(3), 255.

Ewert de Oliveira, B., Junqueira Amorim, O. H., Lima, L. L., Rezende, R. A., Mestnik, N. C., Bagatin, E., & Leonardi, G. R. (2021). 5-Fluorouracil, innovative drug delivery systems to enhance bioavailability for topical use. Journal of Drug Delivery Science and Technology, 61, 102155.

Fares, J., Fares, M. Y., Khachfe, H. H., Salhab, H. A., & Fares, Y. (2020). Molecular principles of metastasis: a hallmark of cancer revisited. Signal Transduction and Targeted Therapy, 5, 28.

Faujan, H.-, Noriham, A., Norrakiah, & Babji. (2007). Antioxidative Activities of Water Extracts of Some Malaysian Herbs 61. ASEAN Food Journal, 14(1), 61–68.

Freund, E., Liedtke, K. R., van der Linde, J., Metelmann, H. R., Heidecke, C. D., Partecke, L. I., & Bekeschus, S. (2019). Physical plasma-treated saline promotes an immunogenic phenotype in CT26 colon cancer cells in vitro and in vivo. Scientific Reports, 9, 634.

Friedenreich, C. M., Ryder-Burbidge, C., & McNeil, J. (2021). Physical activity, obesity and sedentary behavior in cancer etiology: epidemiologic evidence and biologic mechanisms. Molecular Oncology, 15(3), 790–800.

Fu, B., Wang, N., Tan, H. Y., Li, S., Cheung, F., & Feng, Y. (2018). Multi-component herbal products in the prevention and treatment of chemotherapy-associated toxicity and side effects: A review on experimental and clinical evidences. Frontiers in Pharmacology, 9, 411500.

Fukao, A., Tomohiro, T., & Fujiwara, T. (2021). Translation initiation regulated by RNA-binding protein in Mammals: The modulation of translation initiation complex by trans-acting factors. Cells, 10(7), 1711.

Gao, Q., Feng, J., Liu, W., Wen, C., Wu, Y., Liao, Q., Zou, L., Sui, X., Xie, T., Zhang, J., & Hu, Y. (2022). Opportunities and challenges for co-delivery nanomedicines based on combination of phytochemicals with chemotherapeutic drugs in cancer treatment. Advanced Drug Delivery Reviews, 188, 114445.

García-Alfonso, P., Muñoz Martín, A. J., Ortega Morán, L., Soto Alsar, J., Torres Pérez-Solero, G., Blanco Codesido, M., Calvo Ferrandiz, P. A., & Grasso Cicala, S. (2021). Oral drugs in the treatment of metastatic colorectal cancer. Therapeutic Advances in Medical Oncology, 13, 1–16.

Garutti, M., Noto, C., Pastò, B., Cucciniello, L., Alajmo, M., Casirati, A., Pedrazzoli, P., Caccialanza, R., & Puglisi, F. (2023). Nutritional Management of Oncological Symptoms: A Comprehensive Review. Nutrients, 15(24), 5068.

Gash, K. J., Baser, O., & Kiran, R. P. (2017). Factors associated with degree of tumour response to neo-adjuvant radiotherapy in rectal cancer and subsequent corresponding outcomes. European Journal of Surgical Oncology, 43(11), 2052–2059.

Gemoll, T., Habermann, J. K., Becker, S., Szymczak, S., Upender, M. B., Bruch, H. P., Hellman, U., Ried, T., Auer, G., Jörnvall, H., & Roblick, U. J. (2013). Chromosomal aneuploidy affects the global proteome equilibrium of colorectal cancer cells. Analytical Cellular Pathology, 36(5–6), 149–161.

George, A., Chinnappan, S., Choudhary, Y., Bommu, P., & Sridhar, M. (2014). Immunomodulatory activity of an aqueous extract of Polygonum minus Huds on Swiss albino mice using carbon clearance assay. Asian Pacific Journal of Tropical Disease, 4(5), 398–400.

George, A., Ng, C. P., O'Callaghan, M., Jensen, G. S., & Wong, H. J. (2014). In vitro and ex-vivo cellular antioxidant protection and cognitive enhancing effects of an extract of Polygonum minus Huds (LineminusTM) demonstrated in a Barnes Maze animal model for memory and learning. BMC Complementary and Alternative Medicine, 14, 1–10.

Ghafouri-Fard, S., Abak, A., Tondro Anamag, F., Shoorei, H., Fattahi, F., Javadinia, S. A., Basiri, A., & Taheri, M. (2021). 5-Fluorouracil: A Narrative Review on the Role of Regulatory Mechanisms in Driving Resistance to This Chemotherapeutic Agent. Frontiers in Oncology, 11, 658636.

Gizak, A., Wiśniewski, J., Heron, P., Mamczur, P., Sygusch, J., & Rakus, D. (2019). Targeting a moonlighting function of aldolase induces apoptosis in cancer cells. Cell Death and Disease, 10(10), 712.

Gmeiner, W. H. (2020a). Chemistry of fluorinated pyrimidines in the era of personalized medicine. Molecules, 25(15), 3438.

Gmeiner, W. H. (2020b). Fluoropyrimidine modulation of the anti-tumor immune response—prospects for improved colorectal cancer treatment. Cancers, 12(6), 1641.

Gmeiner, W. H. (2021). A narrative review of genetic factors affecting fluoropyrimidine toxicity. Precision Cancer Medicine, 4, 38.

Goh, W. W. Bin, Lee, Y. H., Zubaidah, R. M., Jin, J., Dong, D., Lin, Q., Chung, M. C. M., & Wong, L. (2011). Network-based pipeline for analyzing MS data: An application toward liver cancer. Journal of Proteome Research, 10(5), 2261–2272.

Golshani, G., & Zhang, Y. (2020). Advances in immunotherapy for colorectal cancer: a review. Therapeutic Advances in Gastroenterology, 13, 1–11.

Gomes, L. R., Menck, C. F. M., & Leandro, G. S. (2017). Autophagy roles in the modulation of DNA repair pathways. International Journal of Molecular Sciences, 18(11), 2351.

Gong, J. E., Jin, Y. J., Kim, J. E., Choi, Y. J., Lee, S. J., Kim, K. S., Jung, Y. S., Cho, J. Y., Lim, Y., Kang, H. G., & Hwang, D. Y. (2021). Comparison of cisplatin-induced anti-tumor response in CT26 syngeneic tumors of three BALB/c substrains. Laboratory Animal Research, 37(1), 33.

Gong, K., Hong, Q., Wu, H., Wang, F., Zhong, L., Shen, L., Xu, P., Zhang, W., Cao, H., Zhan, Y. yan, Hu, T., & Hong, X. (2022). Gap junctions mediate glucose transfer to promote colon cancer growth in three-dimensional spheroid culture. Cancer Letters, 531, 27–38.

Gorinstein, S., Vargas, O. J. M., Jaramillo, N. O., Salas, I. A., Ayala, A. L. M., Arancibia-Avila, P., Toledo, F., Katrich, E., & Trakhtenberg, S. (2007). The total polyphenols and the antioxidant potentials of some selected cereals and pseudocereals. European Food Research and Technology, 225, 321–328.

Gramolini, A. O., Kislinger, T., Alikhani-Koopaei, R., Fong, V., Thompson, N. J., Isserlin, R., Sharma, P., Oudit, G. Y., Trivieri, M. G., Fagan, A., Kannan, A., Higgins, D. G., Huedig, H., Hess, G., Arab, S., Seidman, J. G., Seidman, C. E., Frey, B., Perry, M., … Emili, A. (2008). Comparative proteomics profiling of a phospholamban mutant mouse model of dilated cardiomyopathy reveals progressive intracellular stress responses. Molecular and Cellular Proteomics, 7(3), 519–533.

Graziani, V., Scognamiglio, M., Belli, V., Esposito, A., D'Abrosca, B., Chambery, A., Russo, R., Panella, M., Russo, A., Ciardiello, F., Troiani, T., Potenza, N., & Fiorentino, A. (2018). Metabolomic approach for a rapid identification of natural products with cytotoxic activity against human colorectal cancer cells. Scientific Reports, 8(1), 5309.

Gsottberger, F., Meier, C., Ammon, A., Parker, S., Wendland, K., George, R., Petkovic, S., Mellenthin, L., Emmerich, C., Lutzny-Geier, G., Metzler, M., Mackensen, A., Chandramohan, V., & Müller, F. (2023). Targeted inhibition of protein synthesis renders cancer cells vulnerable to apoptosis by unfolded protein response. Cell Death and Disease, 14(8), 1–13.

Gu, J., Zhang, H., Wen, C., Zhang, J., He, Y., Ma, H., & Duan, Y. (2020). Purification, characterization, antioxidant and immunological activity of polysaccharide from Sagittaria sagittifolia L. Food Research International, 136, 109345.

Güçlü, H., Doganlar, Z. B., Gürlü, V. P., Özal, A., Dogan, A., Turhan, M. A., & Doganlar, O. (2018). Effects of cisplatin-5-fluorouracil combination therapy on oxidative stress, DNA damage, mitochondrial apoptosis, and death receptor signalling in retinal pigment epithelium cells. Cutaneous and Ocular Toxicology, 37(3), 291–304.

Gui, Y., Qian, X., Ding, Y., Chen, Q., Fangyu Ye, Ye, Y., Hou, Y., Yu, J., & Zhao, L. (2024). c-Fos regulated by TMPO/ERK axis promotes 5-FU resistance via inducing NANOG transcription in colon cancer. Cell Death and Disease, 15, 61.

Guo, Y., Ye, Q., Deng, P., Cao, Y., He, D., Zhou, Z., Wang, C., Zaytseva, Y. Y., Schwartz, C. E., Lee, E. Y., Mark Evers, B., Morris, A. J., Liu, S., & She, Q. B. (2020). Spermine synthase and MYC cooperate to maintain colorectal cancer cell survival by repressing Bim expression. Nature Communications, 11, 3243.

Gupta, D. Das, Mishra, S., Verma, S. S., Shekher, A., Rai, V., Awasthee, N., Das, T. J., Paul, D., Das, S. K., Tag, H., Chandra Gupta, S., & Hui, P. K. (2021). Evaluation of antioxidant, anti-inflammatory and anticancer activities of diosgenin enriched Paris polyphylla rhizome extract of Indian Himalayan landraces. Journal of Ethnopharmacology, 270, 113842.

Gur, C., Kandemir, F. M., Caglayan, C., & Satıcı, E. (2022). Chemopreventive effects of hesperidin against paclitaxel-induced hepatotoxicity and nephrotoxicity via amendment of Nrf2/HO-1 and caspase-3/Bax/Bcl-2 signaling pathways. Chemico-Biological Interactions, 365, 110073.

Habanjar, O., Diab-Assaf, M., Caldefie-Chezet, F., & Delort, L. (2021). 3D cell culture systems: Tumor application, advantages, and disadvantages. International Journal of Molecular Sciences, 22(22), 12200.

Hamidi, J. A., Ismaili, N., Ahmadi, F., & Lajisi, N. H. (1996). Antiviral and cytotoxic activities of some plants used in Malaysian indigenous medicine. Pertanika Journal of Tropical Agricultural Science, 19(2/3), 129–136.

Han, M., Kasim, S., Yang, Z., Deng, X., Uddin, M. K., Saidi, N. B., & Shuib, E. M. (2024). Application of Polygonum minus extract in enhancing drought tolerance in maize by regulating osmotic and antioxidant system. Phyton-International Journal of Experimental Botany, 93(2), 213–226.

Hanahan, D., & Weinberg, R. A. (2011). Hallmarks of cancer: The next generation. Cell, 144(5), 646–674.

Hashimoto, Y., Yoshida, Y., Yamada, T., Aisu, N., Yoshimatsu, G., Yoshimura, F., & Hasegawa, S. (2020). Current status of therapeutic drug monitoring of 5-fluorouracil prodrugs. Anticancer Research, 40(8), 4655–4661.

Hassan, K. Z., Noor, H. M., & Kader, J. (2015). Antibacterial Efficacy of Three Different Extracts of Polygonum minus (Huds.). International Conference on Waste Management, Ecology and Biological Sciencess, 41–48.

He, C., Liu, Y., Liu, H., Zheng, X., Shen, G., & Feng, J. (2020). Compositional identification and authentication of Chinese honeys by 1H NMR combined with multivariate analysis. Food Research International, 130, 108936.

He, L., Ding, Y., Zhou, X., Li, T., & Yin, Y. (2023). Serine signaling governs metabolic homeostasis and health. Trends in Endocrinology and Metabolism, 34(6), 361–372.

Heiden, M. G. V., Cantley, L. C., & Thompson, C. B. (2009). Understanding the warburg effect: The metabolic requirements of cell proliferation. Science, 324(5930), 1029–1033.

Hofseth, L. J., Hebert, J. R., Chanda, A., Chen, H., Love, B. L., Pena, M. M., Murphy, E. A., Sajish, M., Sheth, A., Buckhaults, P. J., & Berger, F. G. (2020). Early-onset colorectal cancer: initial clues and current views. Nature Reviews Gastroenterology and Hepatology, 17(6), 352–364.

Hosseini, M., Baghaei, K., Hajivalili, M., Zali, M. R., Ebtekar, M., & Amani, D. (2022). The anti-tumor effects of CT-26 derived exosomes enriched by MicroRNA-34a on murine model of colorectal cancer. Life Sciences, 290, 120234.

Hruba, L., Das, V., Hajduch, M., & Dzubak, P. (2023). Nucleoside-based anticancer drugs: Mechanism of action and drug resistance. Biochemical Pharmacology, 215, 115741.

Hsu, P. P., & Sabatini, D. M. (2008). Cancer cell metabolism: Warburg and beyond. Cell, 134(5), 703–707.

Hu, A., Sun, L., Lin, H., Liao, Y., Yang, H., & Mao, Y. (2024). Harnessing innate immune pathways for therapeutic advancement in cancer. Signal Transduction and Targeted Therapy, 9(1), 1–59.

Hu, X., Zhang, Y., Zhang, A., Li, Y., Zhu, Z., Shao, Z., Zeng, R., & Xu, L. X. (2009). Comparative serum proteome analysis of human lymph node negative/positive invasive ductal carcinoma of the breast and benign breast disease controls via label-free semiquantitative shotgun technology. OMICS A Journal of Integrative Biology, 13(4), 291–300.

Huang, B., Abraham, W. D., Zheng, Y., Bustamante López, S. C., Luo, S. S., & Irvine, D. J. (2015). Active targeting of chemotherapy to disseminated tumors using nanoparticle-carrying T cells. Science Translational Medicine, 7(291), 291ra94.

Huang, M., Hou, W., Zhang, J., Li, M., Zhang, Z., Li, X., Chen, Z., Wang, C., & Yang, L. (2022). Evaluation of AMG510 Therapy on KRAS-Mutant Non–Small Cell Lung Cancer and Colorectal Cancer Cell Using a 3D Invasive Tumor Spheroid System under Normoxia and Hypoxia. Bioengineering, 9(12), 792.

Huang, Z., He, Z., Kong, Y., Liu, Z., & Gong, L. (2020). Insight into osteoarthritis through integrative analysis of metabolomics and transcriptomics. Clinica Chimica Acta, 510, 323–329.

Huda-Faujan, N., Noriham, A., Norrakiah, A., & Babji, A. (2009). Antioxidant activity of plants methanolic extracts containing phenolic compounds. African Journal of Biotechnology, 8(3), 484–489.

Imamaki, H., Oura, M., Oguro, F., Nishikawa, Y., Nakagawa, S., Funakoshi, T., Kataoka, S., Horimatsu, T., Yonezawa, A., Matsubara, T., Watanabe, N., Muto, M., Yanagita, M., & Ozaki, Y. (2024). Removal rate of 5-fluorouracil and its metabolites in patients on hemodialysis: a report of two cases of colorectal cancer patients with end-stage renal failure. Cancer Chemotherapy and Pharmacology, 93(2), 161–167.

Isah Tsamiya, R., Mohd Nafi, S. N., Che Jalil, N. A., & Mat Zin, A. A. (2024). The Clinicopathological Characteristics of Young-Onset Versus Adult-Onset Colorectal Cancer: A Tertiary Hospital-Based Study. Malaysian Journal of Medical Sciences, 31(1), 200.

Ishibashi, M., Ishii, M., Yamamoto, S., Mori, Y., & Shimizu, S. (2021). Possible involvement of TRPM2 activation in 5-fluorouracil-induced myelosuppression in mice. European Journal of Pharmacology, 891, 173671.

Ishihama, Y., Oda, Y., Tabata, T., Sato, T., Nagasu, T., Rappsilber, J., & Mann, M. (2005). Exponentially modified protein abundance index (emPAI) for estimation of absolute protein amount in proteomics by the number of sequenced peptides per protein. Molecular and Cellular Proteomics, 4(9), 1265–1272.

Islam, M. R., Akash, S., Rahman, M. M., Nowrin, F. T., Akter, T., Shohag, S., Rauf, A., Aljohani, A. S. M., & Simal-Gandara, J. (2022). Colon cancer and colorectal cancer: Prevention and treatment by potential natural products. Chemico-Biological Interactions, 368, 110170.

Jaaks, P., Coker, E. A., Vis, D. J., Edwards, O., Carpenter, E. F., Leto, S. M., Dwane, L., Sassi, F., Lightfoot, H., Barthorpe, S., van der Meer, D., Yang, W., Beck, A., Mironenko, T., Hall, C., Hall, J., Mali, I., Richardson, L., Tolley, C., … Garnett, M. J. (2022). Effective drug combinations in breast, colon and pancreatic cancer cells. Nature, 603(7899), 166–173.

Jarukamjorn, K., & Nemoto, N. (2008). Pharmacological aspects of Andrographis paniculata on health and its major diterpenoid constituent andrographolide. Journal of Health Science, 54(4), 370–381.

Jin, H., Wang, L., & Bernards, R. (2023). Rational combinations of targeted cancer therapies: background, advances and challenges. Nature Reviews Drug Discovery, 22(3), 213–234.

Johnny, L., Yusuf, U. K., & Nulit, R. (2011). Antifungal activity of selected plant leaves crude extracts against a pepper anthracnose fungus, Colletotrichum capsici (Sydow) butler and bisby (Ascomycota: Phyllachorales). African Journal of Biotechnology, 10(20), 4157–4165.

Jung, G., Hernández-Illán, E., Moreira, L., Balaguer, F., & Goel, A. (2020). Epigenetics of colorectal cancer: biomarker and therapeutic potential. Nature Reviews Gastroenterology and Hepatology, 17(2), 111–130.

Jurczyk, M., Król, M., Midro, A., Kurnik-łucka, M., Poniatowski, A., & Gil, K. (2021). Cardiotoxicity of fluoropyrimidines: Epidemiology, mechanisms, diagnosis, and management. Journal of Clinical Medicine, 10(19), 4426.

Kalachaveedu, M., Senthil, R., Azhagiyamanavalan, S., Ravi, R., Meenakshisundaram, H., & Dharmarajan, A. (2023). Traditional medicine herbs as natural product matrices in cancer chemoprevention: A trans pharmacological perspective (scoping review). Phytotherapy Research, 37(4), 1539–1573.

Kamran, S., Sinniah, A., Chik, Z., & Alshawsh, M. A. (2022). Diosmetin Exerts Synergistic Effects in Combination with 5-Fluorouracil in Colorectal Cancer Cells. Biomedicines, 10(3), 531.

Kanduri, J., More, L. A., Godishala, A., & Asnani, A. (2019). Fluoropyrimidine-Associated Cardiotoxicity. Cardiology Clinics, 37(4), 399–405.

Kang, J., Brajanovski, N., Chan, K. T., Xuan, J., Pearson, R. B., & Sanij, E. (2021). Ribosomal proteins and human diseases: molecular mechanisms and targeted therapy. Signal Transduction and Targeted Therapy, 6(1), 1–22.

Kano, Y., Suenaga, M., & Uetake, H. (2023). Strategic Insight into the Combination Therapies for Metastatic Colorectal Cancer. Current Oncology, 30(7), 6546–6558. https://doi.org/10.3390/curroncol30070480

Karimi, E., Gharib, B., Rostami, N., Navidpour, L., & Afshar, M. (2019). Clinical efficacy of a topical polyherbal formulation in the management of fluorouracil - associated hand-foot syndrome. Journal of Herbal Medicine, 17, 100270.

Karthika, C., Hari, B., Rahman, M. H., Akter, R., Najda, A., Albadrani, G. M., Sayed, A. A., Akhtar, M. F., & Abdel-Daim, M. M. (2021). Multiple strategies with the synergistic approach for addressing colorectal cancer. Biomedicine and Pharmacotherapy, 140, 111704.

Kastrinos, F., Samadder, N. J., & Burt, R. W. (2020). Use of Family History and Genetic Testing to Determine Risk of Colorectal Cancer. Gastroenterology, 158(2), 389–403.

Kershaw, C. J., Nelson, M. G., Castelli, L. M., Jennings, M. D., Lui, J., Talavera, D., Grant, C. M., Pavitt, G. D., Hubbard, S. J., & Ashe, M. P. (2023). Translation factor and RNA binding protein mRNA interactomes support broader RNA regulons for posttranscriptional control. Journal of Biological Chemistry, 299(10), 105195.

Kim, A., Im, M., Gu, M. J., & Ma, J. Y. (2016). Citrus unshiu peel extract alleviates cancer-induced weight loss in mice bearing CT-26 adenocarcinoma. Scientific Reports, 6(1), 24214.

Kim, H. Y., Lee, S. G., Oh, T. J., Lim, S. R., Kim, S. H., Lee, H. J., Kim, Y. S., & Choi, H. K. (2015). Antiproliferative and apoptotic activity of Chamaecyparis obtusa leaf extract against the HCT116 human colorectal cancer cell line and investigation of the bioactive compound by gas chromatography-mass spectrometry-based metabolomics. Molecules, 20(10), 18066–18082.

Kim, J., Lee, J., Oh, J. H., Chang, H. J., Sohn, D. K., Shin, A., & Kim, J. (2020). Plasma inflammatory biomarkers and modifiable lifestyle factors associated with colorectal cancer risk. Clinical Nutrition, 39(9), 2778–2785.

Kim, S. K., & Cho, S. W. (2022). The Evasion Mechanisms of Cancer Immunity and Drug Intervention in the Tumor Microenvironment. Frontiers in Pharmacology, 13, 868695.

Kimmelman, A. C. (2015). Metabolic dependencies in RAS-driven cancers. Clinical Cancer Research, 21(8), 1828–1834.

Knight, J. R. P., & Sansom, O. J. (2021). Tuning protein synthesis for cancer therapy. Molecular and Cellular Oncology, 8(2), 1884034.

Knikman, J. E., Gelderblom, H., Beijnen, J. H., Cats, A., Guchelaar, H. J., & Henricks, L. M. (2021). Individualized Dosing of Fluoropyrimidine-Based Chemotherapy to Prevent Severe Fluoropyrimidine-Related Toxicity: What Are the Options? Clinical Pharmacology and Therapeutics, 109(3), 591–604.

Koenig, H., & Patel, A. (1970). Biochemical Basis for Fluorouracil Neurotoxicity: The Role of Krebs Cycle Inhibition by Fluoroacetate. Archives of Neurology, 23(2), 155–160.

Kojouharov, B. M., Brackett, C. M., Veith, J. M., Johnson, C. P., Gitlin, I. I., Toshkov, I. A., Gleiberman, A. S., Gudkov, A. V., & Burdelya, L. G. (2014). Toll-like receptor-5 agonist entolimod broadens the therapeutic window of 5-fluorouracil by reducing its toxicity to normal tissues in mice. Oncotarget, 5(3), 802–814.

Koosha, S., Mohamed, Z., Sinniah, A., & Alshawsh, M. A. (2019). Investigation into the molecular mechanisms underlying the anti-proliferative and anti-tumorigenesis activities of diosmetin against HCT-116 human colorectal cancer. Scientific Reports, 9, 5148.

Koppenol, W. H., Bounds, P. L., & Dang, C. V. (2011). Otto Warburg's contributions to current concepts of cancer metabolism. Nature Reviews Cancer, 11(5), 325–337.

Krall, A. S., Xu, S., Graeber, T. G., Braas, D., & Christofk, H. R. (2016). Asparagine promotes cancer cell proliferation through use as an amino acid exchange factor. Nature Communications, 7(1), 1–13.

Krampe, B., & Al-Rubeai, M. (2010). Cell death in mammalian cell culture: Molecular mechanisms and cell line engineering strategies. Cytotechnology, 62(3), 175–188.

Krasteva, N., & Georgieva, M. (2022). Promising Therapeutic Strategies for Colorectal Cancer Treatment Based on Nanomaterials. Pharmaceutics, 14(6), 1213.

Kulesza, J., Pawłowska, M., & Augustin, E. (2021). The influence of antitumor unsymmetrical bisacridines on 3d cancer spheroids growth and viability. Molecules, 26(20), 6262.

Kumar, A., Singh, A. K., Singh, H., Thareja, S., & Kumar, P. (2023). Regulation of thymidylate synthase: an approach to overcome 5-FU resistance in colorectal cancer. Medical Oncology, 40(1), 3.

Kumar, S., Parveen, S., Swaroop, S., & Banerjee, M. (2023). TNF-α and MMPs mediated mucus hypersecretion induced by cigarette smoke: An in vitro study. Toxicology in Vitro, 92, 105654.

Lagarto Parra, A., Silva Yhebra, R., Guerra Sardiñas, I., & Iglesias Buela, L. (2001). Comparative study of the assay of Artemia salina L. and the estimate of the medium lethal dose (LD50 value) in mice, to determine oral acute toxicity of plant extracts. Phytomedicine, 8(5), 395–400.

Lai, W. L., Lee, S. C., Chang, K. F., Huang, X. F., Li, C. Y., Lee, C. J., Wu, C. Y., Hsu, H. J., & Tsai, N. M. (2021). Juniperus communis extract induces cell cycle arrest and apoptosis of colorectal adenocarcinoma in vitro and in vivo. Brazilian Journal of Medical and Biological Research, 54(10), e10891.

Lan, M. J., Yao, D. F., Zhu, L. L., & Zhou, Q. (2023). The Rate of Infusion Represents an Important Aspect of Administering Anticancer Agents. Risk Management and Healthcare Policy, 16, 2531–2541.

Leary, M., Heerboth, S., Lapinska, K., & Sarkar, S. (2018). Sensitization of drug resistant cancer cells: A matter of combination therapy. Cancers, 10(12), 483.

Lee, D. S., Musa, N., Seong Wei, L., Tse Seng, C., Wee, W., Kok Leong, L., Biotechnology Sdn Bhd, G., & Serdang Perdana, T. (2008). Potential of Edible Plants as Remedies of Systemic Bacterial Disease Infection in Cultured Fish. Global Journal of Pharmacology, 2(2), 31–36.

Leelakanok, N., Geary, S., & Salem, A. (2018). Fabrication and Use of Poly(D,L-lactide-co-glycolide)-Based Formulations Designed for Modified Release of 5-Fluorouracil. Journal of Pharmaceutical Sciences, 107(2), 513–528.

Li, X., Wei, S., Niu, S., Ma, X., Li, H., Jing, M., & Zhao, Y. (2022). Network pharmacology prediction and molecular docking-based strategy to explore the potential mechanism of Huanglian Jiedu Decoction against sepsis. Computers in Biology and Medicine, 144, 105389.

Li, X., Yu, C., Luo, Y., Lin, J., Wang, F., Sun, X., Gao, Y., Tan, W., Xia, Q., & Kong, X. (2021). Aldolase a enhances intrahepatic cholangiocarcinoma proliferation and invasion through promoting glycolysis. International Journal of Biological Sciences, 17(7), 1782–1794.

Liang, Z., Xie, H., Shen, W., Shao, L., Zeng, L., Huang, X., Zhu, Q., Zhai, X., Li, K., Qiu, Z., Sui, X., Cheng, H., & Wu, Q. (2022). The Synergism of Natural Compounds and Conventional Therapeutics against Colorectal Cancer Progression and Metastasis. Frontiers in Bioscience - Landmark, 27(9), 263.

Lill, J. (2003). Proteomic tools for quantitation by mass spectrometry. Mass Spectrometry Reviews, 22(3), 182–194.

Lin, X., An, T., Fu, D., Duan, S., Jin, H.-L., & Wang, H.-B. (2023). Optimization of central carbon metabolism by Warburg effect of human cancer cell improves triterpenes biosynthesis in yeast. Advanced Biotechnology, 1(4), 4.

Lin, X., Lécuyer, L., Liu, X., Triba, M. N., Deschasaux-Tanguy, M., Demidem, A., Liu, Z., Palama, T., Rossary, A., Vasson, M. P., Hercberg, S., Galan, P., Savarin, P., Xu, G., & Touvier, M. (2021). Plasma metabolomics for discovery of early metabolic markers of prostate cancer based on ultra-high-performance liquid chromatography-high resolution mass spectrometry. Cancers, 13(13), 3140.

Liu, B., Meng, Q., Gao, X., Sun, H., Xu, Z., Wang, Y., & Zhou, H. (2023). Lipid and glucose metabolism in senescence. Frontiers in Nutrition, 10, 1157352.

Liu, C., Zhao, Y., Wang, J., Yang, Y., Zhang, Y., Qu, X., Peng, S., Yao, Z., Zhao, S., He, B., Mi, Q., Zhu, Y., Liu, X., Zou, J., Zhang, X., & Du, Q. (2020). FoxO3 reverses 5-fluorouracil resistance in human colorectal cancer cells by inhibiting the Nrf2/TR1 signaling pathway. Cancer Letters, 470, 29–42.

Liu, H., Sadygov, R. G., & Yates, J. R. (2004). A model for random sampling and estimation of relative protein abundance in shotgun proteomics. Analytical Chemistry, 76(14), 4193–4201.

Liu, K., Zheng, M., Lu, R., Du, J., Zhao, Q., Li, Z., Li, Y., & Zhang, S. (2020). The role of CDC25C in cell cycle regulation and clinical cancer therapy: A systematic review. Cancer Cell International, 20, 1–16.

Liu, Y., Tong, Z., Shi, J., Li, R., Upton, M., & Wang, Z. (2021). Drug repurposing for next-generation combination therapies against multidrug-resistant bacteria. Theranostics, 11(10), 4910.

Liu, Y., Zhang, C., Wang, Q., Wu, K., Sun, Z., Tang, Z., & Zhang, B. (2023). Temporal Trends in the Disease Burden of Colorectal Cancer with Its Risk Factors at the Global and National Level from 1990 to 2019, and Projections Until 2044. Clinical Epidemiology, 15, 55–71.

Lo, E. K. K., Leung, H. K. M., Zhang, F., & El-Nezami, H. (2023). Gut microbiota: Impact on 5-fluorouracil efficacy and toxicity. Current Opinion in Toxicology, 36, 100423.

Loke, M. F., Chua, E. G., Gan, H. M., Thulasi, K., Wanyiri, J. W., Thevambiga, I., Goh, K. L., Wong, W. F., & Vadivelu, J. (2018). Metabolomics and 16S rRNA sequencing of human colorectal cancers and adjacent mucosa. PLoS ONE, 13(12), e0208584.

Lousa, I., Reis, F., Beirão, I., Alves, R., Belo, L., & Santos-Silva, A. (2021). New potential biomarkers for chronic kidney disease management — A review of the literature. International Journal of Molecular Sciences, 22, 43.

Loveday, S. M. (2022). Protein digestion and absorption: the influence of food processing. Nutrition Research Reviews, 36(2), 544–559.

Lyons, S. M., Kharel, P., Akiyama, Y., Ojha, S., Dave, D., Tsvetkov, V., Merrick, W., Ivanov, P., & Anderson, P. (2021). eIF4G has intrinsic G-quadruplex binding activity that is required for tiRNA function. Nucleic Acids Research, 48(11), 6223–6233.

Ma, C., Almasan, A., & Gurkan-Cavusoglu, E. (2022). Computational analysis of 5-fluorouracil anti-tumor activity in colon cancer using a mechanistic pharmacokinetic/pharmacodynamic model. PLOS Computational Biology, 18(11), e1010685.

Mapuskar, K. A., Vasquez-Martinez, G., Mayoral-Andrade, G., Tomanek-Chalkley, A., Zepeda-Orozco, D., & Allen, B. G. (2023). Mitochondrial Oxidative Metabolism: An Emerging Therapeutic Target to Improve CKD Outcomes. Biomedicines, 11(6), 1573.

Marques, R. C. P., De Medeiros, S. R. B., Da Silva Dias, C., Barbosa-Filho, J. M., & Agnez-Lima, L. F. (2003). Evaluation of the mutagenic potential of yangambin and of the hydroalcoholic extract of Ocotea duckei by the Ames test. Mutation Research/Genetic Toxicology and Environmental Mutagenesis, 536(2), 117–120.

Masci, D., Naro, C., Puxeddu, M., Urbani, A., Sette, C., La Regina, G., & Silvestri, R. (2023). Recent Advances in Drug Discovery for Triple-Negative Breast Cancer Treatment. Molecules, 28(22), 7513.

Maugard, M., Vigneron, P. A., Bolaños, J. P., & Bonvento, G. (2021). L-Serine links metabolism with neurotransmission. Progress in Neurobiology, 197, 101896.

Mbemi, A. T., Sims, J. N., Yedjou, C. G., Noubissi, F. K., Gomez, C. R., & Tchounwou, P. B. (2020). Vernonia calvoana shows promise towards the treatment of ovarian cancer. International Journal of Molecular Sciences, 21(12), 4429.

McQuade, R. M., Stojanovska, V., Bornstein, J. C., & Nurgali, K. (2017). Colorectal Cancer Chemotherapy: The Evolution of Treatment and New Approaches. Current Medicinal Chemistry, 24(15), 1537–1557.

Melnikov, S., Manakongtreecheep, K., & Söll, D. (2018). Revising the structural diversity of ribosomal proteins across the three domains of life. Molecular Biology and Evolution, 35(7), 1588–1598.

Melo-Reis, P. R., Bezerra, L. S. A., Vale, M. A. A. B., Canhête, R. F. R., & Chen-Chen, L. (2011). Assessment of the mutagenic and antimutagenic activity of Synadenium umbellatum Pax latex by micronucleus test in mice. Brazilian Journal of Biology, 71(1), 169–174.

Metge, B. J., Alsheikh, H. A., Chen, D., Elhamamsy, A. R., Hinshaw, D. C., Chen, B. R., Sleckman, B. P., Samant, R. S., & Shevde, L. A. (2023). Ribosome biosynthesis and Hedgehog activity are cooperative actionable signaling mechanisms in breast cancer following radiotherapy. Npj Precision Oncology, 7(1), 1–15.

Mezzapesa, M., Losurdo, G., Celiberto, F., Rizzi, S., D'amati, A., Piscitelli, D., Ierardi, E., & Di Leo, A. (2022). Serrated Colorectal Lesions: An Up-to-Date Review from Histological Pattern to Molecular Pathogenesis. International Journal of Molecular Sciences, 23(8), 4461.

Ming, Y. ., N.B.T.Zulkawi, Vandana Kotak Cy, & Y.K.Choudhary. (2013). Acute and sub-acute oral toxicity of Polygonum minus aqueous extract (biotropics®PM101) in wistar rats. International Journal of Pharmacy and Pharmaceutical Sciences, 5(2), 120–124.

Miyazawa, H., Snaebjornsson, M. T., Prior, N., Kafkia, E., Hammarén, H. M., Tsuchida-Straeten, N., Patil, K. R., Beck, M., & Aulehla, A. (2022). Glycolytic flux-signaling controls mouse embryo mesoderm development. ELife, 11, e83299.

Mohammed, A. I., Celentano, A., Paolini, R., Low, J. T., McCullough, M. J., O' Reilly, L. A., & Cirillo, N. (2023). Characterization of a novel dual murine model of chemotherapy-induced oral and intestinal mucositis. Scientific Reports, 13(1), 1396.

Mohd Ghazali, M. A., Al-Naqeb, G., Krishnan Selvarajan, K., Hazizul Hasan, M., & Adam, A. (2014). Apoptosis induction by polygonum minus is related to antioxidant capacity, alterations in expression of apoptotic-related genes, and S-phase cell cycle arrest in HepG2 cell line. BioMed Research International, 2014, 539607.

Moon, J. Y., Lee, M. R., & Ha, G. W. (2022). Prognostic value of tumor deposits for long-term oncologic outcomes in patients with stage III colorectal cancer: a systematic review and meta-analysis. International Journal of Colorectal Disease, 37(1), 1–11.

More, L. A., Lane, S., & Asnani, A. (2021). 5-FU Cardiotoxicity: Vasospasm, Myocarditis, and Sudden Death. Current Cardiology Reports, 23(3), 1–8.

Muhamad, N. A., Ma'amor, N. H., Rosli, I. A., Leman, F. N., Abdul Mutalip, M. H., Chan, H. K., Yusof, S. N., Tamin, N. S. I., Aris, T., Lai, N. M., & Abu Hassan, M. R. (2023). Colorectal cancer survival among Malaysia population: data from the Malaysian National Cancer Registry. Frontiers in Oncology, 13, 1132417.

Muhammad, N., Mansor, E., Sang, Y. C., Shariffudin, N. S., Dahdi, A., Alias, A. F., Mohamed, N., Shuid, A. N., Babji, A. S., & Soelaiman, I. N. (2013). Acute and subacute toxicity of Persicaria minor in wistar rats. Asian Journal of Animal Sciences, 7(2), 47–55.

Muhammad, Z., & Mustafa, A. M. (2015). Traditional Malay medicinal plants. In ITBM (pp. 39–41). Institut Terjemahan Negara Malaysia.

Mullen, N. J., & Singh, P. K. (2023). Nucleotide metabolism: a pan-cancer metabolic dependency. Nature Reviews Cancer, 23(5), 275–294.

Mun, J. G., Jeon, H. D., Yoon, D. H., Lee, Y. S., Park, S. Y., Jin, J. S., Park, N. J., & Kee, J. Y. (2022). Supercritical extract of cannabis sativa inhibits lung metastasis in colorectal cancer cells by increasing AMPK and MAPKs-Mediated apoptosis and cell cycle arrest. Nutrients, 14(21), 4548.

Muneer, M., Kanjal, M. I., Iqbal, M., Saeed, M., Khosa, M. K., Ud Den, N. Z., Ali, S., & Nazir, A. (2020). Gamma and UV radiations induced treatment of anti-cancer methotrexate drug in aqueous medium: Effect of process variables on radiation efficiency evaluated using bioassays. Applied Radiation and Isotopes, 166, 109371.

Muriithi, W., Macharia, L. W., Heming, C. P., Echevarria, J. L., Nyachieo, A., Filho, P. N., & Neto, V. M. (2020). ABC transporters and the hallmarks of cancer: roles in cancer aggressiveness beyond multidrug resistance. Cancer Biology and Medicine, 17(2), 253.

Mwangi, G. G., Wagacha, J. M., Nguta, J. M., & Mbaria, J. M. (2015). Brine shrimp cytotoxicity and antimalarial activity of plants traditionally used in treatment of malaria in Msambweni district. Pharmaceutical Biology, 53(4), 588–593.

MZ, A., M.H, M., & J, M. A. (2015). Antioxidant and Anticancer Activities of Polygonum Minus, Alpinia Galanga and Etlingera Elatior. The Open Conference Proceedings Journal, 4, 203–203.

Nakakaawa, L., Gbala, I. D., Cheseto, X., Bargul, J. L., & Wesonga, J. M. (2023). Oral acute, sub-acute toxicity and phytochemical profile of Brassica carinata A. Braun microgreens ethanolic extract in Wistar rats. Journal of Ethnopharmacology, 305, 116121.

Nannini, G., Meoni, G., Amedei, A., & Tenori, L. (2020). Metabolomics profile in gastrointestinal cancers: Update and future perspectives. World Journal of Gastroenterology, 26(20), 2514.

Negrei, C., Hudita, A., Ginghina, O., Galateanu, B., Voicu, S. N., Stan, M., Costache, M., Fenga, C., Drakoulis, N., & Tsatsakis, A. M. (2016). Colon cancer cells gene expression signature as response to 5-fluorouracil, oxaliplatin, and folinic acid treatment. Frontiers in Pharmacology, 7, 172.

Neve, R. M., Chin, K., Fridlyand, J., Yeh, J., Baehner, F. L., Fevr, T., Clark, L., Bayani, N., Coppe, J. P., Tong, F., Speed, T., Spellman, P. T., DeVries, S., Lapuk, A., Wang, N. J., Kuo, W. L., Stilwell, J. L., Pinkel, D., Albertson, D. G., … Gray, J. W. (2006). A collection of breast cancer cell lines for the study of functionally distinct cancer subtypes. Cancer Cell, 10(6), 515–527.

Ng, C. X., Affendi, M. M., Chong, P. P., & Lee, S. H. (2022). The Potential of Plant-Derived Extracts and Compounds to Augment Anticancer Effects of Chemotherapeutic Drugs. Nutrition and Cancer, 74(9), 3058–3076.

Nguyen, N. H., Nguyen, T. T., Ma, P. C., Ta, Q. T. H., Duong, T. H., & Vo, V. G. (2020). Potential antimicrobial and anticancer activities of an ethanol extract from bouea macrophylla. Molecules, 25(8), 1996.

O'Reilly, M., Linehan, A., Krstic, A., Kolch, W., Sheahan, K., Winter, D. C., & Mc Dermott, R. (2023). Oncotherapeutic Strategies in Early Onset Colorectal Cancer. Cancers, 15(2), 552.

Oh, C. M., Lee, D., Kong, H. J., Lee, S., Won, Y. J., Jung, K. W., & Cho, H. (2020). Causes of death among cancer patients in the era of cancer survivorship in Korea: Attention to the suicide and cardiovascular mortality. Cancer Medicine, 9(5), 1741–1752.

Okeda, R., Shibutani, M., Matsuo, T., Kuroiwa, T., Shimokawa, R., & Tajima, T. (1990). Experimental neurotoxicity of 5-fluorouracil and its derivatives is due to poisoning by the monofluorinated organic metabolites, monofluoroacetic acid and α-fluoroβ-alanine. Acta Neuropathologica, 81(1), 66–73.

Olivo Pimentel, V., Marcus, D., Van Der Wiel, A. M. A., Lieuwes, N. G., Biemans, R., Lieverse, R. I. Y., Neri, D., Theys, J., Yaromina, A., Dubois, L. J., & Lambin, P. (2021). Releasing the brakes of tumor immunity with anti-PD-L1 and pushing its accelerator with L19-IL2 cures poorly immunogenic tumors when combined with radiotherapy. Journal for ImmunoTherapy of Cancer, 9(3), e001764.

Omar, A. H., Kue, C. S., Dianita, R., & Yu, K. X. (2020). Teratogenic potential of traditional Malaysian vegetables (ulam) in the zebrafish model. British Food Journal, 122(10), 3089–3098.

Ong, H. C., & Nordiana, M. (1999). Malay ethno-medico botany in Machang, Kelantan, Malaysia. Fitoterapia, 70(5), 502–513.

Pan, L., Li, Z., Wang, Y., Zhang, B., Liu, G., & Liu, J. (2020). Network pharmacology and metabolomics study on the intervention of traditional Chinese medicine Huanglian Decoction in rats with type 2 diabetes mellitus. Journal of Ethnopharmacology, 258, 112842.

Pan, S., Fan, M., Liu, Z., Li, X., & Wang, H. (2021). Serine, glycine and one-carbon metabolism in cancer (Review). International Journal of Oncology, 58(2), 158–170.

Pan, Y., Gu, H. W., Lv, Y., Yin, X. L., Chen, Y., Long, W., Fu, H., & She, Y. (2022). Untargeted metabolomic analysis of Chinese red wines for geographical origin traceability by UPLC-QTOF-MS coupled with chemometrics. Food Chemistry, 394, 133474.

Parment, R., Dubois, M., Desrues, L., Mutel, A., Dembélé, K. P., Belin, N., Tron, L., Guérin, C., Coëffier, M., Compère, V., Féger, C., Joly, F., Hilber, P., Ribet, D., & Castel, H. (2022). A Panax quinquefolius-Based Preparation Prevents the Impact of 5-FU on Activity/Exploration Behaviors and Not on Cognitive Functions Mitigating Gut Microbiota and Inflammation in Mice. Cancers, 14(18), 4403.

Paternoga, H., Crowe-McAuliffe, C., Bock, L. V., Koller, T. O., Morici, M., Beckert, B., Myasnikov, A. G., Grubmüller, H., Nováček, J., & Wilson, D. N. (2023). Structural conservation of antibiotic interaction with ribosomes. Nature Structural and Molecular Biology, 30(9), 1380–1392.

Pavlova, N. N., Zhu, J., & Thompson, C. B. (2022). The hallmarks of cancer metabolism: Still emerging. Cell Metabolism, 34(3), 355–377.

Perše, M. (2021). Cisplatin mouse models: Treatment, toxicity and translatability. Biomedicines, 9(10), 1406.

Pezzani, R., Salehi, B., Vitalini, S., Iriti, M., Zuñiga, F. A., Sharifi-Rad, J., Martorell, M., & Martins, N. (2019). Synergistic effects of plant derivatives and conventional chemotherapeutic agents: An update on the cancer perspective. Medicina, 55(4), 110.

Pham, E. C., Van, L. V., Nguyen, C. V., Duong, N. T. N., Le Thi, T. V., & Truong, T. N. (2023). Acute and sub-acute toxicity evaluation of Merremia tridentata (L.) stem extract on mice. Toxicon, 227, 107093.

Phatik, T., Das, J., & Boruah, P. (2014). Antifungal activity of Polygonum hydropiper and Solanum melongena against plant pathogenic fungi. Plant Archives, 14(1), 15–17.

Plana, D., Palmer, A. C., & Sorger, P. K. (2022). Independent Drug Action in Combination Therapy: Implications for Precision Oncology. Cancer Discovery, 12(3), 606–624.

Posma, J. M., Garcia-Perez, I., Frost, G., Aljuraiban, G. S., Chan, Q., Van Horn, L., Daviglus, M., Stamler, J., Holmes, E., Elliott, P., & Nicholson, J. K. (2020). Nutriome–metabolome relationships provide insights into dietary intake and metabolism. Nature Food, 1(7), 426–436.

Posse, S., Otazo, R., Dager, S. R., & Alger, J. (2013). MR spectroscopic imaging: Principles and recent advances. Journal of Magnetic Resonance Imaging, 37(6), 1301–1325.

Punt, C. J. A., Heinemann, V., Maughan, T., Cremolini, C., Van Cutsem, E., McDermott, R., Bodoky, G., André, T., Osterlund, P., Teske, A. J., & Pfeiffer, P. (2023). Fluoropyrimidine-induced hand-foot syndrome and cardiotoxicity: recommendations for the use of the oral fluoropyrimidine S-1 in metastatic colorectal cancer. ESMO Open, 8(2), 101199.

Qader, S. W., Abdulla, M. A., Chua, L. S., Najim, N., Zain, M. M., & Hamdan, S. (2011). Antioxidant, total phenolic content and cytotoxicity evaluation of selected Malaysian plants. Molecules, 16(4), 3433–3443.

Qader, S. W., Abdulla, M. A., Chua, L. S., Sirat, H. M., & Hamdan, S. (2012). Pharmacological Mechanisms Underlying Gastroprotective Activities of the Fractions Obtained from Polygonum minus in Sprague Dawley Rats. International Journal of Molecular Sciences, 13(2), 1481–1496.

Rahim, N. A., Nordin, N., Ahmad Rasedi, N. I. S., Mohd Kauli, F. S., Wan Ibrahim, W. N., & Zakaria, F. (2022). Behavioral and cortisol analysis of the anti-stress effect of Polygonum minus (Huds) extracts in chronic unpredictable stress (CUS) zebrafish model. Comparative Biochemistry and Physiology Part C: Toxicology & Pharmacology, 256, 109303.

Rajhard, S., Hladnik, L., Vicente, F. A., Srčič, S., Grilc, M., & Likozar, B. (2021). Solubility of luteolin and other polyphenolic compounds in water, nonpolar, polar aprotic and protic solvents by applying ftir/hplc. Processes, 9(11), 1952.

Randel, K. R., Schult, A. L., Botteri, E., Hoff, G., Bretthauer, M., Ursin, G., Natvig, E., Berstad, P., Jørgensen, A., Sandvei, P. K., Olsen, M. E., Frigstad, S. O., Darre-Næss, O., Norvard, E. R., Bolstad, N., Kørner, H., Wibe, A., Wensaas, K. A., de Lange, T., & Holme, Ø. (2021). Colorectal Cancer Screening With Repeated Fecal Immunochemical Test Versus Sigmoidoscopy: Baseline Results From a Randomized Trial. Gastroenterology, 160(4), 1085–1096.

Redondo-Blanco, S., Fernández, J., Gutiérrez-del-Río, I., Villar, C. J., & Lombó, F. (2017). New insights toward colorectal cancer chemotherapy using natural bioactive compounds. Frontiers in Pharmacology, 8, 242711.

Regner, G. G., Gianesini, J., Von Borowski, R. G., Silveira, F., Semedo, J. G., Ferraz, A. de B. F., Wiilland, E., Von Poser, G., Allgayer, M., Picada, J. N., & Pereira, P. (2011). Toxicological evaluation of Pterocaulon polystachyum extract: A medicinal plant with antifungal activity. Environmental Toxicology and Pharmacology, 31(1), 242–249.

Reina-Campos, M., Diaz-Meco, M. T., & Moscat, J. (2020). The complexity of the serine glycine one-carbon pathway in cancer. Journal of Cell Biology, 219(1), e201907022.

Reyes-Habito, C. M., & Roh, E. K. (2014). Cutaneous reactions to chemotherapeutic drugs and targeted therapies for cancer: Part I. Conventional chemotherapeutic drugs. Journal of the American Academy of Dermatology, 71(2), 203.

Rohin, M. A. K., Hadi, N. A., & Ridzwan, N. (2020). Different Polarity Extracts of Polygonum minus towards Cytotoxic Activities against Colon Cancer Cell Lines (HT-29, HCT-116, CT-26). Journal of Pharmaceutical Research International, 32(14), 168–180.

Saganuwan, S. A. (2017). Toxicity studies of drugs and chemicals in animals: An overview. Bulgarian Journal of Veterinary Medicine, 20(4), 291–318.

Sahandi, J., Sorgeloos, P., & Zhang, W. (2022). Culture of Artemia franciscana nauplii with selected microbes suppressed Vibrio loading and enhanced survival, population stability, enzyme activity, and chemical composition. Aquaculture International, 30(5), 2279–2293.

Saini, R. K., Prasad, P., Shang, X., & Keum, Y. S. (2021). Advances in lipid extraction methods—a review. International Journal of Molecular Sciences, 22(24), 13643.

Saleem, M., Ullah, M., Kamreen, H., Hajri, A. K., Alanazi, A. N., Alraih, A. M., Alsuhaibani, A. M., Albedair, L. A., ur Rehman, K., & Khan, D. (2024). Microwave-assisted extraction of green tea catechins and antioxidant activity of tea extracts: The role of solvents, microwave power, and contact time. Microchemical Journal, 203, 110906.

Saputri, F. C., & Jantan, I. (2011). Effects of selected medicinal plants on human low-density lipoprotein oxidation, 2, 2-diphenyl-1-picrylhydrazyl (DPPH) radicals and human platelet aggregation. Journal of Medicinal Plant Research, 5(26), 6182–6191.

Schiliro, C., & Firestein, B. L. (2021). Mechanisms of metabolic reprogramming in cancer cells supporting enhanced growth and proliferation. Cells, 10(5), 1056. https://doi.org/10.3390/cells10051056

Schmidt, S., Denk, S., & Wiegering, A. (2020). Targeting protein synthesis in colorectal cancer. Cancers, 12(5), 1298.

Schoen, M. S., & Singh, R. H. (2022). Plasma metabolomic profile changes in females with phenylketonuria following a camp intervention. American Journal of Clinical Nutrition, 115(3), 811–821.

Schrimpf, S. P., Weiss, M., Reiter, L., Ahrens, C. H., Jovanovic, M., Malmström, J., Brunner, E., Mohanty, S., Lercher, M. J., Hunziker, P. E., Aebersold, R., Von Mering, C., & Hengartner, M. O. (2009). Comparative functional analysis of the Caenorhabditis elegans and Drosophila melanogaster proteomes. PLoS Biology, 7(3), e48.

Sethy, C., & Kundu, C. N. (2021). 5-Fluorouracil (5-FU) resistance and the new strategy to enhance the sensitivity against cancer: Implication of DNA repair inhibition. Biomedicine and Pharmacotherapy, 137, 111285.

Setyani, W., Murwanti, R., Sulaiman, T. N. S., & Hertiani, T. (2023). Application of Response Surface Methodology (RSM) for the Optimization of Ultrasound-Assisted Extraction (UAE) of Moringa oleifera: Extraction Yield, Content of Bioactive Compounds, and Biological Effects In Vitro. Plants, 12(13), 2455.

Shah, N. A., Khan, M. R., & Nadhman, A. (2014). Antileishmanial, toxicity, and phytochemical evaluation of medicinal plants collected from Pakistan. BioMed Research International, 2014(1), 384204.

Shakibaei, M., Mobasheri, A., Lueders, C., Busch, F., Shayan, P., & Goel, A. (2013). Curcumin Enhances the Effect of Chemotherapy against Colorectal Cancer Cells by Inhibition of NF-κB and Src Protein Kinase Signaling Pathways. PLoS ONE, 8(2), e57218.

Shao, B., Zhu, M., Shen, K., Luo, L., Du, P., Li, J., Xu, J., Deng, Y., Lin, N., Wu, J., & Hu, W. (2023). Disease Burden of Total and Early-Onset Colorectal Cancer in China from 1990 to 2019 and Predictions of Cancer Incidence and Mortality. Clinical Epidemiology, 15, 151–163.

Sharma, M., Bakshi, A. K., Mittapelly, N., Gautam, S., Marwaha, D., Rai, N., Singh, N., Tiwari, P., Agarwal, N., Kumar, A., & Mishra, P. R. (2022). Recent updates on innovative approaches to overcome drug resistance for better outcomes in cancer. Journal of Controlled Release, 346, 43–70.

Sharma, N., Kumar, V., Chopra, M. P., Sourirajan, A., Dev, K., & El-Shazly, M. (2020). Thalictrum foliolosum: A lesser unexplored medicinal herb from the Himalayan region as a source of valuable benzyl isoquinoline alkaloids. Journal of Ethnopharmacology, 255, 112736.

Sharma, S., Zhang, X., Azhar, G., Patyal, P., Verma, A., Grishma, K. C., & Wei, J. Y. (2024). Valine improves mitochondrial function and protects against oxidative stress. Bioscience, Biotechnology and Biochemistry, 88(2), 168–176.

Shaw, R. J. (2009). LKB1 and AMP-activated protein kinase control of mTOR signalling and growth. Acta Physiologica, 196(1), 65–80.

Shen, B. B., Yang, Y. P., Yasamin, S., Liang, N., Su, W., Chen, S. H., Wang, X. J., & Wang, W. (2018). Analysis of the Phytochemistry and Bioactivity of the Genus Polygonum of Polygonaceae. Digital Chinese Medicine, 1(1), 19–36.

Shin, I. S., Seo, C. S., Ha, H. K., Lee, M. Y., Huang, D. S., Huh, J. I., & Shin, H. K. (2011). Genotoxicity assessment of Pyungwi-san (PWS), a traditional herbal prescription. Journal of Ethnopharmacology, 133(2), 696–703.

Shiratori, R., Furuichi, K., Yamaguchi, M., Miyazaki, N., Aoki, H., Chibana, H., Ito, K., & Aoki, S. (2019). Glycolytic suppression dramatically changes the intracellular metabolic profile of multiple cancer cell lines in a mitochondrial metabolism-dependent manner. Scientific Reports, 9(1), 1–15.

Showalter, S. L., Showalter, T. N., Witkiewicz, A., Havens, R., Kennedy, E. P., Hucl, T., Kern, S. E., Yeo, C. J., & Brody, J. R. (2008). Evaluating the drug-target relationship between thymidylate synthase expression and tumor response to 5-fluorouracil: Is it time to move forward?. Cancer Biology and Therapy, 7(7), 986-994.

Shunxi, W., Xiaoxue, Y., Guanbin, S., Li, Y., Junyu, J., & Wanqian, L. (2023). Serine Metabolic Reprogramming in Tumorigenesis, Tumor Immunity, and Clinical Treatment. Advances in Nutrition, 14(5), 1050–1066.

Siegel, R. L., Giaquinto, A. N., Ahmedin, Dvm, J., & Siegel, R. L. (2024). Cancer statistics, 2024. CA: A Cancer Journal for Clinicians, 74(1), 12–49.

Singh, C. K., George, J., & Ahmad, N. (2013). Resveratrol-based combinatorial strategies for cancer management. Annals of the New York Academy of Sciences, 1290(1), 113–121.

Smith, P., Lavery, A., & Turkington, R. C. (2020). An overview of acute gastrointestinal side effects of systemic anti-cancer therapy and their management. Best Practice and Research: Clinical Gastroenterology, 48, 101691.

Song, M., Chan, A. T., & Sun, J. (2020). Influence of the Gut Microbiome, Diet, and Environment on Risk of Colorectal Cancer. Gastroenterology, 158(2), 322–340.

Sumazian, Y., Syahida, A., Hakiman, M., & Maziah, M. (2010). Antioxidant activities, flavonoids, ascorbic acid and phenolic contents of Malaysian vegetables. Journal of Medicinal Plants Research, 4(10), 881–890.

Sun, W., Liu, R., Gao, X., Lin, Z., Tang, H., Cui, H., & Zhao, E. (2023). Targeting serine-glycine-one-carbon metabolism as a vulnerability in cancers. Biomarker Research, 11, 48.

Talbot, S. R., Biernot, S., Bleich, A., van Dijk, R. M., Ernst, L., Häger, C., Helgers, S. O. A., Koegel, B., Koska, I., Kuhla, A., Miljanovic, N., Müller-Graff, F. T., Schwabe, K., Tolba, R., Vollmar, B., Weegh, N., Wölk, T., Wolf, F., Wree, A., … Zechner, D. (2020). Defining body-weight reduction as a humane endpoint: a critical appraisal. Laboratory Animals, 54(1), 99–110.

Tallarida, R. J. (2002). The interaction index: A measure of drug synergism. Pain, 98(1–2), 163–168.

Tamin, N. S. I., Razalli, K. A., Sallahuddin, S. N., Chan, H. K., & Hassan, M. R. A. (2020). A 5-year evaluation of using stool-based test for opportunistic colorectal cancer screening in primary health institutions across Malaysia. Cancer Epidemiology, 69, 101829.

Tan, H. M., Leong, K. H., Song, J., Mohd Sufian, N. S. F., Mohd Hazli, U. H. A., Chew, L. Y., & Kong, K. W. (2020). Antioxidant and LC-QToF-MS/MS analysis of polyphenols in polar and non-polar extracts from Strobilanthes crispus and Clinacanthus nutans. International Food Research Journal, 27(5), 903.

Temaj, G., Chichiarelli, S., Eufemi, M., Altieri, F., Hadziselimovic, R., Farooqi, A. A., Yaylim, I., & Saso, L. (2022). Ribosome-Directed Therapies in Cancer. Biomedicines, 10(9), 2088.

Therizols, G., Bash-Imam, Z., Panthu, B., Machon, C., Vincent, A., Ripoll, J., Nait-Slimane, S., Chalabi-Dchar, M., Gaucherot, A., Garcia, M., Laforêts, F., Marcel, V., Boubaker-Vitre, J., Monet, M. A., Bouclier, C., Vanbelle, C., Souahlia, G., Berthel, E., Albaret, M. A., … Diaz, J. J. (2022). Alteration of ribosome function upon 5-fluorouracil treatment favors cancer cell drug-tolerance. Nature Communications, 13(1), 173.

Tian, J., Afebu, K. O., Bickerdike, A., Liu, Y., Prasad, S., & Nelson, B. J. (2023). Fundamentals of Bowel Cancer for Biomedical Engineers. Annals of Biomedical Engineering, 51(4), 679–701.

Tian, J., Zhang, D., Kurbatov, V., Wang, Q., Wang, Y., Fang, D., Wu, L., Bosenberg, M., Muzumdar, M. D., Khan, S., Lu, Q., Yan, Q., & Lu, J. (2021). 5-Fluorouracil efficacy requires anti-tumor immunity triggered by cancer-cell-intrinsic STING. The EMBO Journal, 40(7), e106065.

Tobias, G. C., Gomes, J. L. P., Fernandes, L. G., Voltarelli, V. A., de Almeida, N. R., Jannig, P. R., de Souza, R. W. A., Negrão, C. E., Oliveira, E. M., Chammas, R., Alves, C. R. R., & Brum, P. C. (2023). Aerobic exercise training mitigates tumor growth and cancer-induced splenomegaly through modulation of non-platelet platelet factor 4 expression. Scientific Reports, 13(1), 21970.

Torres, S., Bartolomé, R. A., Mendes, M., Barderas, R., Fernandez-Aceñero, M. J., Peláez-García, A., Peña, C., Lopez-Lucendo, M., Villar-Vázquez, R., De Herreros, A. G., Bonilla, F., & Casal, J. I. (2013). Proteome profiling of cancer-associated fibroblasts identifies novel proinflammatory signatures and prognostic markers for colorectal cancer. Clinical Cancer Research, 19(21), 6006–6019.

Tu, C., Mojica, W., Straubinger, R. M., Li, J., Shen, S., Qu, M., Nie, L., Roberts, R., An, B., & Qu, J. (2017). Quantitative proteomic profiling of paired cancerous and normal colon epithelial cells isolated freshly from colorectal cancer patients. Proteomics - Clinical Applications, 11(5–6), 1600155.

Tufail, M., Jiang, C.-H., & Li, N. (2024). Altered metabolism in cancer: insights into energy pathways and therapeutic targets. Molecular Cancer, 23(1), 1–40.

Udani, J. K., George, A. A., Musthapa, M., Pakdaman, M. N., & Abas, A. (2014). Effects of a proprietary freeze-dried water extract of Eurycoma longifolia (Physta) and Polygonum minus on sexual performance and well-being in men: A randomized, double-blind, placebo-controlled study. Evidence-Based Complementary and Alternative Medicine, 2014, 1–10.

Uyub, A. M., Nwachukwu, I. N., Azlan, A. A., & Fariza, S. S. (2010). In-vitro antibacterial activity and cytotoxicity of selected medicinal plant extracts from penang island Malaysia on metronidazole-resistanthelicobacter pylori and some pathogenic bacteria. Ethnobotany Research and Applications, 8, 95–106.

Valencia-Lazcano, A. A., Hassan, D., Pourmadadi, M., shamsabadipour, A., Behzadmehr, R., Rahdar, A., Medina, D. I., & Díez-Pascual, A. M. (2023). 5-Fluorouracil nano-delivery systems as a cutting-edge for cancer therapy. European Journal of Medicinal Chemistry, 246(15), 114995.

van Wyk, A. S., & Prinsloo, G. (2020). Health, safety and quality concerns of plant-based traditional medicines and herbal remedies. South African Journal of Botany, 133, 54–62.

Verma, H., Narendra, G., Raju, B., Singh, P. K., & Silakari, O. (2022). Dihydropyrimidine Dehydrogenase-Mediated Resistance to 5-Fluorouracil: Mechanistic Investigation and Solution. ACS Pharmacology and Translational Science, 5(11), 1017–1033.

Vicar, T., Raudenska, M., Gumulec, J., & Balvan, J. (2020). The Quantitative-Phase Dynamics of Apoptosis and Lytic Cell Death. Scientific Reports, 10(1), 1566.

Vikram, P., Chiruvella, K. K., Ripain, I. H. A., & Arifullah, M. (2014). A recent review on phytochemical constituents and medicinal properties of kesum (Polygonum minus Huds.). Asian Pacific Journal of Tropical Biomedicine, 4(6), 430–435.

Vimala, S., Adenan, M. I., Ahmad, A. R., & Shahdan, R. (2003). Nature's choice to wellness: antioxidant vegetables/ulam. Forest Research Institute Malaysia (FRIM).

Vimala, S., Rohana, S., Rashih, A. ., & M, J. (2011). Antioxidant Evaluation in Malaysian Medicinal Plant: Persicaria minor (Huds.) Leaf. Science Journal of Medicine and Clinical Trials, 2012, 9–16.

Vodenkova, S., Buchler, T., Cervena, K., Veskrnova, V., Vodicka, P., & Vymetalkova, V. (2020). 5-fluorouracil and other fluoropyrimidines in colorectal cancer: Past, present and future. Pharmacology and Therapeutics, 206, 107447.

Voss, K., Hong, H. S., Bader, J. E., Sugiura, A., Lyssiotis, C. A., & Rathmell, J. C. (2021). A guide to interrogating immunometabolism. Nature Reviews Immunology, 21(10), 637–652.

Vousden, K. H., & Ryan, K. M. (2009). P53 and metabolism. Nature Reviews Cancer, 9(10), 691–700.

Wahab, N. Z. A., Bunawan, H., & Ibrahim, N. (2015). Cytotoxicity and antiviral activity of methanol extract from Polygonum minus. AIP Conference Proceedings, 1678(1), 030036.

Walter, M., & Herr, P. (2022). Re-Discovery of Pyrimidine Salvage as Target in Cancer Therapy. Cells, 11(4), 739.

Wan-Ibrahim, W. I., Sidik, K., & Kuppusamy, U. R. (2010). A high antioxidant level in edible plants is associated with genotoxic properties. Food Chemistry, 122(4), 1139–1144.

Wang, D., & Wan, X. (2022). Progress in research on the role of amino acid metabolic reprogramming in tumour therapy: A review. Biomedicine and Pharmacotherapy, 156, 113923.

Wang, Z. H., Li, J., Liu, Q., Qian, J. C., Li, Q. Q., Wang, Q. Y., Zeng, L. T., Li, S. J., Gao, X., Pan, J. X., Gao, X. F., Wu, K., Hu, G. X., Iwakuma, T., & Cai, J. P. (2024). A modified nucleoside O6-methyl-2′-deoxyguanosine-5′-triphosphate exhibits anti-glioblastoma activity in a caspase-independent manner. Pharmacological Research, 199, 106990.

Wang, Z., Li, W., Park, J., Gonzalez, K. M., Scott, A. J., & Lu, J. (2022). Camptothesome elicits immunogenic cell death to boost colorectal cancer immune checkpoint blockade. Journal of Controlled Release, 349, 929–939.

War Naw, S., Darli Kyaw Zaw, N., Siti Aminah, N., Amin Alamsjah, M., Novi Kristanti, A., Nege, A. S., & Thanda Aung, H. (2020). Bioactivities, heavy metal contents and toxicity effect of macroalgae from two sites in Madura, Indonesia. Journal of the Saudi Society of Agricultural Sciences, 19(8), 528–537.

Warburg, O. (1924). Über den Stoffwechsel der Carcinomzelle. Naturwissenschaften, 12(50), 1131–1137.

Warburg, O. (1956). On the origin of cancer cells. Science, 123(3191), 309–314.

Ward, R. A., Fawell, S., Floc'H, N., Flemington, V., McKerrecher, D., & Smith, P. D. (2021). Challenges and Opportunities in Cancer Drug Resistance. Chemical Reviews, 121(6), 3297–3351.

Wasman, S. Q., Mahmood, A. A., Salehhuddin, H., Zahra, A. A., & Salmah, I. (2010). Cytoprotective activities of Polygonum minus aqueous leaf extract on ethanol-induced gastric ulcer in rats. Journal of Medicinal Plants Research, 4(24), 2658–2665.

Wei, Z., Chen, G., Zhang, P., Zhu, L., Zhang, L., & Chen, K. (2018). Rhizopus nigricans polysaccharide activated macrophages and suppressed tumor growth in CT26 tumor-bearing mice. Carbohydrate Polymers, 198, 302–312.

Wei, Z., Liu, X., Cheng, C., Yu, W., & Yi, P. (2021). Metabolism of Amino Acids in Cancer. Frontiers in Cell and Developmental Biology, 8, 603837.

Weli, A. M., Al-Harrasi, A., Al Baiti, N. H., Philip, A., Hossain, A., Gilani, S. A., & Banioraba, N. (2020). Biological and toxicological evaluation of aerial parts extracts of locally grown Cleome austroarabica. Journal of King Saud University-Science, 32(1), 753–757.

Weth, F. R., Hoggarth, G. B., Weth, A. F., Paterson, E., White, M. P. J., Tan, S. T., Peng, L., & Gray, C. (2024). Unlocking hidden potential: advancements, approaches, and obstacles in repurposing drugs for cancer therapy. British Journal of Cancer, 130(5), 703–715.

Wiart, C. (2006). Medicinal plants of Asia and the Pacific. In CRC Press.

Wlodarczyk, J. R., & Lee, S. W. (2022). New Frontiers in Management of Early and Advanced Rectal Cancer. Cancers, 14(4), 938.

Xi, Y., & Xu, P. (2021). Global colorectal cancer burden in 2020 and projections to 2040. Translational Oncology, 14(10), 101174.

Xia, C., He, Z., & Cai, Y. (2020). Quantitative proteomics analysis of differentially expressed proteins induced by astragaloside IV in cervical cancer cell invasion. Cellular and Molecular Biology Letters, 25(1), 1–14.

Xia, X., Li, X., Xie, F., Yuan, G., Cheng, D., & Peng, C. (2022). Non-targeted metabonomic analysis of plasma in patients with atherosclerosis by liquid chromatography-mass spectrometry. Annals of Translational Medicine, 10(3), 133.

Xia, Y., Sun, M., Huang, H., & Jin, W. L. (2024). Drug repurposing for cancer therapy. Signal Transduction and Targeted Therapy, 9(1), 92.

Xiao, H., Zheng, Y., Ma, L., Tian, L., & Sun, Q. (2021). Clinically-Relevant ABC Transporter for Anti-Cancer Drug Resistance. Frontiers in Pharmacology, 12, 648407.

Xie, D., Song, X., & Tong, L. (2021). Stage migration resulting from inadequate number of examined lymph nodes impacts prognosis in stage II colon cancer after radical surgery. International Journal of Colorectal Disease, 36(5), 959–969.

Xie, L., Shen, M., Huang, R., Liu, X., Yu, Y., Lu, H., & Xie, J. (2023). Apoptosis of colon cancer CT-26 cells induced polysaccharide from Cyclocarya paliurus and its phosphorylated derivative via intrinsic mitochondrial passway. Food Science and Human Wellness, 12(5), 1545–1556.

Xu, M., Xi, S., Li, H., Xia, Y., Mei, G., & Cheng, Z. (2024). Prognosis significance and potential association between ALDOA and AKT expression in colorectal cancer. Scientific Reports, 14, 6488.

Yan, H., Wang, P., Yang, F., Cheng, W., Chen, C., Zhai, B., & Zhou, Y. (2024). Anticancer therapy-induced adverse drug reactions in children and preventive and control measures. Frontiers in Pharmacology, 15, 1329220.

Yang, L. C., Hsieh, C. C., Lu, T. J., & Lin, W. C. (2014). Structurally characterized arabinogalactan from Anoectochilus formosanus as an immuno-modulator against CT26 colon cancer in BALB/c mice. Phytomedicine, 21(5), 647–655.

Yang, Y., Ma, L., Xu, Y., Liu, Y., Li, W., Cai, J., & Zhang, Y. (2020). Enalapril overcomes chemoresistance and potentiates antitumor efficacy of 5-FU in colorectal cancer by suppressing proliferation, angiogenesis, and NF-κB/STAT3-regulated proteins. Cell Death and Disease, 11(6), 477.

Yang, Z., Deng, X., Yang, Z., Han, M., Chan, K. W., Abdull Razis, A. F., Esa, N. M., Ho, K. L., & Abu Bakar, M. Z. (2024). Polygonum minus: A tropical medicinal herb with vast applications in food, agricultural, and medicinal fields. Food Bioscience, 60, 104511.

Yang, Z., Yang, Z., Abu Bakar, M. Z., & Deng, X. (2025). Exploring the anti-colon cancer potential of Polygonum minus: Integrating in vitro and in silico studies. Food Bioscience, 64, 105853.

Youssef, A. M. M., Maaty, D. A. M., & Al-Saraireh, Y. M. (2023). Phytochemistry and Anticancer Effects of Mangrove (Rhizophora mucronata Lam.) Leaves and Stems Extract against Different Cancer Cell Lines. Pharmaceuticals, 16(1), 4.

Yu, Y., Hai, Y., Zhou, H., Bao, W., Hu, X., Gao, Y., & Wu, J. (2024). METTL3 Inhibition Suppresses Cell Growth and Survival in Colorectal Cancer via ASNS Downregulation. Journal of Cancer, 15(15), 4853–4865.

Yuan, M., Zhang, G., Bai, W., Han, X., Li, C., & Bian, S. (2022). The Role of Bioactive Compounds in Natural Products Extracted from Plants in Cancer Treatment and Their Mechanisms Related to Anticancer Effects. Oxidative Medicine and Cellular Longevity, 2022, 1429869.

Yusoh, N. A., Tiley, P. R., James, S. D., Harun, S. N., Thomas, J. A., Saad, N., Hii, L. W., Chia, S. L., Gill, M. R., & Ahmad, H. (2023). Discovery of ruthenium (II) metallocompound and olaparib synergy for cancer combination therapy. Journal of Medicinal Chemistry, 66(10), 6922–6937.

Zafar, A., Drobni, Z. D., Mosarla, R., Alvi, R. M., Lei, M., Lou, U. Y., Raghu, V. K., Murphy, S. P., Jones-O'Connor, M., Hartmann, S., Gilman, H. K., Weekes, C. D., Clark, J. R., Clark, J., Blaszkowsky, L., Tavares, E., & Neilan, T. G. (2021). The Incidence, Risk Factors, and Outcomes With 5-Fluorouracil–Associated Coronary Vasospasm. JACC: CardioOncology, 3(1), 101–109.

Zargar, T., Kumar, D., Sahni, B., Shoket, N., Bala, K., & Angurana, S. (2021). Dietary risk factors for colorectal cancer: A hospital-based case-control study. Cancer Research, Statistics, and Treatment, 4(3), 479–485.

Zhang, B., VerBerkmoes, N. C., Langston, M. A., Uberbacher, E., Hettich, R. L., & Samatova, N. F. (2006). Detecting differential and correlated protein expression in label-free shotgun proteomics. Journal of Proteome Research, 5(11), 2909–2918.

Zhang, C., Yu, J. J., Yang, C., Yuan, Z. L., Zeng, H., Wang, J. J., Shang, S., Lv, X. X., Liu, X. T., Liu, J., Xue, Q., Cui, B., Tan, F. W., & Hua, F. (2023). Wild-type IDH1 maintains NSCLC stemness and chemoresistance through activation of the serine biosynthetic pathway. Science Translational Medicine, 15(726), eade4113.

Zhang, W. li, Li, N., Shen, Q., Fan, M., Guo, X. dong, Zhang, X. wen, Zhang, Z., & Liu, X. (2020). Establishment of a mouse model of cancer cachexia with spleen deficiency syndrome and the effects of atractylenolide I. Acta Pharmacologica Sinica, 41(2), 237–248.

Zhang, Y., Wang, Q., Liang, J., Liu, L., Liu, P., & Zhao, H. (2022). Serum proteomic analysis of differentially expressed proteins and pathways involved in the mechanism of endemic osteoarthritis. Molecular Omics, 18(8), 745–753.

Zhao, M., van Straten, D., Broekman, M. L. D., Préat, V., & Schiffelers, R. M. (2020). Nanocarrier-based drug combination therapy for glioblastoma. Theranostics, 10(3), 1355.

Zhao, Y., Feng, X., Zhang, L., Huang, W., & Liu, Y. (2023). Antitumor Activity of Carboxymethyl Pachymaran with Different Molecular Weights Based on Immunomodulatory and Gut Microbiota. Nutrients, 15(21), 4527.

Zhou, H., Zhang, M., Cao, H., Du, X., Zhang, X., Wang, J., & Bi, X. (2023). Research Progress on the Synergistic Anti-Tumor Effect of Natural Anti-Tumor Components of Chinese Herbal Medicine Combined with Chemotherapy Drugs. Pharmaceuticals, 16(12), 1734.

Zhu, D., Wang, J., Ren, L., Li, Y., Xu, B., Wei, Y., Zhong, Y., Yu, X., Zhai, S., Xu, J., & Qin, X. (2013). Serum proteomic profiling for the early diagnosis of colorectal cancer. Journal of Cellular Biochemistry, 114(2), 448–455.

Zhu, L., Cao, J., Chen, G., Xu, Y., Lu, J., Fang, F., & Chen, K. (2016). Anti-tumor and immunomodulatory activities of an exopolysaccharide from Rhizopus nigricans on CT26 tumor-bearing mice. International Immunopharmacology, 36, 218–224.

Zhu, Y., Ouyang, Z., Du, H., Wang, M., Wang, J., Sun, H., Kong, L., Xu, Q., Ma, H., & Sun, Y. (2022). New opportunities and challenges of natural products research: When target identification meets single-cell multiomics. Acta Pharmaceutica Sinica B, 12(11), 4011–4039.

Zong, Y., Li, H., Liao, P., Chen, L., Pan, Y., Zheng, Y., Zhang, C., Liu, D., Zheng, M., & Gao, J. (2024). Mitochondrial dysfunction: mechanisms and advances in therapy. Signal Transduction and Targeted Therapy, 9(1), 1–29.

Zou, J. Y., Chen, Q. L., Luo, X. C., Damdinjav, D., Abdelmohsen, U. R., Li, H. Y., Battulga, T., Chen, H. B., Wang, Y. Q., & Zhang, J. Y. (2024). Natural products reverse cancer multidrug resistance. Frontiers in Pharmacology, 15, 1348076.

BIODATA OF STUDENT

Yang Zhongming was born on July 5, 1993, in Bazhong, Sichuan, China. In 2011, he was successfully admitted to the Faculty of Veterinary Medicine of Southwest University, majoring in veterinary medicine. In 2015, he successfully graduated and obtained a bachelor's degree in agriculture. In the same year, he was admitted to the Faculty of Veterinary Medicine of Southwest University to pursue a master's degree in agriculture and graduated in 2017. After graduating in 2017, he joined Yibin Vocational and Technical College, where he served as a lead lecturer in the Animal Medicine program. In 2018, he moved to Sichuan Vocational and Technical College of Chemical Technology, taking up the role of lead lecturer at the Modern Agriculture College. A year later, he became a lead lecturer at Yangtze Normal University. In 2022, demonstrating his commitment to academic excellence, he opted to pursue a PhD. program starting in March 2022 at the Institute of Bioscience, UPM, supported by his family.

LIST OF PUBLICATIONS

Yang, Z., Deng, X., Yang, Z., Han, M., Chan, K. W., Abdull Razis, A. F., Esa, N. M., Ho, K. L., & Abu Bakar, M. Z. (2024). Polygonum minus: A tropical medicinal herb with vast applications in food, agricultural, and medicinal fields. *Food Bioscience*, 60, 104511.